



Review

# Significance of Singlet Oxygen Molecule in Pathologies

Kazutoshi Murotomi <sup>1,†</sup> , Aya Umeno <sup>2,†</sup>, Mototada Shichiri <sup>3,\*</sup> , Masaki Tanito <sup>2</sup> and Yasukazu Yoshida <sup>4</sup>

<sup>1</sup> Biomedical Research Institute, National Institute of Advanced Industrial Science and Technology (AIST), Tsukuba 305-8566, Japan

<sup>2</sup> Department of Ophthalmology, Shimane University Faculty of Medicine, Izumo 693-8501, Japan

<sup>3</sup> Biomedical Research Institute, National Institute of Advanced Industrial Science and Technology (AIST), Ikeda 563-8577, Japan

<sup>4</sup> LG Japan Lab Inc., Yokohama 220-0011, Japan

\* Correspondence: mototada-shichiri@aist.go.jp; Tel.: +81-72-751-8234

† These authors contributed equally to this work.

**Abstract:** Reactive oxygen species, including singlet oxygen, play an important role in the onset and progression of disease, as well as in aging. Singlet oxygen can be formed non-enzymatically by chemical, photochemical, and electron transfer reactions, or as a byproduct of endogenous enzymatic reactions in phagocytosis during inflammation. The imbalance of antioxidant enzymes and antioxidant networks with the generation of singlet oxygen increases oxidative stress, resulting in the undesirable oxidation and modification of biomolecules, such as proteins, DNA, and lipids. This review describes the molecular mechanisms of singlet oxygen production in vivo and methods for the evaluation of damage induced by singlet oxygen. The involvement of singlet oxygen in the pathogenesis of skin and eye diseases is also discussed from the biomolecular perspective. We also present our findings on lipid oxidation products derived from singlet oxygen-mediated oxidation in glaucoma, early diabetes patients, and a mouse model of bronchial asthma. Even in these diseases, oxidation products due to singlet oxygen have not been measured clinically. This review discusses their potential as biomarkers for diagnosis. Recent developments in singlet oxygen scavengers such as carotenoids, which can be utilized to prevent the onset and progression of disease, are also described.

**Keywords:** reactive oxygen species; singlet oxygen; biomarkers; lipid peroxidation



**Citation:** Murotomi, K.; Umeno, A.; Shichiri, M.; Tanito, M.; Yoshida, Y. Significance of Singlet Oxygen Molecule in Pathologies. *Int. J. Mol. Sci.* **2023**, *24*, 2739. <https://doi.org/10.3390/ijms24032739>

Academic Editors: Rossana Morabito and Alessia Remigante

Received: 11 December 2022

Revised: 22 January 2023

Accepted: 26 January 2023

Published: 1 February 2023



**Copyright:** © 2023 by the authors. Licensee MDPI, Basel, Switzerland. This article is an open access article distributed under the terms and conditions of the Creative Commons Attribution (CC BY) license (<https://creativecommons.org/licenses/by/4.0/>).

## 1. Introduction

Oxygen can be recognized as a “double-edged sword” because aerobic organisms cannot live without it, even though the oxidative metabolism produces toxic by-products. Most deleterious phenomena arise because of free radicals. Hence, for survival, the elimination of highly reactive oxygen species (ROS) is important for living organisms. The human body is also constantly threatened by oxidative injury and radicals. Over the course of evolution, humans have developed defense systems to counteract oxidative damage, including the transformation and/or elimination of ROS, as a part of normal physiological homeostasis. When this homeostatic balance is disturbed by stress caused by environmental or radiation exposure, it is termed oxidative stress, that is, a state in which the homeostatic balance between oxidation reactions and antioxidant defenses is lost, leading to the oxidation of vital biomolecules and, finally, the onset of disease.

Thousands of studies have been reported over the past decade on the role of ROS in cell and tissue injury. ROS are generally accepted to be involved in various pathologies, including inflammation, asthma, muscular dystrophy, dementia, anaphylaxis, rheumatoid arthritis, reperfusion injury following ischemic stroke or heart attacks, cardiac toxicity of anti-cancer drugs, carcinogenicity of various chemicals, and smoking [1–5].

In this review, we focus on singlet oxygen (<sup>1</sup>O<sub>2</sub>) in ROS. However, we exclude photodynamic therapy (PDT), in which <sup>1</sup>O<sub>2</sub> is stimulated by the light irradiation of a photosensitizing agent to induce a therapeutic effect on cancer [6], because many interesting review

articles on PDT have already been published in recent years. The molecular aspects of (1) the mechanism of  $^1\text{O}_2$  production in vivo, (2) methods for detecting  $^1\text{O}_2$  and its oxidation-modification products, (3) implications in the pathogenesis of skin and eye diseases, and (4) compounds that scavenge  $^1\text{O}_2$  are presented. Furthermore, we present our findings on the measurement of  $^1\text{O}_2$ -mediated oxidation products in diabetes, bronchial asthma, and ocular diseases. Although  $^1\text{O}_2$  has been known to potentially be involved in the pathogenesis of certain diseases, lipid peroxidation products and other products produced by  $^1\text{O}_2$  have not been actively measured clinically. In this review, we examine the usefulness of lipid peroxidation products produced by  $^1\text{O}_2$  in diagnosing and understanding the pathophysiology of diseases.

## 2. Chemical Properties and Possible Production of Singlet Oxygen In Vivo

ROS are redox-active intermediates that are formed by the chemical, photochemical, or biochemical reduction in oxygen that, at least partially, triggers a chain of oxidative reactions. ROS are grouped into non-radical and radical species, the former including  $^1\text{O}_2$  and hydrogen peroxide ( $\text{H}_2\text{O}_2$ ), and the latter including superoxide anions ( $\text{O}_2^{\bullet-}$ ), hydroxyl radicals ( $\text{HO}^\bullet$ ), hydroperoxyl radicals ( $\text{HO}_2^\bullet$ ), alkoxy radicals ( $\text{RO}^\bullet$ ), and peroxy radicals ( $\text{ROO}^\bullet$ ) [7].  $^1\text{O}_2$  is generated by energy transfer via chemical or photochemical pathways from an activated species to the oxygen molecule (triplet oxygen,  $^3\text{O}_2$ ) (Figure 1). Other species are formed by a series of reactions initiated by  $^1\text{O}_2$ , or by certain one-electron reduction processes [7]. Therefore, ROS have been actively studied over the past three decades to determine whether they are beneficial or harmful.

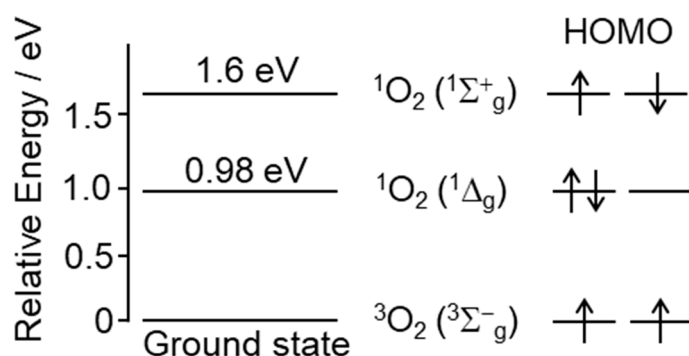


**Figure 1.** Relationship between energy levels of ground state triplet oxygen molecule  $^3\text{O}_2$  and singlet oxygen molecule  $^1\text{O}_2$ . The ground state oxygen molecule, triplet oxygen  $^3\text{O}_2$  ( $^3\Sigma_g^-$ ), has two unpaired and spin-parallel electrons in  $\pi^*$  antibonding orbitals.  $^3\text{O}_2$  ( $^3\Sigma_g^-$ ) in the ground state receives energy and is excited to the singlet state, forming singlet oxygen ( $^1\text{O}_2$ ).  $^1\text{O}_2$  is the spin-flipped electron state of  $^3\text{O}_2$  ( $^3\Sigma_g^-$ ). There are two states of  $^1\text{O}_2$ :  $^1\text{O}_2$  ( $^1\Sigma_g^+$ ) and  $^1\text{O}_2$  ( $^1\Delta_g$ ).  $^1\text{O}_2$  ( $^1\Sigma_g^+$ ) and  $^1\text{O}_2$  ( $^1\Delta_g$ ) have energies that are 1.6 eV and 0.98 eV higher than the ground state  $^3\text{O}_2$  ( $^3\Sigma_g^-$ ), respectively. The lifetime of  $^1\text{O}_2$  ( $^1\Sigma_g^+$ ) is a few picoseconds, and it is rapidly converted to  $^1\text{O}_2$  ( $^1\Delta_g$ ). Since the lifetime of  $^1\text{O}_2$  ( $^1\Delta_g$ ) is several microseconds, which is significantly longer than that of  $^1\text{O}_2$  ( $^1\Sigma_g^+$ ), the  $^1\text{O}_2$  generated in vivo can be  $^1\text{O}_2$  ( $^1\Delta_g$ ). The arrows indicate the direction of the electron spin of the highest occupied molecular orbital (HOMO).

High-energy radiations, such as X- and  $\gamma$ -rays, generate radical ROS directly by the ionization of  $\text{H}_2\text{O}$  or oxygen, whereas various chemical and photochemical reactions produce  $^1\text{O}_2$  (Figure 2A), which in turn creates other ROS [8]. In the energy transfer mechanism, a photoactivated chromophore causes intersystem crossing to the triplet state, and triplet–triplet annihilation transfers part of the electronic energy to oxygen to generate  $^1\text{O}_2$  [9,10]. Since the energy of most photoactivated molecules is higher than the excitation energy of  $^1\text{O}_2$  (0.98 eV) (Figure 1),  $^1\text{O}_2$  is readily produced by endogenous chromophores activated by ultraviolet (UV) irradiation [11]. Hatz et al. showed that the lifetime of  $^1\text{O}_2$  generated by pulsed laser irradiation of a photosensitizer (5,10,15,20-tetrakis(N-methyl-4-pyridyl)-21H, 23H-phthalocyanine (TMPyP)) incorporated into the nucleus of HeLa cells is about

3  $\mu\text{s}$ . They also found that the generated  $^1\text{O}_2$  diffuses from the formation point to a sphere radius of about 100 nm [12,13]. On the other hand, Liang et al. created a system that generates organelle-specific  $^1\text{O}_2$  by irradiating 660 nm light using a photosensitizer that is locally expressed in the membrane, cytosol, endoplasmic reticulum, mitochondria, and nucleus [14]. Using this system, they observed differences in the irradiation energy required to induce cell death depending on the organelle in which the photosensitizer is expressed, as well as differences in the type of cell death (early apoptosis, necrosis, or late apoptosis) [14]. This result indicates that  $^1\text{O}_2$  generated in intracellular organelles may not spread to other organelles. These reports indicate that  $^1\text{O}_2$  generated by intracellular photosensitizers may induce cell death by oxidizing the components of the organelle containing the photosensitizer, rather than diffusing widely within the cell.

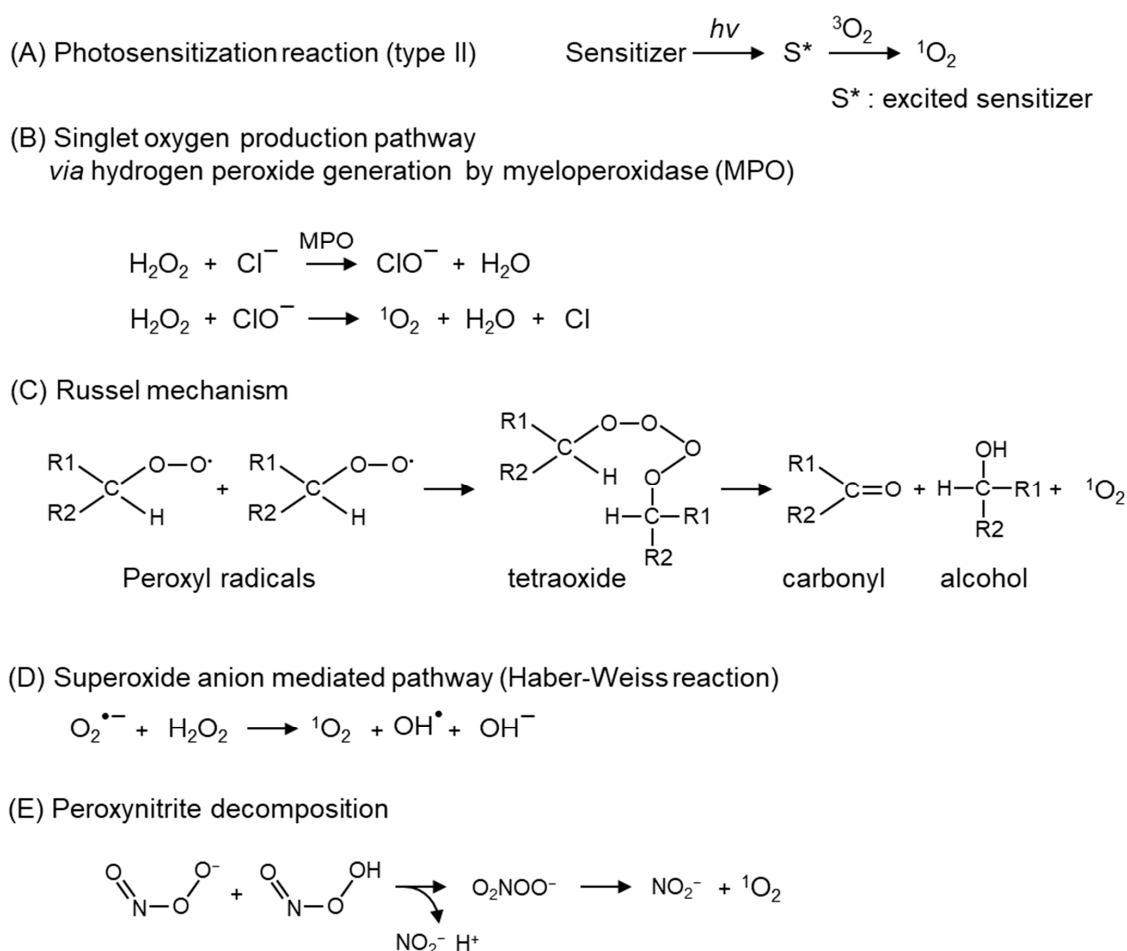


**Figure 2.** Major  $^1\text{O}_2$  production mechanisms.  $^1\text{O}_2$  production pathways; (A) photochemical reaction, (B) reactions mediated by hydrogen peroxide produced by myeloperoxidase (MPO), (C) decomposition of peroxy radicals (Russel mechanism), (D) reaction mediated by superoxide anion ( $\text{O}_2^{\bullet-}$ ), (E) pathway via peroxynitrite decomposition.

The secretion of myeloperoxidase (MPO) from phagocytes generates hypochlorite ( $\text{ClO}^-$ ), which reacts with  $\text{H}_2\text{O}_2$  to form  $^1\text{O}_2$  (Figure 2B) [15]. In leukocytes,  $^1\text{O}_2$  generated via peroxidases and nicotinamide adenine dinucleotide phosphate (NADPH) oxidase critically contributes to an antimicrobial role [16]. Another endogenous pathway of  $^1\text{O}_2$  is the degradation of lipid peroxides or  $\text{ROO}^\bullet$  via the Russel mechanism (Figure 2C) [17,18].  $\text{ROO}^\bullet$  and lipid peroxides, which are the substrates of the Russel mechanism, are derived from the peroxidation of polyunsaturated fatty acids (PUFA) by auto-oxidation and enzymatic-oxidation, such as cytochrome c, lactoperoxidase [19], and lipoxygenases [20]. In addition, the light-independent generation pathways of  $^1\text{O}_2$  include reactions involving

$O_2^{\bullet-}$  (Figure 2D) [21], peroxyxynitrite (Figure 2E) [22,23], and ozone [24–26]. Atmospheric particulates also catalyze the  $^1O_2$  generation [27,28].

### 3. Damage to Biomolecules by $^1O_2$ -Mediated Oxidation

Notably, because  $^1O_2$  has electrophilic properties, it attacks the  $\pi$ -bonds of the compound to form hydroperoxide by the ene reaction or endoperoxide by the 1,4-addition reaction (Figure 3A).  $^1O_2$  oxidatively modifies biomolecules, such as amino acids (Figure 3B) [29,30], nucleic acids (Figure 3C) [31,32], and lipids (Figure 3D) [33,34], either by a direct reaction or by the induction of ROS.

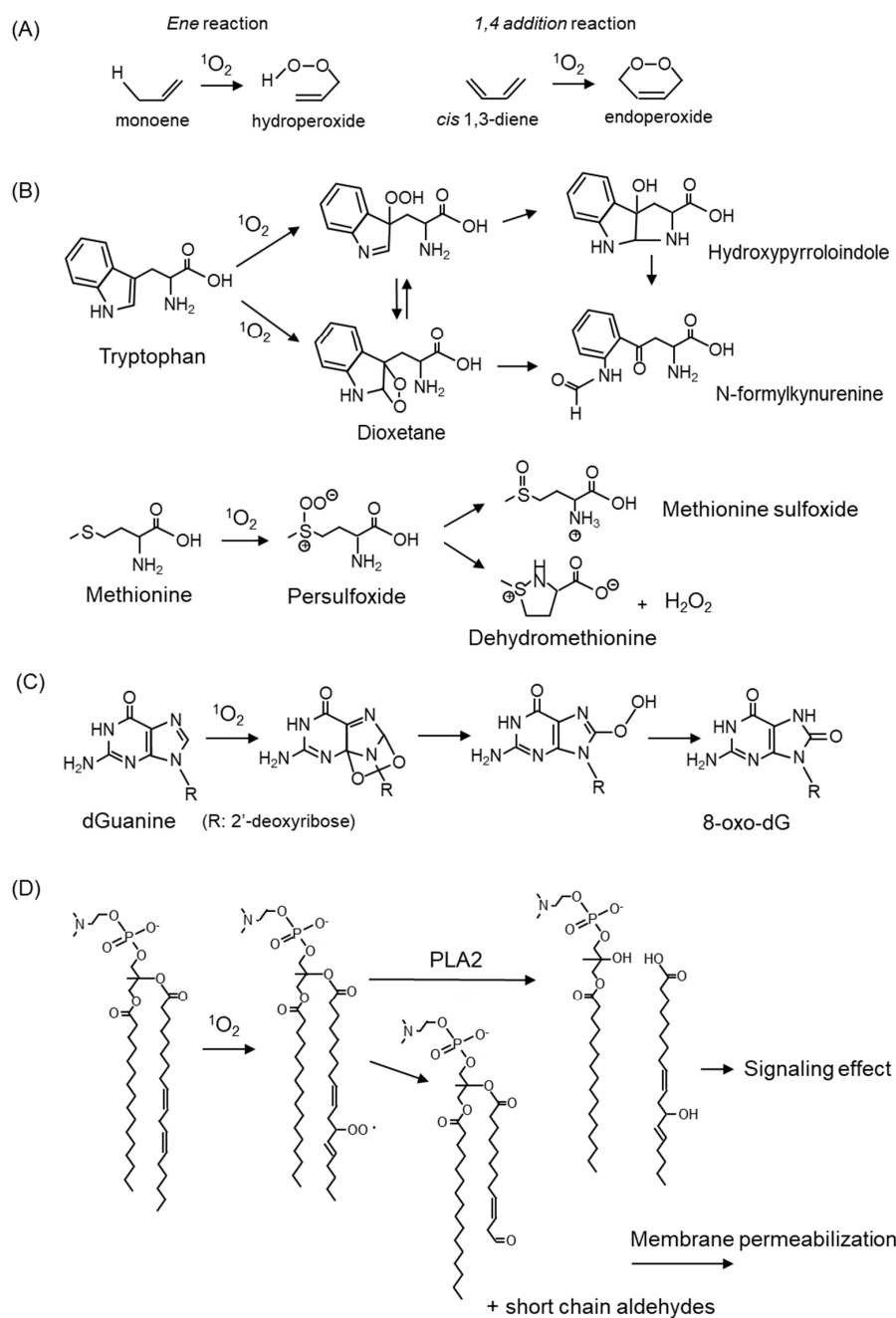


**Figure 3.**  $^1O_2$ -mediated oxidation of amino acid, nucleic acid, and lipids. (A) Oxygenation reaction by  $^1O_2$ . (B) Reaction products of tryptophan and methionine with  $^1O_2$ . (C) Formation of 8-oxo-2'-deoxyguanosine (8-oxo-dG) by  $^1O_2$  oxidation to deoxyguanosine (dG). (D) Oxidative modification of fatty acids in membrane phospholipids by  $^1O_2$ .

Amino acids, which are components of proteins, are the targets of  $^1\text{O}_2$ . Among the 20 natural amino acids, tryptophan, histidine, tyrosine, and the sulfur-containing amino acids cysteine and methionine, are susceptible to reaction with  $^1\text{O}_2$  because of their structural properties. The reaction products of tryptophan and methionine with  $^1\text{O}_2$  are shown in Figure 3B. Tryptophan reacts with  $^1\text{O}_2$  to form a hydroperoxide at the C3 position as an intermediate, which undergoes ring closure to form hydroxypyrroloindole, and finally, N-formylkynurenine [35]. Tryptophan reacts with  $^1\text{O}_2$  to form C2-C3 cross-linked dioxetanes as intermediates, followed by the conversion to N-formylkynurenine [35]. Methionine reacts with  $^1\text{O}_2$  to form methionine sulfoxide and the cyclic product dehydromethionine via a persulfoxide intermediate [30]. Oxidative modifications to amino acids cause alterations in protein properties, resulting in cellular damage accompanied by reduced enzyme activity and disruption of the cell structure.

$^1\text{O}_2$  reacts specifically with the guanine portion of DNA bases converting to 7,8-dihydro-8-oxo-2'-deoxy-guanin (8-oxo-dG) (Figure 3C) [36]. 8-oxo-dG is a potential mutagenic substance because it pairs with adenine to cause a G  $\rightarrow$  T transversion, and it is widely recognized as one of the indicators for evaluating oxidative DNA damage [37]. The details are discussed below in Section 5.1.4. on skin cancer.

Phospholipids in the membrane react with  $^1\text{O}_2$ , resulting in the oxidative modification of fatty acids (Figure 3D). Oxidized fatty acids are cleaved and serve as signaling molecules involved in carcinogenesis and skin aging. The cleavage of short-chain aldehydes from fatty acids also results in membrane instability and increased permeability. The oxidation products derived from linoleic acid and cholesterol by  $^1\text{O}_2$  are described below.

$^1\text{O}_2$  also oxidatively modifies steroids [38], vitamins [39,40], carbohydrates, terpenes [41], and flavonoids [42]. In addition,  $^1\text{O}_2$  contributes to the stimulation of stress-activated kinases and the regulation of gene expression [43].

#### 4. Detection Methods of $^1\text{O}_2$ In Vivo and In Vitro

The oxidative modification of biomolecules by  $^1\text{O}_2$  has been related in several diseases, including skin and eye diseases [44]. The development of methods to precisely detect and quantify  $^1\text{O}_2$  contributes not only to an understanding of its roles in physiological and pathological conditions, but also in cancer therapy, by understanding the mechanism of PDT. Detection methods for  $^1\text{O}_2$  have been developed to verify  $^1\text{O}_2$  production in living systems [45]. The detection of  $^1\text{O}_2$  is mainly performed using the following methods: spectroscopic measurement of near-infrared (NIR) luminescence [46,47], electron spin resonance (ESR) with sterically hindered amine [48,49], fluorescence measurement by reaction with fluorescence probes [50,51], and the measurement of oxidation products produced by the reaction of  $^1\text{O}_2$  with biomolecules [52,53]. These methods were utilized for in vitro and in vivo experiments.

##### 4.1. Direct Detection of $^1\text{O}_2$

The measurement of  $^1\text{O}_2$  NIR luminescence is a reliable method for the direct spectroscopic detection of  $^1\text{O}_2$ , as  $^1\text{O}_2$  emission (1270 nm) can be excited by an argon laser [54]. This luminescence emission was first used for the time-resolved detection of  $^1\text{O}_2$  in solution by Krasnovsky in 1976. This measurement method has been used as a standard technique for  $^1\text{O}_2$  formation yields, lifetimes, and deactivation constants in various solutions. The in vivo detection of  $^1\text{O}_2$  luminescence has been attempted previously, and it has been reported that  $^1\text{O}_2$  in a suspension of leukemia cells [55,56] and red cell ghost [57] can be detected using a sophisticated near-infrared photomultiplier device. However, this luminescence signal is weak because the inactivation of  $^1\text{O}_2$  is dominated by nonradiative pathways; typical phosphorescence yields are of the order of  $10^{-5}$  to  $10^{-7}$  [58]. In addition, these methods require the usage of deuterium oxide ( $\text{D}_2\text{O}$ ) to extend the lifetime of  $^1\text{O}_2$  and remove the 1270 nm emission absorption due to  $\text{H}_2\text{O}$  [59]. This difficulty in detecting  $^1\text{O}_2$  in vivo can be attributed to the short lifetime of  $^1\text{O}_2$  in cells and tissues and the lack of sufficient sensitive detectors at NIR wavelengths.

ESR spectroscopy, which has been proposed for paramagnetic materials and organic compounds with unpaired electrons, has been used for the detection of free radicals [60]. To detect  $^1\text{O}_2$ , a method was developed for measuring nitroxide radicals produced by the reaction of  $^1\text{O}_2$  with sterically hindered secondary amine probes such as 2,2,6,6-tetramethylpiperidine (TEMP) (Figure 4A) [61–63] and hydroxy-TEMP (Figure 4B) [64]. This method has been applied to the *in vitro*  $^1\text{O}_2$  scavenging activity of various substances in solution, and there is considerable evidence demonstrating the  $^1\text{O}_2$  scavenging effects of various substances using this method [48,65,66]. However, ESR spectroscopy is not considered suitable for the detection of intracellular  $^1\text{O}_2$ , which may be because the time resolution in ESR measurements is not suitable for the short lifetime of  $^1\text{O}_2$  in cells existing in  $^1\text{O}_2$  quenching molecules.

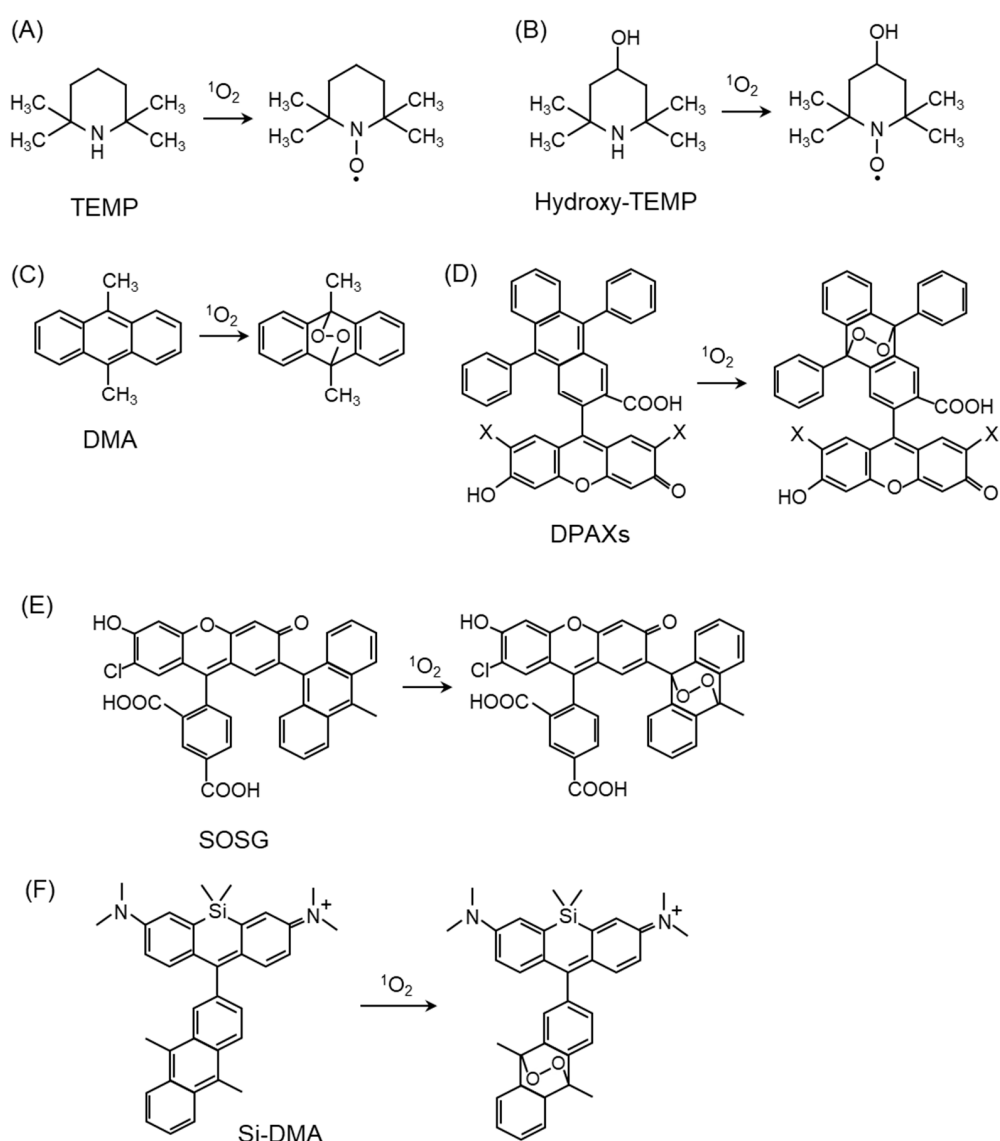


**Figure 4.** Structures and oxidation modification of probes for  $^1\text{O}_2$  detection. (A) 2,2,6,6-tetramethylpiperidine (TEMP), (B) Hydroxy-TEMP, (C) 9,10-dimethylanthracene (DMA), (D) 9-[2-(3-Carboxy-9,10-diphenyl)anthryl]-6-hydroxy-3H-xanthen-3-ones (DPAXs), (E) Singlet Oxygen Sensor Green (SOSG), (F) silicone-containing rhodamine-9,10-dimethylanthracene (Si-DMA).

#### 4.2. $^1\text{O}_2$ Detection by Fluorescent Probes

Fluorescent probes are excellent sensors for the detection of ROS because of their high sensitivity, simplicity of data acquisition, and high spatial resolution in microscopic imaging [67–69]. Fluorescent probes, including 9,10-dimethylanthracene (DMA) (Figure 4C) [68,70,71] and 9-[2-(3-Carboxy-9,10-diphenyl)anthryl]-6-hydroxy-3H-xanthen-3-ones (DPAXs) (Figure 4D) [72], have been developed for the detection of  $^1\text{O}_2$  in neutral or basic aqueous solutions. These probes react specifically and rapidly with  $^1\text{O}_2$  to form stable endoperoxides with a high rate constant. Singlet Oxygen Sensor Green (SOSG) (Figure 4E) is a fluorescent probe for in vitro detection because of its high  $^1\text{O}_2$  selectivity [73–75]. To apply fluorescence probes in biological samples, the probes must penetrate the cell membrane and be localized in the cell. Recently, a far-red fluorescent probe consisting of DMA and silicon-containing rhodamine (Si-rhodamine) moieties, namely Si-DMA (Figure 4F), was developed for detecting  $^1\text{O}_2$  in the mitochondria. The advantages of Si-DMA are its cell-permeable ability and increased sensitivity to specifically detect mitochondrial  $^1\text{O}_2$  by the Si-rhodamine moiety [76]. It is important to precisely measure intracellular  $^1\text{O}_2$  generation to clarify the characteristics of fluorescence probes in terms of their signal-to-noise ratio and dynamic changes. We have demonstrated that intracellular  $^1\text{O}_2$  can be quantitatively measured using Si-DMA in living cells, as time-lapse imaging using Si-DMA provides an apparent signal-to-noise ratio in the treatments of a  $^1\text{O}_2$  generator and quencher [77]. Other fluorescent probes have been used to detect intracellular  $^1\text{O}_2$  using nanoparticles, including SOSG-based nanoprobe [50], super-pH-resolved nanosensors encoding SOSG [78], and biocompatible polymeric nanosensors encapsulating SOSG within their hydrophobic core [79]. The use of these fluorescence probes will improve our understanding of the  $^1\text{O}_2$  generation mechanism and the biological function of  $^1\text{O}_2$  in the physiological and pathological conditions of cultured cells.

#### 4.3. Detection of $^1\text{O}_2$ -Mediated Peroxidation Products

$^1\text{O}_2$  generated in vivo quickly reacts with biomolecules, including lipids, proteins, and nuclei, and the subsequent comparatively stable oxidized products remain in the  $^1\text{O}_2$  generation site. This chemical property has been used for the development of in vivo ROS detection methods, and these oxidation products are widely used as oxidative stress biomarkers because they can be detected stably and correlate with oxidative stress status in vivo [80,81].

The oxidation product of linoleic acid, hydroxyoctadecadienoic acid (HODE), contains six isomers.  $^1\text{O}_2$  reacts with molecules containing double bonds to form hydroperoxides as primary products, which are subsequently reduced to hydroxides (Figure 5).  $^1\text{O}_2$  produces 9-, 10-, 12-, and 13-(Z,E)-hydroperoxyoctadecadienoic acid (HPODE) from linoleates; however, only 10- and 12-(Z,E)-HPODE are specific products by  $^1\text{O}_2$  because 9- and 13-(Z,E)-HPODE are also formed by both free radical- and enzyme-mediated oxidation. The chemical structures of 10- and 12-(Z,E)-HPODE differ significantly from those of 9- and 13-(Z,E)-HPODE: the latter contains a conjugated diene, while the former does not. These structural features cause differences in physiological functions; for example, 10- and 12-(Z,E)-HODE cause adaptive responses to UV-derived oxidative damage in cultured cells, whereas 9- and 13-(Z,E)-HODE do not [82,83].

Cholesterol is an important lipid that constitutes biological membranes and undergoes oxidative modification to produce 7-, 24-, and 27-hydroxycholesterol. Cholesterol, as well as unsaturated fatty acids, are substrates for the oxidative reaction of  $^1\text{O}_2$ . When  $^1\text{O}_2$  reacts with cholesterol, it forms 5 $\alpha$ -hydroperoxide (cholesterol 5 $\alpha$ -OOH), 6 $\alpha$ -hydroperoxide (cholesterol 6 $\alpha$ -OOH), and 6 $\beta$ -hydroperoxide (cholesterol 6 $\beta$ -OOH) (Figure 6). Cholesterol 5 $\alpha$ -OOH is produced in larger amounts than 6 $\alpha$ /6 $\beta$ -OOH. Therefore, cholesterol 5 $\alpha$ -OOH could be used as a biomarker for oxidative reactions involving  $^1\text{O}_2$  in vivo. Furthermore, the Hock cleavage of cholesterol 5 $\alpha$ -OOH converts to cholesterol 5,6-secosterol. Cholesterol 5,6-secosterol, also called ateronal, is involved in the development of cardiovascular diseases [84] and neurodegeneration [85].

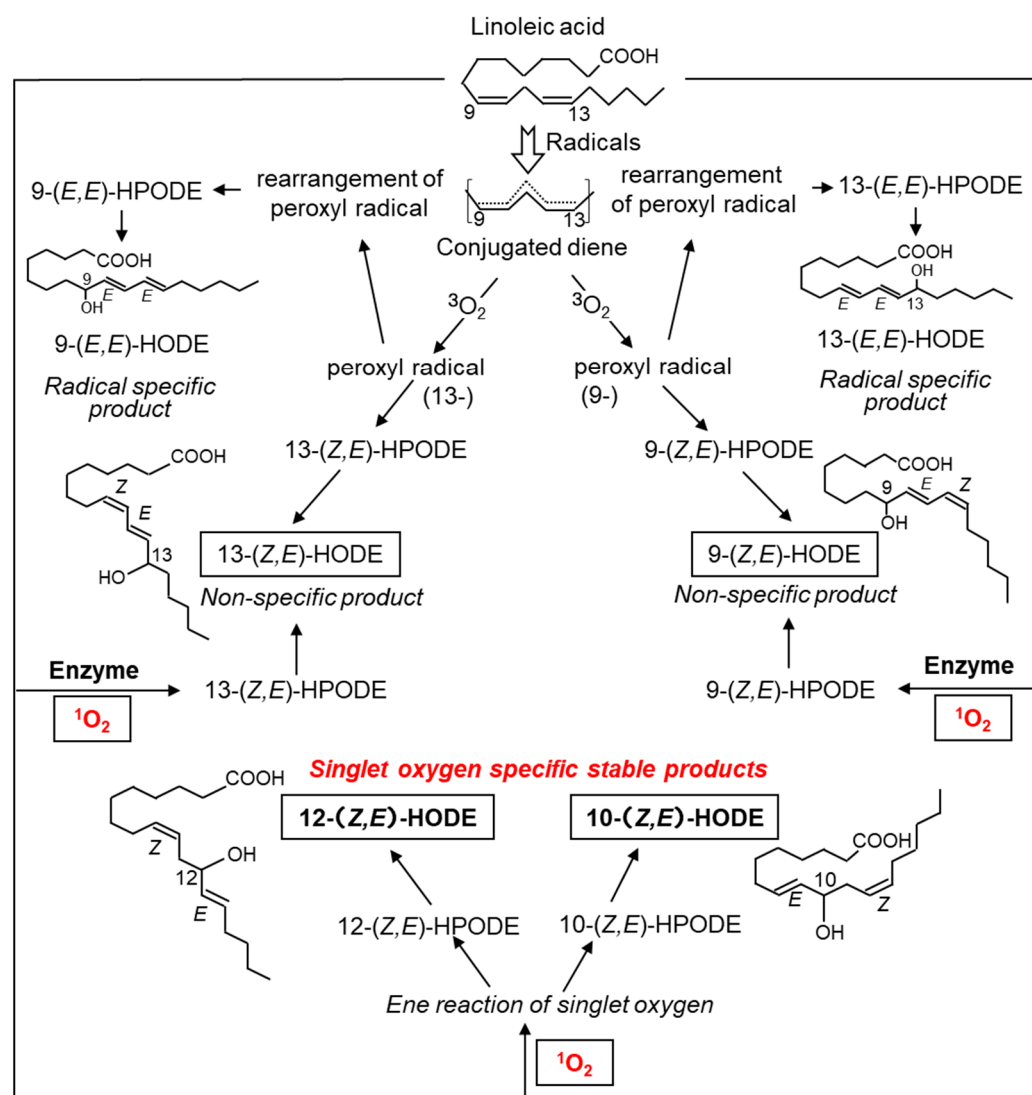


**Figure 5.** Structures and formation mechanism of hydroxyoctadecadienoic acid (HODE), an oxidation product derived from linoleic acid.  $^1O_2$  oxidizes linoleic acid to produce 13-(Z,E)-HODE, 9-(Z,E)-HODE, 12-(Z,E)-HODE, and 10-(Z,E)-HODE. 13-(Z,E)-HODE and 9-(Z,E)-HODE are also produced by ROS other than  $^1O_2$  and by enzymatic oxidation reactions via lipid oxidases. 9-(E,E)-HODE and 13-(E,E)-HODE are produced in a radical-specific manner.

We have developed a method to comprehensively measure lipid peroxidation and proposed the measurement of HODEs and hydroxycholesterol [86–91]. In this method, lipid components are extracted from biological samples after reduction and saponification. These pretreatments result in the measurement of both free and esterified forms of hydroperoxides and hydroxides as free hydroxides. HODEs and hydroxycholesterol are analyzed by liquid chromatography–tandem mass spectrometry (LC-MS/MS) and gas chromatography–mass spectrometry (GC-MS), respectively. Biological samples to be measured with this method include plasma, urine, erythrocytes, as well as cultured cells and tissues. This method allows for the measurement of not only radical-mediated oxidation products, but also  $^1O_2$ -specific oxidation products using the HODEs isomer as an indicator [89–91], in other words, indirect in vivo  $^1O_2$  detection is possible. We have determined the relationship between  $^1O_2$ -mediated oxidation and the early diagnosis of diabetes in humans and mice based on the production of 10- and 12-(Z,E)-HODEs [83,92,93], which will be discussed in more detail later.  $^1O_2$  measurements using 10- and 12-(Z,E)-HODEs as indicators can

evaluate  $^1\text{O}_2$  generation not only in living cells, but also in humans and animals in vivo, and they can precisely analyze the involvement of  $^1\text{O}_2$  generation and diseases.

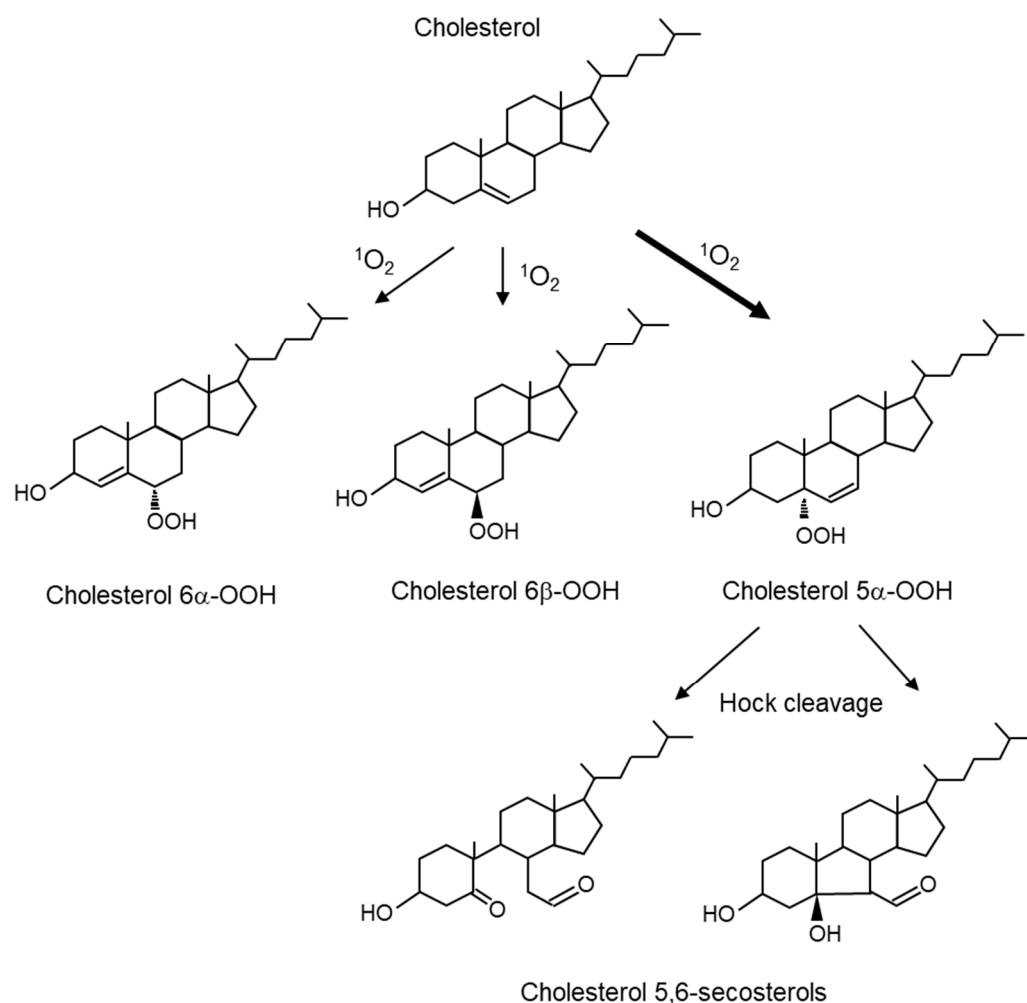


**Figure 6.** Structures of cholesterol peroxides produced by  $^1\text{O}_2$ -mediated oxidation reactions.  $^1\text{O}_2$  oxidizes cholesterol to produce 5 $\alpha$ -hydroperoxide (cholesterol 5 $\alpha$ -OOH), 6 $\alpha$ -hydroperoxide (cholesterol 6 $\alpha$ -OOH), and 6 $\beta$ -hydroperoxide (cholesterol 6 $\beta$ -OOH). Hock cleavage of cholesterol 5 $\alpha$ -OOH converts it to cholesterol 5,6-secosterols.

While ESR and fluorescent probes are useful for detecting  $^1\text{O}_2$  in vitro and in cells, it is difficult to use these tools to assess the degree of damage caused by  $^1\text{O}_2$  in tissues. Therefore, it is better to measure oxidation products that are relatively stable and retained in biological samples. Table 1 summarizes the methods for measuring  $^1\text{O}_2$  itself or its oxidation products and both their advantages and disadvantages. Table 2 summarizes reports of the measurements of linoleic acid- or cholesterol-derived oxidation products produced by  $^1\text{O}_2$ -mediated oxidation reactions in human and animal samples.  $^1\text{O}_2$ -derived lipid oxidation products have been measured in the blood and tissue samples obtained from patients with borderline diabetes, glaucoma, alcoholism, and atherosclerosis. In animal experiments, cholesterol 5 $\alpha$ -hydroperoxide in the skin tissue was measured following UVA irradiation in mice. These results are important to understand the contribution of  $^1\text{O}_2$  to the pathogenesis of various disorders.

**Table 1.** Characterization of  $^1\text{O}_2$  detection methods in vivo and in vitro.

Detection Method of $^1\text{O}_2$	Principle	Pros/Cons	Ref.
Near-infrared luminescence	$^1\text{O}_2$ emission at 1270 nm	<ul style="list-style-type: none"> <li>• A standard technique for the <math>^1\text{O}_2</math> yields, lifetimes, and deactivation constants in vitro.</li> <li>• Weak signal (phosphorescence yields are of the order <math>10^{-5}</math> to <math>10^{-7}</math>)</li> <li>• Requirement of deuterium oxide (<math>\text{D}_2\text{O}</math>) for longer lifetime</li> </ul>	[54,57–59]
ESR spectroscopy	Measurement of nitroxide radicals produced by the reaction of $^1\text{O}_2$ with sterically hindered secondary amine probes	<ul style="list-style-type: none"> <li>• Applied for in vitro <math>^1\text{O}_2</math> scavenging activity in solution</li> <li>• Time resolution is longer for the short lifetime of <math>^1\text{O}_2</math> in cells</li> </ul>	[48,60,61,65,66]
Fluorescent probes 9,10-dimethylanthracene (DMA)		<ul style="list-style-type: none"> <li>• Detection of <math>^1\text{O}_2</math> in neutral or basic aqueous solutions</li> </ul>	[67–69]
9-[2-(3-Carboxy-9,10-diphenyl)anthryl]-6-hydroxy-3H-xanthen-3-ones (DPAXs)		<ul style="list-style-type: none"> <li>• React rapidly with <math>^1\text{O}_2</math> in a high rate constant</li> <li>• Impermeable cell membrane</li> </ul>	[68,70–72]
Singlet Oxygen Sensor Green (SOSG)	React with $^1\text{O}_2$ and form stable endoperoxides with high-fluorescence quantum yield (high sensitivity,	<ul style="list-style-type: none"> <li>• Commercially available highly selective <math>^1\text{O}_2</math> indicator</li> <li>• Impermeable cell membrane</li> </ul>	[73–75]
SOSG-based nanosensors NanoSOSG SPR-SOSG PAM-SOSG	simplicity of data acquisition, and high spatial resolution in microscopic imaging)	<ul style="list-style-type: none"> <li>• Using nanoparticles for detection of intracellular <math>^1\text{O}_2</math></li> <li>• Permeable cell membrane</li> <li>• Visualization of <math>^1\text{O}_2</math> signal at the subcellular level</li> </ul>	[50,78,79]
Si-DMA		<ul style="list-style-type: none"> <li>• Cell-permeable and localization of mitochondria</li> <li>• Specifically detect mitochondrial <math>^1\text{O}_2</math></li> <li>• Relatively quantitative</li> </ul>	[76,77]
$^1\text{O}_2$ -mediated peroxidation products			
10- and 12-(Z,E)-HODEs	Products mediated by the reaction of $^1\text{O}_2$ with linoleic acid	<ul style="list-style-type: none"> <li>• Relatively stable</li> <li>• Abundant in living organisms (cell membrane)</li> <li>• Can be used to evaluate in vivo oxidative damage</li> </ul>	[83,89–93]
Cholesterol 5 $\alpha$ -OOH Cholesterol 6 $\alpha$ -OOH Cholesterol 6 $\beta$ -OOH	Products mediated by the reaction of $^1\text{O}_2$ with cholesterol	<ul style="list-style-type: none"> <li>• Relatively stable</li> <li>• Can be used to evaluate in vivo oxidative damage</li> </ul>	[52]

**Table 2.** Report on the results of the determination of linoleic acid- or cholesterol-derived peroxides produced by  $^1\text{O}_2$ -mediated oxidation reactions using human and animal samples.

$^1\text{O}_2$ -Mediated Oxidation Product	Sample Species	Disease/Model	Ref.
10- and/or 12-(Z,E)-HODE	Human	Borderline diabetes/oral glucose tolerance test	[92,93]
	Human	High serum levels in patients with primary open-angle glaucoma	[94]
	Pig	Increased by kidney tissue damage	[95]
	Mouse	High in the plasma of model mice with prediabetes	[83,96]
	Mouse	Increased in the lungs of model mice with asthma and positively correlated with MPO activity and nerve growth factor (NGF)	[97]
Cholesterol 5 $\alpha$ -hydroperoxide	Human	Alcoholic patients	[98]
	Rat	Pheophorbide a and visible light irradiation	[99]
	Mouse	UVA irradiation of hairless mice	[100]
	Mouse	Effect of beta-carotene on UVA irradiation of hairless mice	[101,102]
Cholesterol 5,6-secosterol	Human	Cholesterol 5,6-secosterol detected in atherosclerotic plaques	[103]
	Human	Cortex in patients with Alzheimer's disease	[104]
	Rat	Higher in the plasma of amyotrophic lateral sclerosis (ALS) rats than before disease onset	[85]

## 5. Diseases Involving $^1\text{O}_2$ and Their Pathophysiology

### 5.1. Skin Diseases

The skin is the organ with the largest area exposed to sunlight. The skin is regularly exposed to sunlight and is at a high risk of oxidative stress. UV radiation from the sun generates ROS in keratinocytes, the major cells of the epidermis and the outermost layer of the skin [105]. UV exposure also increases the activities of cyclooxygenase and lipoxygenase, which produce eicosanoids from arachidonic acid. UV exposure of the skin causes erythema and acute inflammation, and long-term UV exposure causes photo-carcinogenesis [106] and skin aging [107]. Lipid oxidation on the skin surface is important in relation to sunburn, hyperpigmentation, wrinkle formation, freckles, atopic dermatitis, acne, and skin cancer.

UVA (320–400 nm) penetrates the dermis, whereas UVB (280–320 nm) only attacks the epidermis. Both UVA and UVB produce ROS and free radicals in the presence of photosensitizers (Figure 7). In type I reactions, an excited photosensitizer reacts with an organic compound to produce  $\text{O}_2^{\bullet-}$  and lipid peroxy radical ( $\text{LOO}^\bullet$ ). In a type II reaction, the excited photosensitizer reacts with a triplet oxygen molecule, producing  $^1\text{O}_2$  primarily by energy transfer and, to a minor extent,  $\text{O}_2^{\bullet-}$  by electron transfer.

#### 5.1.1. Photosensitizers

Porphyryns such as protoporphyrin IX (Figure 8A) [108] have been examined as endogenous photosensitizers, and their derivatives [8] and 5-aminolevulinic acid [109], a component of porphyryns, have been investigated for application as PDT in therapeutic modalities against diseases such as cancer. Interestingly, coproporphyrin (Figure 8B) produced by *Propionibacterium acnes*, an acne-causing bacterium, also acts as a photosensitizer and generates  $^1\text{O}_2$ , which is associated with skin inflammation [110,111]. Hemin (Figure 8C) [112] and chlorophyll (Figure 8D) [113], which are metal complexes of porphyrin and similar compounds, also exhibit photosensitizing effects. Hemin is an iron-containing protoporphyrin IX, and chlorophyll is a chemical responsible for absorbing light energy in the light reaction of photosynthesis. Pheophytin (Figure 8E), from which magnesium ions are removed during chlorophyll degradation, and pheophorbide (Figure 8F), from which the phytol group is eliminated from pheophytin, also act as photosensitizers [114,115].

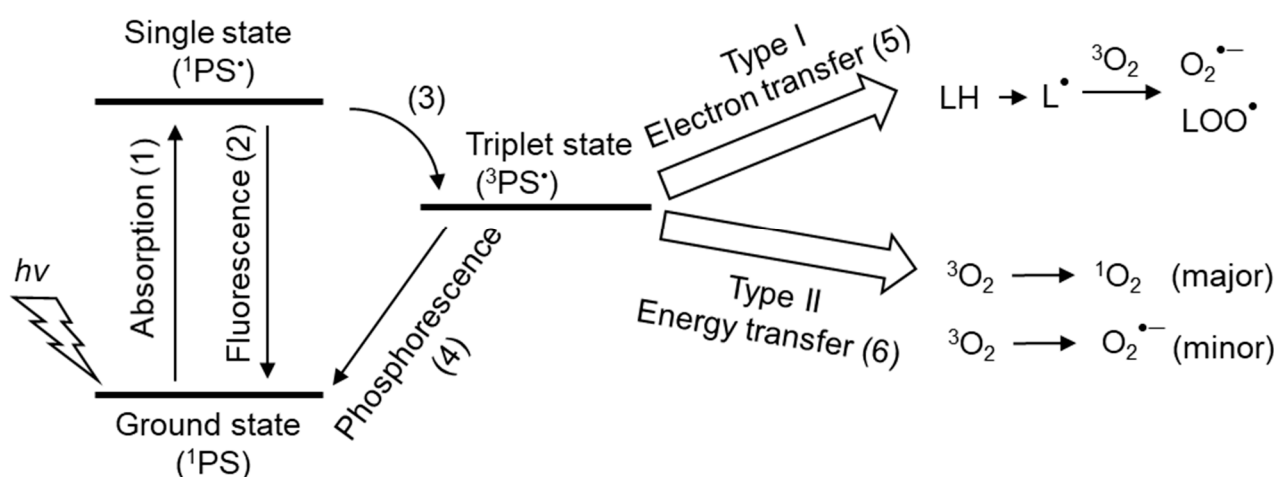


**Figure 7.** Photosensitizers and the mechanisms of  $^1O_2$  production. (1) Photosensitizers (PS) absorb photons ( $h\nu$ ) from light and transform them to the excited singlet state ( $^1PS^*$ ). (2)  $^1PS^*$  returns to the ground singlet state ( $^1PS$ ) by losing energy via fluorescence emission. (3)  $^1PS^*$  was converted to the long-lived triplet state ( $^3PS^*$ ). (4)  $^3PS^*$  can return to the ground singlet state ( $^1PS$ ) via light emission (phosphorescence). (5)  $^3PS^*$  forms organic radicals ( $L^\bullet$ ) from organic compounds (LH) through the transfer of electrons in the type I photochemical reaction.  $L^\bullet$  affects oxygen ( $^3O_2$ ) to produce ROS (superoxide anion  $O_2^{\bullet-}$ , lipid peroxyl radical ( $LOO^\bullet$ )).  $O_2^{\bullet-}$  leads to the production of  $H_2O_2$  and hydroxyl radicals ( $OH^\bullet$ ), resulting in the induction of radical chain reactions. (6) In type II photochemical reactions, the energy of  $^3PS^*$  is transferred to  $^3O_2$  to mainly produce  $^1O_2$ , but  $O_2^{\bullet-}$  is produced as a minor product via electron transfer from  $^3PS^*$ .

In addition to porphyrins, tryptophan and tryptophan metabolites (kynurenine and 3-hydroxykynurenine) (Figure 8G) [116] and riboflavin (Figure 8H) [117,118] are endogenous photosensitizers. Riboflavin, a water-soluble vitamin B2, is distributed in the skin, eyes, brain, and blood vessels and increases the production of  $^1O_2$ . Cholesta-5,7,9(11)-trien-3 $\beta$ -ol (9-DDHC) (Figure 8I), a metabolite of 7-dehydrocholesterol (7-DHC), is a photosensitizer involved in rare cholesterol metabolism disorders [119]. Psoralen (Figure 8J), found in citrus fruits, is a dietary photosensitizer that causes photosensitivity [120,121].

#### 5.1.2. Lipids in the Skin and Lipid Peroxidation Products Mediated by $^1O_2$

The lipid composition of the epidermis is a mixture of free fatty acids, ceramide, and cholesterol at approximately 30–35% each [122]. The fatty acids in the epidermis include linoleic acid (21%), oleic acid (15%), palmitic acid (14%), stearic acid (11%), and arachidonic acid (6%) [123]. In contrast, the lipid composition of sebum is triacylglycerol (45–50%), wax ester (25%), squalene (Sq) (12%), and free fatty acids (10%) [122]. The fatty acid composition of sebum is palmitic acid (22%), palmitoleic acid (21%), oleic acid (15%), myristic acid (12%), and myristoleic acid (5%) [124]. The lipid composition of the sebum differs significantly from that of the epidermis.

Squalene (Sq) is a triterpene compound characteristically present in sebum, and six Sq monohydroperoxides (2-, 3-, 6-, 7-, 10-, and 11-OOH-Sq) are produced in similar amounts by the peroxidation of  $^1O_2$  (Figure 9) [125]. In contrast, 2- and 3-OOH-Sq were recently reported to be produced by free radical oxidation [125]. Considering these results, 6-, 7-, 10-, and 11-OOH-Sq may be the specific products of  $^1O_2$ . SqOOHs are also associated with wrinkle formation [126] and inflammatory acne [127]. As SqOOHs are unstable, further photooxidation was revealed to produce 2-OOH-3-(1,2-dioxane)-Sq (Figure 9) as a secondary oxidation product [128]. SqOOH concentrations in sebum collected from skin exposed to tobacco heating products or electronic cigarette aerosols are lower than that in sebum from skin exposed to tobacco smoke, indicating consumer hygiene and cosmetic benefits [129].

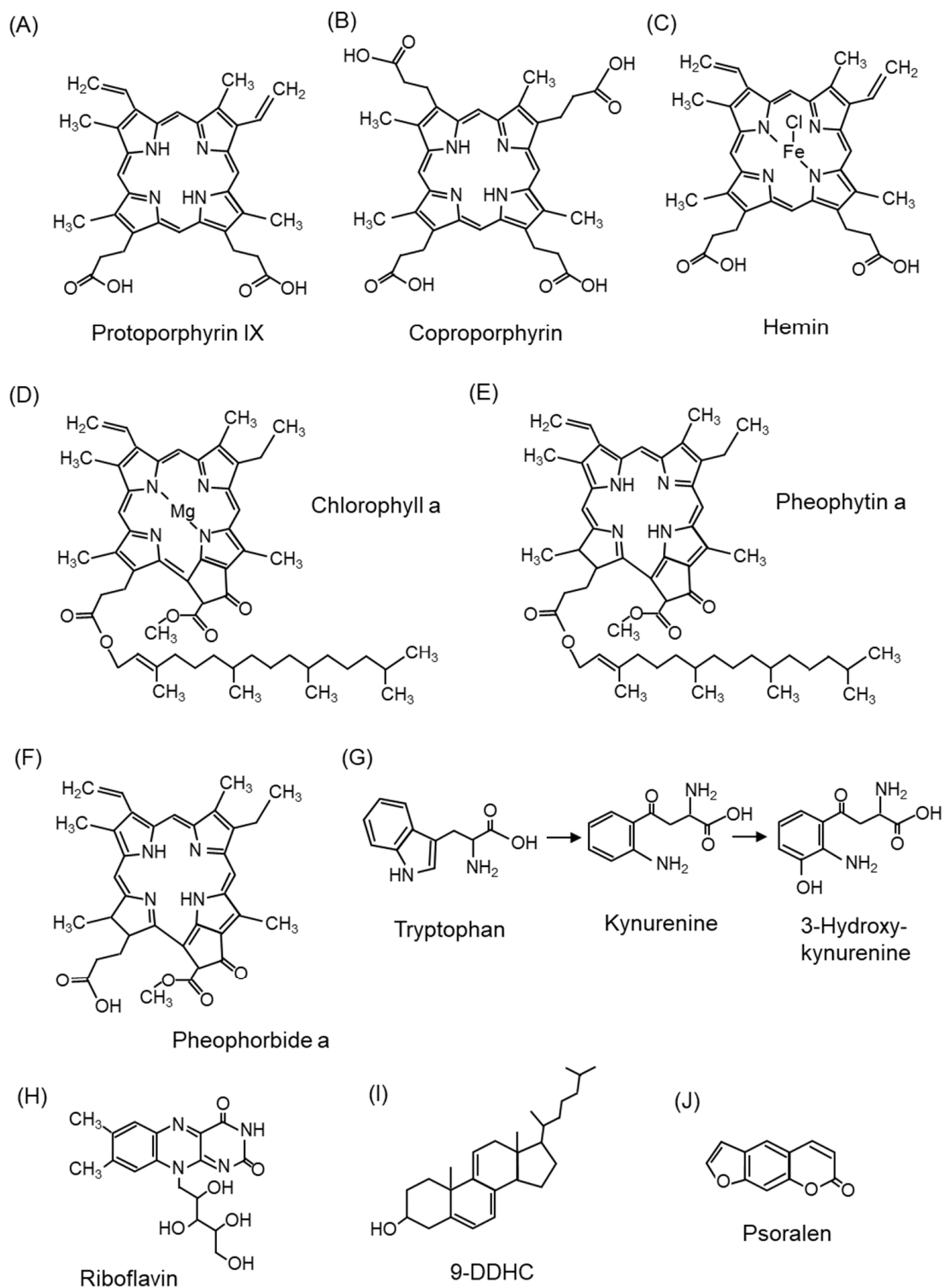


**Figure 8.** The structures of photosensitizers. (A) Protoporphyrin IX, (B) coproporphyrin, (C) hemin, (D) chlorophyll a, (E) pheophytin a, (F) pheophorbide a, (G) tryptophan, (H) riboflavin, (I) cholesta-5,7,9(11)-trien-3beta-ol (9-DDHC), (J) psoralen.

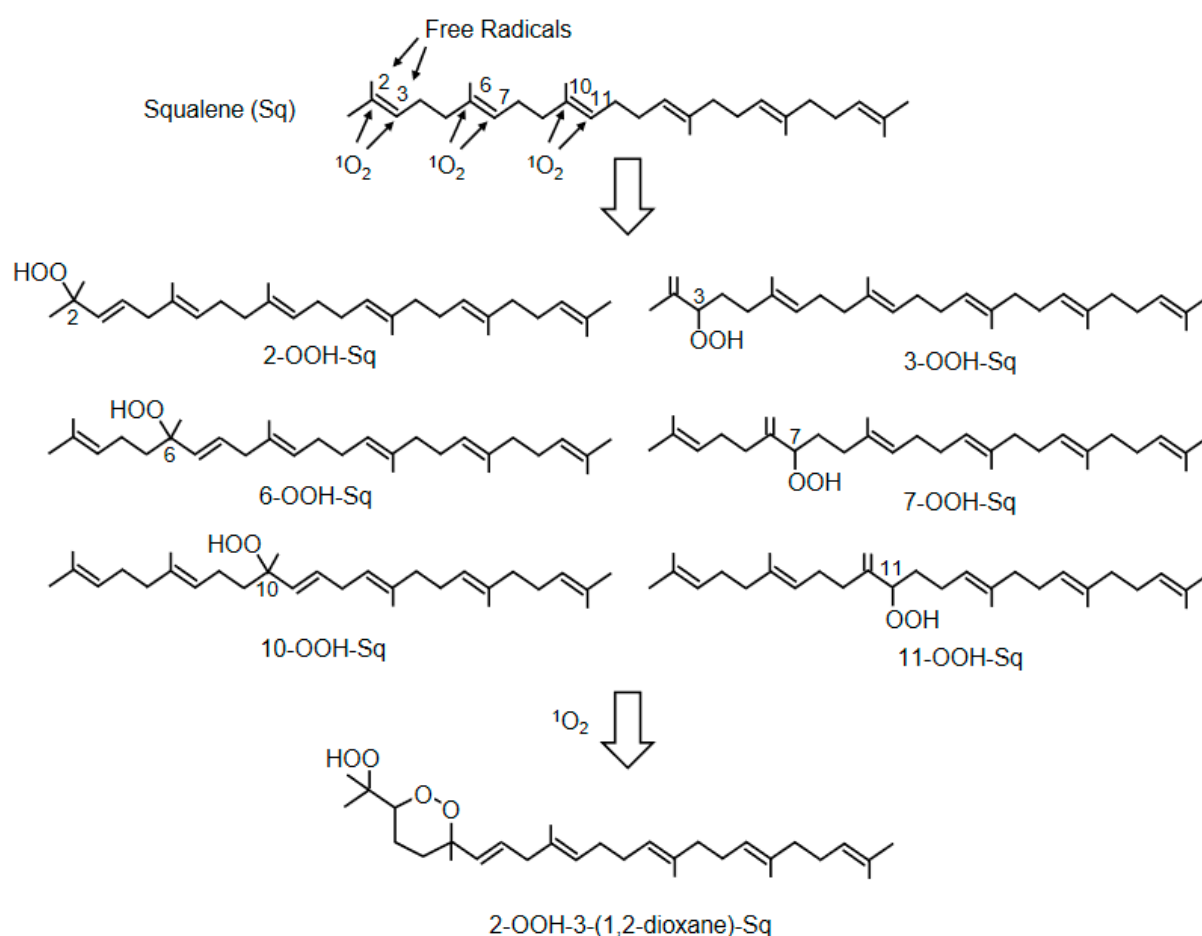


**Figure 9.** The structures of squalene and its peroxidation products. Squalene (Sq) is converted by  $^1\text{O}_2$  to six monohydroperoxides (2-, 3-, 6-, 7-, 10-, and 11-OOH-Sq). The monohydroperoxides of Sq are further photo-oxidized to 2-OOH-3-(1,2-dioxane)-Sq.

Table 3 shows the results of SqOOH measurements in human and animal sebum samples. The fact that SqOOHs, which are specifically produced by  $^1\text{O}_2$ , can be detected using sebum, which can be collected without severe invasion, makes it possible to assess the effects of pollutants, sunlight, and UV. In the future, techniques for the measurement of the SqOOH content in sebum could be further developed in the field of skin diseases, including cosmetology.

As mentioned above,  $^1\text{O}_2$  peroxidation products from cholesterol are caused by ene reactions to 5,6 double bonds to form cholesterol 5 $\alpha$ -OOH, 6 $\alpha$ -OOH, and 6 $\beta$ -OOH (Figure 6). However, cholesterol 5 $\alpha$ -OOH is more abundant than cholesterol 6 $\alpha$ - and 6 $\beta$ -OOH [52].

PUFAs in the skin are also target molecules for peroxidation by  $^1\text{O}_2$ . UVA irradiation of hairless mice has also been reported to increase 10-HPODE and 12-HPODE levels (Figure 5), which are  $^1\text{O}_2$ -specific lipid hydroperoxides of linoleic acid [130].

**Table 3.** Report on the results of the determination of squalene-derived peroxides produced by oxidation reactions mediated by  $^1\text{O}_2$  using human and animal samples.

$^1\text{O}_2$ -Mediated Oxidation Product	Sample Species	Disease/Model	Ref.
Squalene monohydroperoxides	Human	Increased by exposure of human skin to tobacco smoke	[131]
	Human	Sunlight exposure increases SqOOH in sebum	[132]
	Human	UV irradiation to human sebum	[133–135]
	Human	SqOOH reduction in sebum by application of cosmetics	[136]
	Human	Human skin surface lipids	[137]
	Human	Increased SqOOH in the scalp due to high dandruff	[138]
	Human	Detection using human fingerprints	[139]
	Human	Increase in SqOOH in the sebum due to ambient dust and ozone	[140]
	Human	Less SqOOH in sebum exposed to tobacco heating products and electronic cigarettes compared to cigarette smoke exposure	[129]
	Pig	Cigarette smoke exposure to pig skin	[141]
	Rabbit	UVA irradiation of rabbit ears	[127]
	Guinea pig	Carotene reduces the increase in SqOOH caused by UV irradiation of the skin	[142]
	2-OOH-3-(1,2-dioxane)-squalene	Human	Identification of cyclic peroxides of SqOOH

### 5.1.3. Skin Aging

The main clinical sign of skin aging is the dysfunction of the dermis, with ultrastructural disruption of elastic fibers [143]. This is due to an imbalance in collagen remodeling relative to proteolysis that occurs in the extracellular matrix. UVA-irradiated cultured human fibroblasts and human epidermis have been shown to induce the expression of collagenase, a protease that degrades elastic fibers in the dermis [144]. Moreover, the addition of cholesterol oxidants derived from the  $^1\text{O}_2$  oxidation reaction to mouse fibroblasts causes them to accumulate in lipid rafts, as well as upregulates matrix metalloproteinase-9 (MMP-9) activity [145]. The UVA irradiation of cells under protoporphyrin administration results in the upregulation of MMP-9 activity with the formation of cholesterol oxide [145]. This suggests that cholesterol oxidation products produced by  $^1\text{O}_2$  may alter the structure of lipid rafts, resulting in the activation of signaling pathways that induce MMP-9 expression, leading to skin aging.

### 5.1.4. Skin Cancer

DNA nucleobases are targets of oxidation reactions [44].  $^1\text{O}_2$ , as well as highly reactive  $\text{HO}^\bullet$ , are oxidants that can damage cellular DNA [146–148]. Since UVA is among the carcinogens to which organisms are exposed, it is important to understand the mechanisms that cause DNA damage [149]. UVA in sunlight is a potential source of oxidative DNA damage in the skin [150,151]. As discussed in the previous chapter, exposing skin to UVA radiation produces  $^1\text{O}_2$ . The reactivity of  $^1\text{O}_2$  to nucleobases tends to occur in the order guanine > cytosine > adenine > uracil > thymine [152].

The introduction of an oxo group into the C8 of guanine and the addition of a hydrogen atom to the nitrogen of N7 yields 8-oxo-dG (Figure 3C). The presence of 8-oxo-dG in DNA causes problems in the S phase of the cell cycle. In the S phase, cells must replicate an exact copy of the genome. Unlike most other types of DNA damage, 8-oxo-dG does not stop the replication process but rather creates a point mutation. Normally, guanine pairs with cytosine (C), whereas 8-oxo-dG mimics thymine (T), thus forming a pair with adenine (A) [153]. Furthermore, the A:8-oxo-dG mispair does not cause helix distortion in the DNA backbone, thus avoiding correction by the error detection mechanism of replication polymerase [154]. This results in mutations that are essentially C:G→A:T mutations. The presence of C:G→A:T mutations in many cancers emphasizes the importance of 8-oxo-dG in cancer pathogenesis [155]. The amount of 8-oxo-dG produced is approximately  $10^3$ /cell

per day in normal cells, but increases to  $10^5$ /cell in cancer cells [156]. 8-oxo-dG is also markedly increased in human skin cells after UVA irradiation [157]. There are reports that 8-oxo-dG is involved in photocarcinogenesis [158,159]. It has also been reported that 8-oxo-dG is increased in epidermal cells after chronic broadband UVB irradiation in Ogg1 knockout mice, which are unable to eliminate oxidized bases and are susceptible to skin cancer [160]. However, cyclobutane pyrimidine dimers observed in UV-irradiated DNA are also known to correlate with skin cancer development [161]. It is thought that DNA mutation due to  $^1\text{O}_2$  generation is not the only cause of UV-induced carcinogenesis, but that various mutagenic molecules are involved in the pathogenesis in a complex manner.

Furthermore, 8-oxo-dG has been used as a biomarker to evaluate the degree of oxidative stress, and its application has been attempted as a risk assessment for many diseases [162].

#### 5.1.5. Porphyria

Porphyria is a rare genetic disorder caused by a deficiency in any of the eight enzymes involved in the heme metabolism, resulting in the accumulation of the photosensitizing substance porphyrin or its precursors [163]. Porphyrin accumulation in the skin also causes photosensitivity, resulting in burn-like skin lesions [164]. The nine porphyria are divided into “cutaneous porphyria” and “acute porphyria”. Among cutaneous porphyria, photosensitivity symptoms begin to appear shortly after birth for congenital erythropoietic porphyria (CEP) and hepato-erythropoietic porphyria (HEP), around age 5–6 for erythropoietic protoporphyria (EPP), and after age 50 for late-onset porphyria (PCT). Exposure to sunlight causes pain, itching, redness, and swelling, and, in severe cases, blister-like burns. Porphyrins accumulated in skin tissue become excited by the absorption of light and induce the production of  $^1\text{O}_2$ , resulting in tissue and vascular damage due to complement activation. In addition, the release of histamine, kinins, and chemotactic factors is thought to cause skin damage [165]. Currently, there is no cure for porphyria, and photoprotection is the only way to treat this disease. Beta-carotene, a scavenger of  $^1\text{O}_2$ , is widely used to treat photosensitivity caused by EPP [166,167], but it has also been reported to be less useful for photosensitivity associated with PCT [167,168].

The  $^1\text{O}_2$  produced via porphyrins causes protein oxidation and aggregation [169,170]. In a porphyria model mouse, in which porphyrin accumulation was induced by 3,5-diethoxycarbonyl-1,4-dihydrocollidine, protein aggregation in liver tissue was observed upon safelight exposure compared to non-exposure [171]. Moreover, overexposure to sunlight in EPP and PCT is associated with liver dysfunction, cirrhosis, gallstones, and acute liver failure, and the relationship between hepatic damage in porphyria and  $^1\text{O}_2$  production by irradiation is becoming clearer.

#### 5.1.6. Smith–Lemli–Opitz Syndrome and Statin-Induced Skin Disorders

Smith–Lemli–Opitz syndrome (SLOS) is caused by mutations in the *DHCR7* gene, which encodes 7-dehydrocholesterol (7-DHC) reductase, involved in the final step of cholesterol biosynthesis [172,173]. SLOS shows a cholesterol deficiency and increased 7-DHC in the plasma and tissues [173]. A variety of symptoms are recognized in SLOS, including growth retardation, microcephaly, intellectual disability, characteristic facial features, and external malformations; however, hypersensitivity to ultraviolet light is recognized as a symptom of SLOS [174]. Although 7-DHC itself does not absorb UVA and is not a direct source of photosensitivity in SLOS, 9-DDHC (Figure 8I), a 7-DHC metabolite found in the plasma of SLOS patients, is highly absorbable to UVA [119]. Furthermore, UVA exposure to 9-DDHC generates  $^1\text{O}_2$ , providing a mechanism for the pathogenesis of photosensitivity in SLOS [119].

In addition, some statins inhibit 7-DHC reductase [175]; thus, the accumulation of 9-DDHC may also be involved in statin-induced skin photosensitivity [176] and cataracts [177].

### 5.1.7. Skin Disorders Caused by Exogenous Photosensitizers

Pheophorbide (Figure 8F), a degradation product of chlorophyll (Figure 8D), is a photosensitizing substance [178]. Pheophorbide is sometimes found in food, and the exposure of humans [179] and animals [180] to light after ingesting this compound can cause dermatitis due to photosensitivity. Cholesterol 5 $\alpha$ -OOH (Figure 6) was detected in rat skin administered with pheophorbide and exposed to visible light [99].

The thiopurine prodrugs azathioprine and 6-mercaptopurine are widely prescribed for the treatment of leukemia and autoimmune diseases [181]. Although these drugs have shown therapeutic efficacy, long-term administration has been reported to increase the risk of basal cell carcinoma and squamous cell carcinoma by 10- and 65- to 250-fold, respectively [182]. These adverse effects are induced by sunlight exposure. Thiopurine derivatives absorb UVA, which is believed to be responsible for producing  $^1\text{O}_2$ .

Ibuprofen and ketoprofen, both marketed as nonsteroidal anti-inflammatory drugs with antipyretic and analgesic properties, also produce  $^1\text{O}_2$  due to their photosensitizing effects and have been associated with adverse skin symptoms, including photosensitivity [183]. Some commonly used pharmaceutical compounds whose side effects include skin disorders associated with photosensitivity may also produce  $^1\text{O}_2$ .

### 5.1.8. Diagnosis and Evaluation of Skin Diseases by Measuring $^1\text{O}_2$ -Mediated Products

In skin diseases, the measurement of  $^1\text{O}_2$ -derived lipid peroxidation products in sebum, especially SqOOHs, may be useful in the diagnosis of skin aging and photosensitivity. On the other hand, while the diagnosis of porphyria and SLOS can be made by measuring porphyrin and 7-DHC, respectively, the measurement of  $^1\text{O}_2$ -derived lipid peroxidation products in sebum may be useful in elucidating the pathogenesis and understanding a patient's disease status. In skin cancer, 8-oxo-dG may be useful in assessing the risk of DNA mutations induced by UV, but it should be evaluated in combination with the analysis of compounds produced by UV irradiation, such as cyclobutane pyrimidine dimers.

## 5.2. Ophthalmological Diseases

Since sunlight directly impacts the skin and eyes, oxidative stress is involved not only in the skin, but also in the eyes. In this section, we focus on eye structures, light permeation, and dysfunctions, followed by diseases related to  $^1\text{O}_2$ -mediated oxidative stress.

### 5.2.1. Structure and Optical Transparency of the Ocular Bulb

Light passes through the cornea, aqueous humor, and pupil through the lens and vitreous body, to reach the retina. The pupil regulates light, and the crystalline lens acts as the lens. The retina is a transparent membrane that lines the inside of the eyeball. It mainly consists of a layered structure of four types of cells: retinal ganglion cells, communication/glia cells, photoreceptors, and retinal pigment epithelium (RPE) cells of the vitreous. Light is received by photoreceptors; the pigment cell layer is located outside the photoreceptor layer. Under visible light, the light that passes through the eye differs depending on its wavelength, and UVA (320–400 nm), UVB (280–320 nm), and UVC (100–280 nm) are absorbed by the cornea and lens [184,185], although UV can reach the retina in an aphakic eye (i.e., an eye with no crystalline lens). In the human eye, light with a wavelength of 400–760 nm reaches the retina with little absorption from the cornea to the vitreous body. Since mid- and far-infrared rays are absorbed by water, they are absorbed by water in the cornea, lens, and aqueous humor and do not reach the fundus of the eye. Since near-infrared light has low water absorption, it penetrates the choroid [186].

### 5.2.2. Photooxidative Stress

Visual cells, which are photoreceptors, contain visual substances of chromoproteins that receive light. They are composed of two types of cone cells that sense colors and rod cells that sense the intensity (brightness and darkness) of light. Cone cells have photopsins, and rod cells have rhodopsins.  $^1\text{O}_2$  is produced by the oxygen present in

photoreceptors [187]. In addition, photoreceptor cells and retinal pigment epithelial cells accumulate waste products, called lipofuscin, with aging [188], and these are also activated by light absorption to produce radicals [189,190].

Lipofuscin is considered a waste product in the lysosome, consisting primarily of 30–58% protein, 19–51% lipid-like substances (oxidation products of PUFA), carbohydrates, and trace metals (2%), including iron, copper, aluminum, zinc, zinc calcium, and manganese [191]. Lipofuscin cannot be degraded by lysosomal hydrolytic enzymes because of the polymerization and cross-linking of peptides with aldehydes, resulting in a plastic-like structure that is not biologically degradable and accumulates in neurons and cardiomyocytes with age. Retinal lipofuscin has been shown to exhibit strong photosensitizing properties when photoexcited in the presence of oxygen [189].

Recently, fluorescent bis-retinoid N-retinyl-N-retinylidene ethanolamine (A2E) (Figure 10A,B) has been implicated in photooxidation in the retina [192,193]. A2E is the main component of lipofuscin that accumulates in RPE cells during aging. Rhodopsin, a pigment protein present in photoreceptor cells, is composed of a protein moiety called opsin and 11-*cis*-retinal (Figure 10A,B). The retina contains vitamin A (retinol). Rhodopsin is broken down into opsin and all-*trans*-retinal when it absorbs light. The RPE regenerates all-*trans*-retinal to 11-*cis*-retinal (a process called the visual cycle) (Figure 10B). During this regeneration process, all-*trans*-retinal reacts with phospholipids and another all-*trans*-retinal generates A2E (Figure 10A,B). A2E, a major component of lipofuscin, generates  $^1\text{O}_2$  upon light stimulation, especially high-energy blue light [194].

ROS and radicals generated by light act on the cell membrane lipids of photoreceptors to form lipid radicals [195,196]. Recently, photo-oxidative stress has been found to lead to retinal aging and is a factor in the onset of age-related macular degeneration [195,196].

### 5.2.3. Compounds Protecting against $^1\text{O}_2$ in the Macular Pigment and Lens

The macula is susceptible to oxidative damage owing to the lack of a retinal inner layer, which is affected by intense light. Therefore, the retina has a macular pigment composed of lutein and zeaxanthin, which are carotenoids, and meso-zeaxanthin [197], which is converted from lutein by the RPE-65 enzyme [198,199].

The lens contains lutein and vitamin C, which have a protective mechanism against blue light, with an absorption peak at 400–500 nm. In addition, these macular pigments and carotenoids have an antioxidant ability to eliminate  $^1\text{O}_2$  and are thought to maintain retinal homeostasis [198].

### 5.2.4. Blue Light Hazard

Visible blue light (400–500 nm) from light-emitting diode (LED), mobile phones, and industrial equipment is increasingly being used, and we are susceptible to this in our daily lives. The accumulation of photo-oxidative stress caused by blue light, called blue light hazard, has been reported to cause chronic retinal changes [200,201].

Marie et al. exposed a 10 nm wide light band, range 390–520 nm, to primary retinal pigment epithelial cells treated with A2E and measured the precise action spectrum that produced the highest amount of ROS in the cells [194]. Of the spectrum of sunlight reaching the retina, blue light at 415–455 nm produced the highest amount of ROS and induced mitochondrial dysfunction. Lipofuscin and A2E accumulate in the RPE with aging, and blue light induce a photooxidative reaction that promotes cell death and angiogenesis. The need for the elderly to filter these wavelengths of light is emphasized.

Exposure to blue light (415–455 nm) for 15 h decreased activities of SOD and catalase and increased oxidized glutathione (GSSG) and ROS in A2E-treated RPE cells [194], suggesting that the balance between the oxidant and antioxidants is readily disrupted by massive blue light exposure [194].

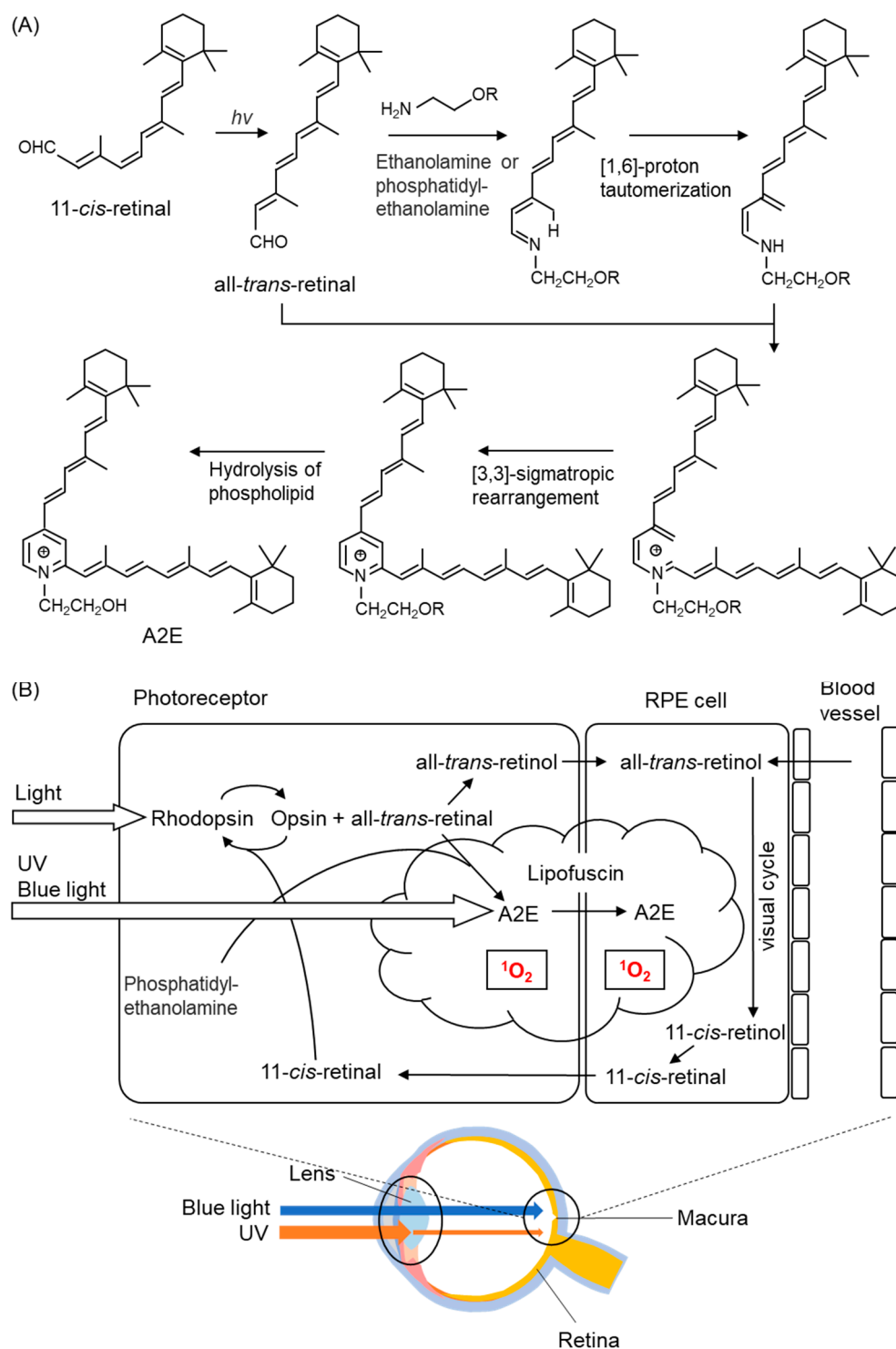


**Figure 10.** The structures of biosynthesis of A2E. (A) After Schiff base formation between all-*trans*-retinal and ethanolamine or phosphatidylethanolamine, a [1,6]-proton tautomerization to enamine follows. After further Schiff base formation with a second molecule of all-*trans*-retinal, a [3,3]-sigmatropic rearrangement is followed by the hydrolysis of the linked phosphatidylethanolamine adduct, resulting in the formation of N-retinyl-N-retinylidene ethanolamine (A2E). (B)  $^1\text{O}_2$  production process mediated by A2E in the retina. Light irradiation of A2E accumulated in lipofuscin generates  $^1\text{O}_2$ .

### 5.2.5. Age-Related Macular Degeneration

Age-related macular degeneration (AMD) is a disease in which the photoreceptor cells in the macula of the central fundus of the eye are damaged. There are two types: the exudative type with neovascularization generated from the choroid that feeds the retina, and the atrophic type without it. AMD is a multifactorial disease characterized by high oxygen consumption, massive radiation exposure, and high PUFA content in the retina. Photooxidative stress is presumed to be one of the causes of retinal disorders such as AMD [200]. PUFAs in the membranes are targets for ROS, which drastically increases the susceptibility of the retina to photochemical damage. In addition, as described above, A2E-containing lipofuscin, which accumulates in RPE cells with aging, is activated by light, and  $^1\text{O}_2$  is generated from abundant oxygen in the retina. In the early stages of the disease, the body's defense mechanism acts. However, the lesion begins to progress as the body's defense mechanisms decline with age.

### 5.2.6. Glaucoma

Glaucoma is a progressive glaucomatous optic neuropathy that causes visual field loss and irreversible blindness [202–204]. The death and axon loss of retinal ganglion cells (RGCs) cause glaucomatous optic neuropathy [202]. Elevated intraocular pressure (IOP) is a primary risk factor for open-angle glaucoma (OAG) including primary OAG (POAG) [202]. In OAGs, the elevation of IOP is explained by a reduction in aqueous humor (AH) outflow at the trabecular meshwork (TM) due to qualitative and quantitative changes in the extracellular matrix in the TM [205]. Numerous reports have shown that various oxidative stressors induce RGC damage [206,207]. For example, antioxidant thioredoxins prevent glaucomatous tissue injury, specifically glutamate- and IOP-induced RGC death [208,209], indicating that oxidative stress is thought to be involved in IOP elevation and then RGC loss in POAG.

We previously demonstrated the involvement of oxidative stress in the pathogenesis of glaucoma by measuring AH and serum HODE levels derived from free radical-mediated oxidation [94,210,211], suggesting that systemic oxidation is at least partially involved in the disease. Furthermore, the levels of HODEs/LA (oxidized/parent molecules ratio, LA; linoleic acid) in AH correlated with those in serum, suggesting that ocular oxidative injury proceeds simultaneously with systemic oxidative stress [211]. The serum levels of 10- and 12-(Z,E)-HODEs/LA formed via  $^1\text{O}_2$  specific oxidation were correlated with IOP [94], which are indices of glaucoma severity derived from TM cell dysfunction. One possible process by which  $^1\text{O}_2$  is produced in the eye is type II photooxidation via a sensitizer present in the vicinity of the reaction milieu, similar to a cataract [212]. The specific region of oxidative injury has not been identified because sunlight does not reach TM cells. In addition, the pathways of the excretion and circulation of HODEs formed in the eyes remain undefined. However, our findings suggested that cerebrospinal HODE levels were well reflected in plasma levels [213,214]. Other studies have simultaneously analyzed the systemic and local redox status, suggesting that alterations in systemic oxidant and antioxidant levels reflect local redox status [215–217].

### 5.2.7. Cataract

Epidemiological approaches have indicated that sun exposure is a risk factor in age-related cataracts [218,219]. UVB is mostly filtered out by the cornea and aqueous humor [220]. For this reason, UVA, which occupies nearly 95% of the UV in sunlight, has been associated with cataracts [221]. It has been proposed that chromophores with UVA-visible light absorption properties, which accumulate in the lens with age, influence the development of cataracts through the ROS generation by photosensitizing reactions [222].

The major protein components of the lens are crystallins, of which there are three main types:  $\alpha$ -,  $\beta$ -, and  $\gamma$ -crystallin. The most abundant of these is  $\alpha$ -crystallin, which functions to maintain lens transparency and acts as a protective chaperone for the lens [223]. As  $\alpha$ -

crystallin is not turned over, damage to the amino acids/proteins constituting  $\alpha$ -crystallin accumulates. This leads to changes in refraction and lens opacity (cataract formation) [224].

Tryptophan metabolites (kynurenine (Figure 8G), 3-hydroxykynurenine (Figure 8G), 3-hydroxykynurenine *o*- $\beta$ -D-glucoside, and 4-(2-amino-3-hydroxyphenyl)-4-oxobutanoic acid *o*- $\beta$ -D glucoside) are present in significant concentrations in the lens and act as endogenous chromophores and UV-absorbing filters [225]. These endogenous chromophores absorb UV and become excited but regenerate to their original ground state without producing radicals or  $^1\text{O}_2$ . These chromophores undergo deamination under physiological conditions and are covalently bound to proteins (crystallin) via Michael addition reactions [226]. As covalent modification progresses gradually with age, the lens turns yellow. Paradoxically, tryptophan derivatives, which act as UV filters, have also been shown to generate  $^1\text{O}_2$  by acting as photosensitizers when bound to proteins [226]. However, the association between cataract development and  $^1\text{O}_2$  remains undefined and has not been confirmed in our studies [94,210].

### 5.2.8. $^1\text{O}_2$ -Derived Peroxidation Products in the Diagnosis and Evaluation of Ophthalmological Diseases

The measurement of  $^1\text{O}_2$ -derived lipid peroxidation products in tissues removed during cataract and glaucoma surgery may provide assistance in elucidating the pathophysiology and in selecting the use of singlet oxygen scavengers. As our results indicate, measuring lipid oxides in circulation may also be useful for diagnosis and pathophysiological evaluation.

## 5.3. Diabetes Mellitus

### 5.3.1. Biomarkers for Diabetes and Diabetic Complications

Diabetes is characterized by a deficiency of the secretion or action of insulin, resulting in microvasculature damage to the retina, renal glomerulus, and heart, as well as peripheral neuropathy. Diabetes can be fatal if its complications include nephritis and atherosclerosis. Type 2 diabetes mellitus (T2D) indicates elevated blood glucose levels caused by the impairment of insulin secretion and insulin resistance. Prediabetic states, including impaired fasting glucose, impaired glucose tolerance (IGT), or slightly elevated blood glucose levels, may precede T2D for the year [227,228]. Progression from prediabetes to T2D can be prevented or delayed by improving diet and increasing physical activity.

Diabetic vascular complications include nephropathy, myocardial infarction, and glaucoma. The early detection of diabetes is important to prevent complications. Several studies have been conducted on the early detection of these complications. Biomarkers of diabetic nephropathy include urinary heme oxygenase-1 (HO-1) [229] and 8-hydroxydeoxyguanosine [230,231], and circulating microRNA 130b [232]. S-glutathionylation [233] and oxidized dityrosine-containing protein [234] are considered candidate markers of vasculopathy in diabetes. Angiotensin-II, protein kinase C (PKC), and advanced glycation end products (AGEs) activate NADPH oxidase and upregulate the production of ROS, leading to cardiac dysfunction [235,236]. The metallic elements selenium [237], copper, and zinc [238] are associated with the detection of diabetes risk in pregnant women. Recently, band 3 anion transport protein, also known as anion exchanger 1 or band 3, or solute carrier family 4 member 1, was proposed for the early detection of the glycation of hemoglobin leading to AGEs [239–241]. To completely detect diabetes and its complications, a combination of several biomarkers is necessary.

### 5.3.2. Diabetic Biomarkers of Lipid Peroxidation

Several studies have examined the association of oxidation products with diabetes pathology [242–246]. Griesser et al. revealed the interplay between lipid and protein modifications using animal models. A large cohort study showed that imbalances in the redox system contribute to the development of T2D [245]. Leinish et al. clarified that the

structural and functional alterations in RNase A result from oxidation by  $^1\text{O}_2$  and  $\text{ROO}^\bullet$ , not solely from histidine and tyrosine cross-linking [246].

We recently found that 10- and 12-(*Z,E*)-HODE,  $^1\text{O}_2$ -specific products derived from linoleic acid, significantly correlated with a risk index for impaired glucose tolerance and insulin resistance in oral glucose tolerance tests performed on healthy volunteers [92,247,248]. Free radical-specific lipid oxidation products, such as 9- and 13-(*E,E*)-HODE and  $7\beta$ -hydroxycholesterol, and hydroxyeicosatetraenoic acids (HETEs), which are oxidation products derived from arachidonic acid, have not been detected. The process by which these  $^1\text{O}_2$ -specific lipid oxidation products are produced in diabetic pathology is speculated to involve the reaction between  $\text{H}_2\text{O}_2$  and  $\text{ClO}^-$  derived from MPO (Figure 2B). This  $^1\text{O}_2$  generation mechanism is mediated by MPO from activated phagocytes [249,250] or eosinophils peroxidase [251,252]. Several reports have shown that neutrophil-derived MPO plays an important role in diabetic vascular injury (Figure 11) [253–255]. The source of  $\text{H}_2\text{O}_2$  in diabetic pathology is thought to be NADPH oxidase in the vascular endothelial cells [253]. MPO released from activated neutrophils is known to bind to the vessel wall for several days [256,257]. The  $\text{H}_2\text{O}_2$  derived from hyperglycemia-activated NADPH oxidase may be used by MPO bound to the vascular endothelium to produce HOCl, resulting in the production of  $^1\text{O}_2$  and vascular injury. Compounds that inhibit the activity of MPO, such as hydroxamic acids, hydrazides, and azides, have potentially harmful side effects. In contrast, quercetin was recently reported to inhibit MPO-dependent HOCl production and prevent vascular endothelial injury [258]. Onyango et al. reviewed the contribution of  $^1\text{O}_2$  to insulin resistance and reported that  $^1\text{O}_2$  generates bioactive aldehydes and induces mitochondrial DNA modification and endoplasmic reticulum stress, which lead to insulin resistance [259].

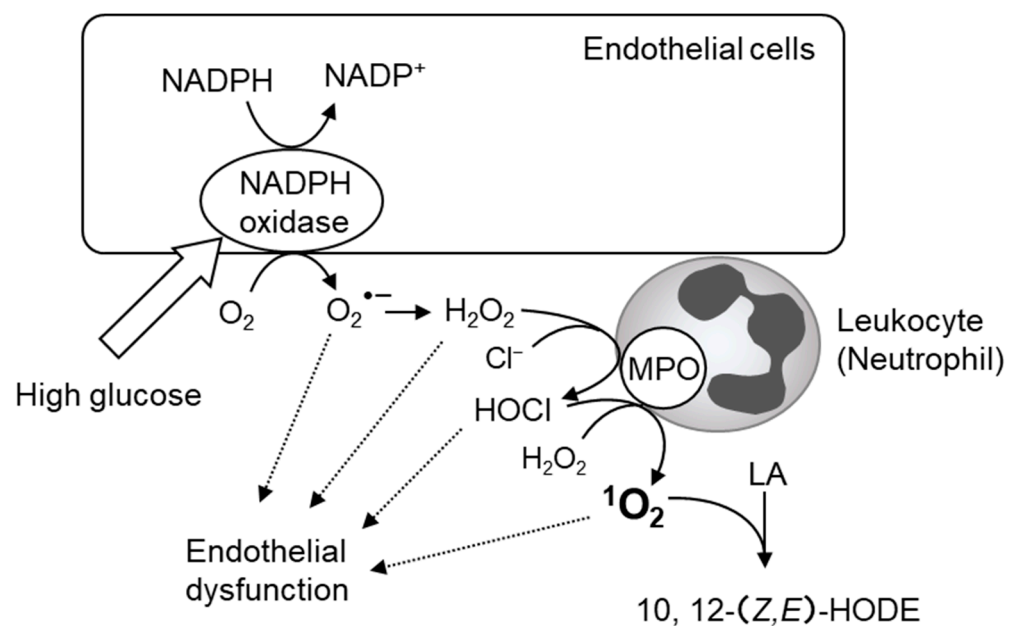


**Figure 11.** Assumed scheme of  $^1\text{O}_2$  production via NADPH oxidase and myeloperoxidase (MPO) in vascular injury in diabetes mellitus. High glucose produces hydrogen peroxide ( $\text{H}_2\text{O}_2$ ) by NADPH oxidase in vascular endothelial cells.  $^1\text{O}_2$  is generated via MPO in activated neutrophils bound to the vessel wall.

Clinicians may be able to manage and/or advise patients regarding their food and exercise habits before the onset of diabetes, by evaluating the levels of  $^1\text{O}_2$ -induced lipid peroxidation products in the near future. In any event, more information and studies are needed to determine the pathological significance of  $^1\text{O}_2$  and 10,12-(*Z,E*)-HODE.

#### 5.4. Bronchial Asthma

Bronchial asthma is characterized by chronic airway inflammation, reversible air-flow obstruction, airway hyperresponsiveness, and structural changes in the airways, and its clinical manifestations include variable airway narrowing, cough, dyspnea, and wheezing [260]. Asthma is caused by multiple interactions between epigenetic regulation and environmental factors. Although this heterogeneity has made it difficult to define biologically distinct subgroups based on the differences in clinical phenotypes, recent advances in genetics and molecular biology have led to the pathogenetic classification of endotypes [261]. These characteristics of asthma may be helpful for understanding the pathophysiology and precision of medicine.

More than 300 million people worldwide suffer from asthma, of which approximately 10% have severe asthma. Symptom control in severe refractory asthma is difficult to achieve despite optimal treatment with high-dose inhaled corticosteroids (ICS) and long-acting adrenergic receptor  $\beta_2$  agonists [262]. Airway inflammation in asthma is typically involved in the submucosal infiltration of activated Th2 lymphocytes, neutrophils, eosinophils, mast cells, and macrophages [263,264]. Although Th2 cytokines and eosinophilic inflammation are typical factors in the development of mild to moderate asthma in response to ICS, a subset of asthmatics with Th2 high-eosinophil-predominant have a refractory course despite optimal treatment [265]. In more severe cases of steroid-resistance, the cellular environment is characterized by airway inflammation induced by Th1/Th2 cytokine expression and neutrophil, with poorly reversible airflow obstruction [265–267]. In adults, elevated neutrophil counts in sputum are related to disease severity [268] and the persistence of symptoms [269]. These reports suggest an important role for neutrophils in asthma and their association with a more steroid-refractory subtype.

Neutrophils are recruited to the site of pathogen invasion for immune defense [270,271]. Several proinflammatory mediators, including cytokines, chemokines, and complements, contribute to the regulation of lung neutrophilic recruitment. Accumulated neutrophils release chemotactic factors that attract monocytes and/or macrophages to the infection site and, subsequently, exacerbate airway inflammation [272]. In particular, Th17/IL-17 and IL-8 are involved in the pathogenesis of steroid-resistant asthma [273,274]. Neutrophil extracellular traps (NETs) comprising neutrophil DNA, whose formation is facilitated by proinflammatory cytokines, are also thought to be implicated in the pathological condition of neutrophilic asthma [274–277]. Activated neutrophils release not only inflammatory cytokines, but also ROS and MPO, which damage airway endothelial cells and exacerbate allergic inflammation [278–281]. Plasma MPO levels in asthmatic patients have been proposed as biomarkers for the evaluation of asthma severity in adults [277,282]. As described in Sections 2 and 5.3.2, MPO contributes to the production of  $^1\text{O}_2$  mediated by the progression of the reaction with  $\text{H}_2\text{O}_2$  and  $\text{Cl}^-$  producing HClO. These suggest that  $^1\text{O}_2$  may be associated with pathogenesis phenotypes in refractory asthma. We have demonstrated a positive correlation between the levels of  $^1\text{O}_2$ -mediated oxidation products 10- and 12-(Z,E)-HODEs, and the levels of MPO activity and IL-17-derived nerve growth factor (NGF) in the bronchoalveolar lavage fluid (BALF) of an asthmatic mouse model with mixed inflammation [97]. As increased NGF in the BALF of asthmatic patients induces smooth muscle hyperplasia in the airway [283,284] and anti-NGF antibodies improve airway hyperresponsiveness [285], NGF is also considered a therapeutic target for lung disease [286]. Interestingly, the generation of  $^1\text{O}_2$  with an endoperoxide [(3-(1, 4-epidioxy-4-methyl-1, 4-dihydro-1- naphthyl) propionic acid] increased NGF and IL-8 levels in human bronchial epithelial cells, suggesting that  $^1\text{O}_2$  generation may be an upstream event of increase in NGF.

Recent studies have described neutrophil-derived MPO as a potential biomarker for neutrophilic asthma [277,282]. Therefore, we would expect that 10, 12-(Z,E)-HODEs, which are elevated according to neutrophil recruitment, could also be a prominent biomarker with more stability than MPO for neutrophilic asthma. Glucocorticoids, which are used as the first choice for asthma therapy, fail to attenuate neutrophilic inflammation and may even

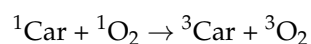
promote neutrophil survival [268,287]. It seems reasonable to choose macrolide antibiotics for the treatment of asthma rather than steroids when the levels of 10- and 12-(*Z,E*)-HODEs are increased. However, the use of macrolides is not appropriate for the long-term treatment of neutrophilic asthma due to the risk of bacterial resistance. Although future studies are needed to determine how  $^1\text{O}_2$  is related to the pathological condition of asthma patients, 10- and 12-(*Z,E*)-HODEs may be useful in stratifying patients with refractory asthma and in selecting treatment options.

## 6. $^1\text{O}_2$ Scavengers

The living body contains superoxide dismutase and catalase, which can scavenge ROS such as  $\text{O}_2^{\bullet-}$  and  $\text{H}_2\text{O}_2$ , but it does not have enzymes that can scavenge  $^1\text{O}_2$ . Substances that can effectively scavenge  $^1\text{O}_2$  depend on exogenous compounds such as dietary carotenoids.

### 6.1. Carotenoids

Carotenoids are plant pigments that are pro-vitamin A and potent scavengers of  $^1\text{O}_2$ . The  $^1\text{O}_2$  scavenging of carotenoids is mainly based on physical scavenging. The excitation energy of  $^1\text{O}_2$  is transferred to carotenoids (singlet carotenoids;  $^1\text{Car}$ ) to produce triplet oxygen ( $^3\text{O}_2$ ) and triplet carotenoids ( $^3\text{Car}$ ).  $^3\text{Car}$ , which receives excitation energy, returns to ground state carotenoids by releasing heat as energy. Thus, carotenoids can repeatedly scavenge  $^1\text{O}_2$  [288].



Carotenoids are the most potent  $^1\text{O}_2$  scavengers found in nature, and carotenoids with 11 carbon atoms involved in the  $\pi$ -conjugation length, such as lycopene (Figure 12A),  $\beta$ -carotene (Figure 12B), and astaxanthin (Figure 11C), are the most efficient  $^1\text{O}_2$  scavengers [288]. Among carotenoids, studies have mainly been conducted on the products associated with the  $^1\text{O}_2$  scavenging of  $\beta$ -carotene, and  $\beta$ -carotene 5,8-endoperoxide (Figure 12B) is a specific product mediated by  $^1\text{O}_2$  oxidation [102,289,290]. In contrast,  $\beta$ -carotene 5,6-epoxide is formed by a free radical-mediated reaction.  $\beta$ -Carotene-5,8-endoperoxide has been detected in vitro [291,292] and in vivo [289]. Among carotenoids, lycopene has the strongest  $^1\text{O}_2$  scavenging capacity [293]. The second-order rate constants of physical quenching (kq) in ethanol/chloroform were  $31,000 \times 10^6 \text{ M}^{-1}\text{s}^{-1}$  for lycopene,  $14,000 \times 10^6 \text{ M}^{-1}\text{s}^{-1}$  for  $\beta$ -carotene,  $8000 \times 10^6 \text{ M}^{-1}\text{s}^{-1}$  for lutein, and  $10,000 \times 10^6 \text{ M}^{-1}\text{s}^{-1}$  for zeaxanthin, indicating that lycopene was the most efficient  $^1\text{O}_2$  quencher [294]. Lycopene and  $\beta$ -carotene also exhibited the fastest  $^1\text{O}_2$  scavenging rate constants under the conditions of the model membrane system using liposomes [295]. Unlike other carotenoids, lycopene does not possess a ring structure. Since 2-methyl-2-hepten-6-one (Figure 12A) and apo-6'-lycopenal (Figure 12A) were detected under 500 W light irradiation in the presence of methylene blue, a photosensitizer, lycopene is assumed to react with  $^1\text{O}_2$  via a dioxetane intermediate [296,297].

Carotenoids in plants exist in close proximity to chlorophyll in chloroplasts and scavenge  $^1\text{O}_2$  generated by the photosensitizing effect of chlorophyll during light absorption. Thus, carotenoids have a protective property against light stress in plants. In addition, carotenoids, such as xanthophylls (lutein (Figure 12D) and zeaxanthin (Figure 12E)), specifically accumulate in the macula of the retina, which is an organ exposed to light. In sunlight, the energy of blue light (400 nm), in particular, is 100-fold greater than that of red light (590 nm) and causes severe damage to cells. Since lutein and zeaxanthin have absorption maxima for light at approximately 440 nm, these carotenoids can efficiently absorb blue light. Therefore, the accumulation of lutein and zeaxanthin in the retinal macula can prevent the oxidative degeneration of macular tissue and reduce the risk of AMD and other diseases. Lutein and zeaxanthin are also present in the lens, where they prevent the development of cataract [298,299]. The consumption of tomatoes rich in  $\beta$ -carotene and lycopene can reduce the formation of erythema in human skin due to UV irradiation [300,301].

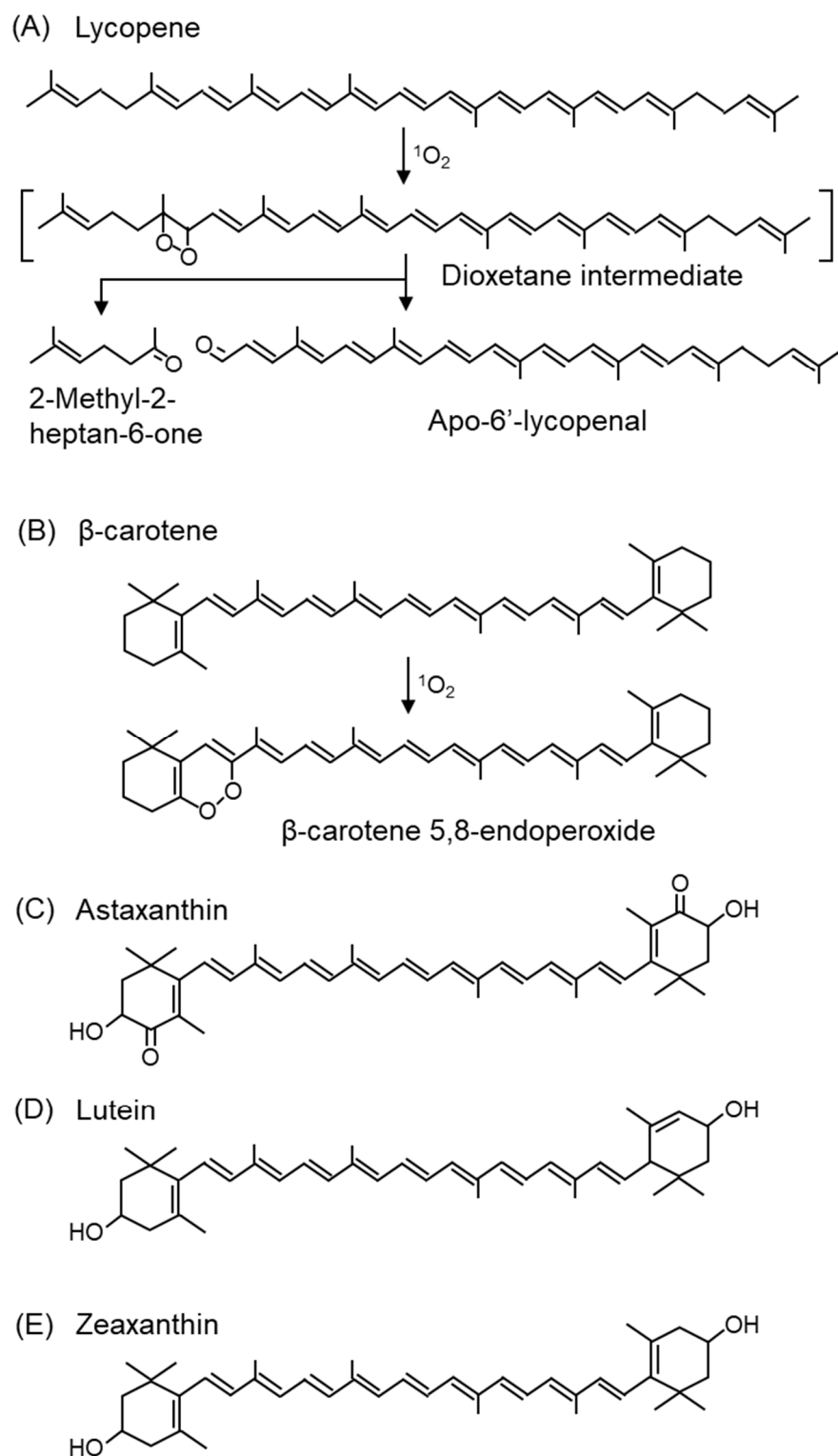


**Figure 12.** The structures of carotenoid and peroxidation products from lycopene and  $\beta$ -carotene. (A) Lycopene, (B)  $\beta$ -carotene, (C) astaxanthin, (D) lutein, (E) zeaxanthin.

### 6.2. Vitamin E (Tocopherol)

$\alpha$ -Tocopherol, a primary fat-soluble antioxidant *in vivo*, also has  $^1\text{O}_2$  scavenging capacity that is approximately 30–100 times weaker than that of carotenoids [302]. However, the  $^1\text{O}_2$  scavenging capacity of carotenoids is also reported to be reduced in liposomes, which are biomembrane models, compared to solution [303]. Considering the level of tocopherols

in vivo, the in vivo  $^1\text{O}_2$  scavenging activity of  $\alpha$ -tocopherol is considered to be functional. Among tocopherols,  $\alpha$ - $\beta$ - $\gamma$ - $\delta$ -tocopherol have  $^1\text{O}_2$  capacities in this order [304,305]. Tocotrienols, which are homologues of tocopherols, also have  $^1\text{O}_2$  scavenging ability in the order of  $\alpha$ - $\beta$ - $\gamma$ - $\delta$ -tocotrienol [304].

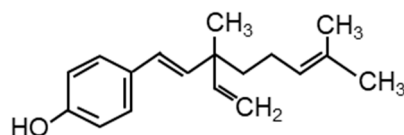
The oxidation product of  $\alpha$ -tocopherol produced by  $^1\text{O}_2$  is  $\alpha$ -tocopherylquinone, which can be measured in biological samples [306–308].  $\alpha$ -Tocopherylquinone is not an  $^1\text{O}_2$ -specific marker because it is also produced by ROS other than  $^1\text{O}_2$ .

### 6.3. Other Compounds

As previously mentioned, PUFA is susceptible to oxidation by  $^1\text{O}_2$  and has  $^1\text{O}_2$  scavenging capacity, although it is very weak compared to carotenoids [309].

Bakuchiol (Figure 13A), a terpeno-phenolic compound, is a functional analog of retinol that has attracted attention in skincare for its ability to induce retinol gene expression and stimulate collagen production [310]. Bakuchiol protects retinol from degradation by  $^1\text{O}_2$  produced by  $\text{H}_2\text{O}_2$  and lithium molybdenum. It was shown to inhibit the  $^1\text{O}_2$ -induced peroxidation of squalene, prevent pore clogging, and reduce the onset of acne by 42% with topical bakuchiol treatment in 54 volunteers [311]. In addition, the 12-week application of a cream containing bakuchiol (0.5%) improved wrinkles and pigmentation [312].

#### (A) Bakuchiol



#### (B) Acetyl zingerone

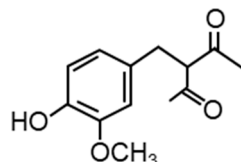


**Figure 13.** Compounds with  $^1\text{O}_2$  scavenging activity other than carotenoids. The structures of (A) bakuchiol and (B) acetyl zingerone.

Zingerone (4-[4-hydroxy-3-methoxyphenyl]-2-butanone) from *Zingiber officinale* Roscoe (ginger) scavenges  $^1\text{O}_2$  [313]. The structure of zingerone is similar to that of turmeric-derived curcumin (1,7-bis[4-hydroxy-3-methoxyphenyl]-1,6-heptane-3,5-dione). Zingerone and curcumin can both prevent skin aging. Acetyl zingerone (3-(4-hydroxy-3-methoxybenzyl)pentane-2,4-dione) (Figure 13B), a multifunctional skincare ingredient, was synthesized using the molecular structures of zingerone and curcumin [314]. Curcumin has been shown to have  $^1\text{O}_2$  scavenging activity in an in vitro experimental system by ESR spectroscopy using TEMP as a spin-trap [315]. Acetyl zingerone, which has a higher  $^1\text{O}_2$  scavenging activity than  $\alpha$ -tocopherol [316], decreases the expression of genes associated with extracellular matrix degradation (MMP-3 and cathepsin V) and inhibits the activity of MMP-1, -3, and -12 [314]. Clinical reports have demonstrated that treatment with a cream containing 1% acetyl zingerone applied twice daily for 8 weeks improves wrinkles, hyperpigmentation, and erythema [317].

## 7. Summary and Outlook

As previously described, diseases and dysfunctions mediated by or, at least, related to  $^1\text{O}_2$  can be categorized into two groups: those caused by the UV irradiation of photosensitizers accumulated in the living body, and those resulting from the activation of MPO in leukocytes. The former includes cutaneous photosensitivity and retinal diseases, which have been clinically investigated. For the latter, we have previously reported findings in diabetic patients, glaucoma patients, and in an asthma mouse model. MPO is expressed in leukocytes and is implicated in many inflammatory diseases [318]. MPO is associated with cardiovascular disease, atherosclerosis, glomerulonephritis, arthritis, and Alzheimer's disease. Practical biomarkers are required for the early diagnosis, assessment, and progression of diseases, and for the evaluation of treatment efficacy. However, as summarized in Tables 2 and 3, there are few reports on the analysis of lipid peroxidation products formed by  $^1\text{O}_2$  in clinical samples, except for SqOOHs. SqOOHs can be measured noninvasively as they are found in sebum; therefore, an increasing number of reports are available (Table 3), especially in the cosmetics and beauty industries. SqOOHs are lipid peroxidation products, but not specific products of  $^1\text{O}_2$ . Since lipid peroxidation is a major oxidative injury in vivo, lipid peroxidation products, especially hydroxides, may be useful biomarkers. It should be noted, however, that lipid peroxidation products are generally not diagnostic indicators of specific diseases. Their usefulness should be enhanced by combination with other biomarkers. Further prospective studies and analysis of the correlation between lipid peroxidation products, specifically from  $^1\text{O}_2$ , and the severity of disease progression should be conducted in the future. When disease risk can be assessed by a prominent biomarker, advice on diet, including carotenoids, and exercise habits can be provided.

**Author Contributions:** Writing—original draft preparation, K.M., A.U., M.S., M.T. and Y.Y.; writing—review and editing, K.M., A.U., M.S., M.T. and Y.Y.; visualization, K.M. and M.S. All authors have read and agreed to the published version of the manuscript.

**Funding:** This study was partially supported by a Grant-in-Aid for JSPS KAKENHI Grant Number JP18K17951.

**Institutional Review Board Statement:** Not applicable.

**Informed Consent Statement:** Not applicable.

**Data Availability Statement:** Not applicable.

**Conflicts of Interest:** Yasukazu Yoshida is an employee of LG Japan Lab, Inc. This paper has not received any form of financial support from LG Japan Lab, Inc. The findings of this paper do not result in any commercial or economic interest to LG Japan Lab, Inc. or any of the authors.

## References

1. Chen, Z.H.; Yoshida, Y.; Saito, Y.; Noguchi, N.; Niki, E. Adaptive response induced by lipid peroxidation products in cell cultures. *FEBS Lett.* **2006**, *580*, 479–483. [[CrossRef](#)]
2. Haugaard, N. Cellular mechanisms of oxygen toxicity. *Physiol. Rev.* **1968**, *48*, 311–373. [[CrossRef](#)]
3. Gottlieb, S.F. Effect of hyperbaric oxygen on microorganisms. *Annu. Rev. Microbiol.* **1971**, *25*, 111–152. [[CrossRef](#)]
4. Gilbert, D.L. Symposium on oxygen. Introduction: Oxygen and life. *Anesthesiology* **1972**, *37*, 100–111. [[CrossRef](#)]
5. Chance, B.; Sies, H.; Boveris, A. Hydroperoxide metabolism in mammalian organs. *Physiol. Rev.* **1979**, *59*, 527–605. [[CrossRef](#)] [[PubMed](#)]
6. Hackbarth, S.; Islam, W.; Fang, J.; Šubr, V.; Röder, B.; Etrych, T.; Maeda, H. Singlet oxygen phosphorescence detection in vivo identifies PDT-induced anoxia in solid tumors. *Photochem. Photobiol. Sci.* **2019**, *18*, 1304–1314. [[CrossRef](#)] [[PubMed](#)]
7. Collin, F. Chemical Basis of Reactive Oxygen Species Reactivity and Involvement in Neurodegenerative Diseases. *Int. J. Mol. Sci.* **2019**, *20*, 2407. [[CrossRef](#)] [[PubMed](#)]
8. Wang, X.; Lv, H.; Sun, Y.; Zu, G.; Zhang, X.; Song, Y.; Zhao, F.; Wang, J. New porphyrin photosensitizers-Synthesis, singlet oxygen yield, photophysical properties and application in PDT. *Spectrochim. Acta. A Mol. Biomol. Spectrosc.* **2022**, *279*, 121447. [[CrossRef](#)]
9. You, Z.Q.; Hsu, C.P.; Fleming, G.R. Triplet-triplet energy-transfer coupling: Theory and calculation. *J. Chem. Phys.* **2006**, *124*, 044506. [[CrossRef](#)]
10. Dzebo, D.; Moth-Poulsen, K.; Albinsson, B. Robust triplet-triplet annihilation photon upconversion by efficient oxygen scavenging. *Photochem. Photobiol. Sci. Off. J. Eur. Photochem. Assoc. Eur. Soc. Photobiol.* **2017**, *16*, 1327–1334. [[CrossRef](#)] [[PubMed](#)]

11. Turro, N.J. Singlet oxygen and chemiluminescent organic reactions. In *Modern Molecular Photochemistry*; University Science Books: Melville, NY, USA, 1991; pp. 583–593.
12. Hatz, S.; Poulsen, L.; Ogilby, P.R. Time-resolved singlet oxygen phosphorescence measurements from photosensitized experiments in single cells: Effects of oxygen diffusion and oxygen concentration. *Photochem. Photobiol.* **2008**, *84*, 1284–1290. [[CrossRef](#)] [[PubMed](#)]
13. Pedersen, B.W.; Sinks, L.E.; Breitenbach, T.; Schack, N.B.; Vinogradov, S.A.; Ogilby, P.R. Single cell responses to spatially controlled photosensitized production of extracellular singlet oxygen. *Photochem. Photobiol.* **2011**, *87*, 1077–1091. [[CrossRef](#)] [[PubMed](#)]
14. Liang, P.; Kolodieznyi, D.; Creeger, Y.; Ballou, B.; Bruchez, M.P. Subcellular Singlet Oxygen and Cell Death: Location Matters. *Front. Chem.* **2020**, *8*, 592941. [[CrossRef](#)] [[PubMed](#)]
15. Denys, G.A.; Devoe, N.C.; Gudis, P.; May, M.; Allen, R.C.; Stephens, J.T., Jr. Mechanism of Microbicidal Action of E-101 Solution, a Myeloperoxidase-Mediated Antimicrobial, and Its Oxidative Products. *Infect. Immun.* **2019**, *87*, e00261-19. [[CrossRef](#)]
16. Neale, T.J.; Ullrich, R.; Ojha, P.; Poczewski, H.; Verhoeven, A.J.; Kerjaschki, D. Reactive oxygen species and neutrophil respiratory burst cytochrome b558 are produced by kidney glomerular cells in passive Heymann nephritis. *Proc. Natl. Acad. Sci. USA* **1993**, *90*, 3645–3649. [[CrossRef](#)] [[PubMed](#)]
17. Russell, G.A. Deuterium-isotope Effects in the Autoxidation of Alkyl Hydrocarbons. Mechanism of the Interaction of Peroxy Radicals. *J. Am. Chem. Soc.* **1957**, *79*, 3871–3877. [[CrossRef](#)]
18. Gonçalves, L.C.P.; Massari, J.; Licciardi, S.; Prado, F.M.; Linares, E.; Klassen, A.; Tavares, M.F.M.; Augusto, O.; Di Mascio, P.; Bechara, E.J.H. Singlet oxygen generation by the reaction of acrolein with peroxy nitrite via a 2-hydroxyvinyl radical intermediate. *Free Radic. Biol. Med.* **2020**, *152*, 83–90. [[CrossRef](#)]
19. Sun, S.; Bao, Z.; Ma, H.; Zhang, D.; Zheng, X. Singlet oxygen generation from the decomposition of alpha-linolenic acid hydroperoxide by cytochrome c and lactoperoxidase. *Biochemistry* **2007**, *46*, 6668–6673. [[CrossRef](#)]
20. Chen, T.; Cohen, D.; Itkin, M.; Malitsky, S.; Fluhr, R. Lipoygenase functions in  $^1\text{O}_2$  production during root responses to osmotic stress. *Plant Physiol.* **2021**, *185*, 1638–1651. [[CrossRef](#)]
21. Khan, A.U.; Kasha, M. Singlet molecular oxygen in the Haber-Weiss reaction. *Proc. Natl. Acad. Sci. USA* **1994**, *91*, 12365–12367. [[CrossRef](#)]
22. Miyamoto, S.; Ronsein, G.E.; Corrêa, T.C.; Martinez, G.R.; Medeiros, M.H.; Di Mascio, P. Direct evidence of singlet molecular oxygen generation from peroxy nitrate, a decomposition product of peroxy nitrite. *Dalton Trans.* **2009**, *29*, 5720–5729. [[CrossRef](#)] [[PubMed](#)]
23. Bauer, G. The synergistic effect between hydrogen peroxide and nitrite, two long-lived molecular species from cold atmospheric plasma, triggers tumor cells to induce their own cell death. *Redox Biol.* **2019**, *26*, 101291. [[CrossRef](#)] [[PubMed](#)]
24. Kanofsky, J.R.; Sima, P. Singlet oxygen production from the reactions of ozone with biological molecules. *J. Biol. Chem.* **1991**, *266*, 9039–9042. [[CrossRef](#)]
25. Cerkovnik, J.; Erzen, E.; Koller, J.; Plesnicar, B. Evidence for HOOO radicals in the formation of alkyl hydrotrioxides (ROOOH) and hydrogen trioxide (HOOOH) in the ozonation of C-H bonds in hydrocarbons. *J. Am. Chem. Soc.* **2002**, *124*, 404–409. [[CrossRef](#)]
26. Pershin, A.A.; Torbin, A.P.; Zagidullin, M.V.; Mebel, A.M.; Mikheyev, P.A.; Azyazov, V.N. Rate constants for collision-induced emission of  $\text{O}(2)(a(1)\Delta(g))$  with He, Ne, Ar, Kr, N(2), CO(2) and SF(6) as collisional partners. *Phys. Chem. Chem. Phys.* **2018**, *20*, 29677–29683. [[CrossRef](#)]
27. Tao, F.; Gonzalez-Flecha, B.; Kobzik, L. Reactive oxygen species in pulmonary inflammation by ambient particulates. *Free Radic. Biol. Med.* **2003**, *35*, 327–340. [[CrossRef](#)] [[PubMed](#)]
28. Gurgueira, S.A.; Lawrence, J.; Coull, B.; Murthy, G.G.; González-Flecha, B. Rapid increases in the steady-state concentration of reactive oxygen species in the lungs and heart after particulate air pollution inhalation. *Environ. Health Perspect.* **2002**, *110*, 749–755. [[CrossRef](#)]
29. Jensen, R.L.; Arnbjerg, J.; Ogilby, P.R. Reaction of singlet oxygen with tryptophan in proteins: A pronounced effect of the local environment on the reaction rate. *J. Am. Chem. Soc.* **2012**, *134*, 9820–9826. [[CrossRef](#)]
30. Nascimento, R.O.; Prado, F.M.; Massafra, M.P.; Di Mascio, P.; Ronsein, G.E. Dehydromethionine is a common product of methionine oxidation by singlet molecular oxygen and hypohalous acids. *Free Radic. Biol. Med.* **2022**, *187*, 17–28. [[CrossRef](#)]
31. Fouquerel, E.; Barnes, R.P.; Uttam, S.; Watkins, S.C.; Bruchez, M.P.; Opreko, P.L. Targeted and Persistent 8-Oxoguanine Base Damage at Telomeres Promotes Telomere Loss and Crisis. *Mol. Cell* **2019**, *75*, 117–130.e116. [[CrossRef](#)] [[PubMed](#)]
32. Lu, W.; Sun, Y.; Tsai, M.; Zhou, W.; Liu, J. Singlet  $\text{O}(2)$  Oxidation of a Deprotonated Guanine-Cytosine Base Pair and Its Entangling with Intra-Base-Pair Proton Transfer. *Chemphyschem* **2018**, *19*, 2645–2654. [[CrossRef](#)]
33. Kato, S.; Shimizu, N.; Otoki, Y.; Ito, J.; Sakaino, M.; Sano, T.; Takeuchi, S.; Imagi, J.; Nakagawa, K. Determination of acrolein generation pathways from linoleic acid and linolenic acid: Increment by photo irradiation. *NPJ Sci. Food* **2022**, *6*, 21. [[CrossRef](#)] [[PubMed](#)]
34. Ishikawa, A.; Ito, J.; Shimizu, N.; Kato, S.; Kobayashi, E.; Ohnari, H.; Sakata, O.; Naru, E.; Nakagawa, K. Linoleic acid and squalene are oxidized by discrete oxidation mechanisms in human sebum. *Ann. N. Y. Acad. Sci.* **2021**, *1500*, 112–121. [[CrossRef](#)] [[PubMed](#)]
35. Carroll, L.; Pattison, D.I.; Davies, J.B.; Anderson, R.F.; Lopez-Alarcon, C.; Davies, M.J. Superoxide radicals react with peptide-derived tryptophan radicals with very high rate constants to give hydroperoxides as major products. *Free Radic. Biol. Med.* **2018**, *118*, 126–136. [[CrossRef](#)]

36. Moe, M.M.; Tsai, M.; Liu, J. Singlet Oxygen Oxidation of the Radical Cations of 8-Oxo-2'-deoxyguanosine and Its 9-Methyl Analogue: Dynamics, Potential Energy Surface, and Products Mediated by C5-O(2) -Addition. *Chempluschem* **2021**, *86*, 1243–1254. [[CrossRef](#)] [[PubMed](#)]
37. Monzo-Beltran, L.; Vazquez-Tarragón, A.; Cerdà, C.; Garcia-Perez, P.; Iradi, A.; Sánchez, C.; Climent, B.; Tormos, C.; Vázquez-Prado, A.; Girbés, J.; et al. One-year follow-up of clinical, metabolic and oxidative stress profile of morbid obese patients after laparoscopic sleeve gastrectomy. 8-oxo-dG as a clinical marker. *Redox Biol.* **2017**, *12*, 389–402. [[CrossRef](#)] [[PubMed](#)]
38. Ponce, M.A.; Ramirez, J.A.; Galagovsky, L.R.; Gros, E.G.; Erra-Balsells, R. Singlet-oxygen ene reaction with 3β-substituted stigmastanes. An alternative pathway for the classical Schenck rearrangement. *J. Chem. Soc. Perkin Trans.* **2000**, *2*, 2351–2358. [[CrossRef](#)]
39. Samuel, D.; Norrell, K.; Hilmey, D.G. Novel ring chemistry of vitamin B6 with singlet oxygen and an activated ene: Isolated products and identified intermediates suggesting an operable [3 + 2] cycloaddition. *Org. Biomol. Chem.* **2012**, *10*, 7278–7281. [[CrossRef](#)]
40. Petrou, A.L.; Petrou, P.L.; Ntanos, T.; Liapis, A. A Possible Role for Singlet Oxygen in the Degradation of Various Antioxidants. A Meta-Analysis and Review of Literature Data. *Antioxidants* **2018**, *7*, 35. [[CrossRef](#)]
41. Zeinali, N.; Oluwoye, I.; Altarawneh, M.K.; Almatarneh, M.H.; Dlugogorski, B.Z. Probing the Reactivity of Singlet Oxygen with Cyclic Monoterpenes. *ACS Omega* **2019**, *4*, 14040–14048. [[CrossRef](#)]
42. Morales, J.; Günther, G.; Zanooco, A.L.; Lemp, E. Singlet oxygen reactions with flavonoids. A theoretical-experimental study. *PLoS ONE* **2012**, *7*, e40548. [[CrossRef](#)] [[PubMed](#)]
43. Chen, L.H.; Tsai, H.C.; Yu, P.L.; Chung, K.R. A Major Facilitator Superfamily Transporter-Mediated Resistance to Oxidative Stress and Fungicides Requires Yap1, Skn7, and MAP Kinases in the Citrus Fungal Pathogen *Alternaria alternata*. *PLoS ONE* **2017**, *12*, e0169103. [[CrossRef](#)] [[PubMed](#)]
44. Di Mascio, P.; Martinez, G.R.; Miyamoto, S.; Ronsein, G.E.; Medeiros, M.H.G.; Cadet, J. Singlet Molecular Oxygen Reactions with Nucleic Acids, Lipids, and Proteins. *Chem. Rev.* **2019**, *119*, 2043–2086. [[CrossRef](#)] [[PubMed](#)]
45. Kanofsky, J.R. Singlet oxygen production by biological systems. *Chem. Biol. Interact.* **1989**, *70*, 1–28. [[CrossRef](#)]
46. Dong, S.; Xu, J.; Jia, T.; Xu, M.; Zhong, C.; Yang, G.; Li, J.; Yang, D.; He, F.; Gai, S.; et al. Upconversion-mediated ZnFe<sub>2</sub>O<sub>4</sub> nanoplatforform for NIR-enhanced chemodynamic and photodynamic therapy. *Chem. Sci.* **2019**, *10*, 4259–4271. [[CrossRef](#)]
47. Choi, J.; Kim, S.Y. Synthesis of near-infrared-responsive hexagonal-phase upconversion nanoparticles with controllable shape and luminescence efficiency for theranostic applications. *J. Biomater. Appl.* **2022**, *37*, 646–658. [[CrossRef](#)]
48. Takajo, T.; Kurihara, Y.; Iwase, K.; Miyake, D.; Tsuchida, K.; Anzai, K. Basic Investigations of Singlet Oxygen Detection Systems with ESR for the Measurement of Singlet Oxygen Quenching Activities. *Chem. Pharm. Bull.* **2020**, *68*, 150–154. [[CrossRef](#)]
49. Yu, Y.Y.; Quan, W.Z.; Cao, Y.; Niu, Q.; Lu, Y.; Xiao, X.; Cheng, L. Boosting the singlet oxygen production from H<sub>2</sub>O<sub>2</sub> activation with highly dispersed Co-N-graphene for pollutant removal. *RSC Adv* **2022**, *12*, 17864–17872. [[CrossRef](#)]
50. Ruiz-González, R.; Bresolí-Obach, R.; Gulías, Ò.; Agut, M.; Savoie, H.; Boyle, R.W.; Nonell, S.; Giuntini, F. NanoSOSG: A Nanostructured Fluorescent Probe for the Detection of Intracellular Singlet Oxygen. *Angew Chem. Int. Ed. Engl.* **2017**, *56*, 2885–2888. [[CrossRef](#)]
51. Liu, H.; Carter, P.J.H.; Laan, A.C.; Eelkema, R.; Denkova, A.G. Singlet Oxygen Sensor Green is not a Suitable Probe for (<sup>1</sup>O<sub>2</sub>) in the Presence of Ionizing Radiation. *Sci. Rep.* **2019**, *9*, 8393. [[CrossRef](#)]
52. Girotti, A.W.; Korytowski, W. Cholesterol as a singlet oxygen detector in biological systems. *Methods Enzymol.* **2000**, *319*, 85–100. [[PubMed](#)]
53. Miyamoto, S.; Di Mascio, P. Lipid hydroperoxides as a source of singlet molecular oxygen. *Subcell Biochem.* **2014**, *77*, 3–20. [[PubMed](#)]
54. Torinuki, W.; Miura, T. Singlet oxygen emission at 1270 nm in protoporphyrin solution excited by argon laser. *Tohoku J. Exp. Med.* **1983**, *140*, 297–299. [[CrossRef](#)] [[PubMed](#)]
55. Baker, A.; Kanofsky, J.R. Direct observation of singlet oxygen phosphorescence at 1270 nm from L1210 leukemia cells exposed to polyporphyrin and light. *Arch. Biochem. Biophys.* **1991**, *286*, 70–75. [[CrossRef](#)]
56. Baker, A.; Kanofsky, J.R. Time-resolved studies of singlet-oxygen emission from L1210 leukemia cells labeled with 5-(N-hexadecanoyl)amino eosin. A comparison with a one-dimensional model of singlet-oxygen diffusion and quenching. *Photochem. Photobiol.* **1993**, *57*, 720–727. [[CrossRef](#)]
57. Oelckers, S.; Ziegler, T.; Michler, I.; Roder, B. Time-resolved detection of singlet oxygen luminescence in red-cell ghost suspensions: Concerning a signal component that can be attributed to <sup>1</sup>O<sub>2</sub> luminescence from the inside of a native membrane. *J. Photochem. Photobiol. B* **1999**, *53*, 121–127. [[CrossRef](#)] [[PubMed](#)]
58. Schweitzer, C.; Schmidt, R. Physical mechanisms of generation and deactivation of singlet oxygen. *Chem. Rev.* **2003**, *103*, 1685–1757. [[CrossRef](#)] [[PubMed](#)]
59. Niedre, M.; Patterson, M.S.; Wilson, B.C. Direct near-infrared luminescence detection of singlet oxygen generated by photodynamic therapy in cells in vitro and tissues in vivo. *Photochem. Photobiol.* **2002**, *75*, 382–391. [[CrossRef](#)]
60. Nosaka, Y.; Nosaka, A.Y. Generation and Detection of Reactive Oxygen Species in Photocatalysis. *Chem. Rev.* **2017**, *117*, 11302–11336. [[CrossRef](#)]
61. Lion, Y.; Delmelle, M.; van de Vorst, A. New method of detecting singlet oxygen production. *Nature* **1976**, *263*, 442–443. [[CrossRef](#)]
62. Moan, J.; Wold, E. Detection of singlet oxygen production by ESR. *Nature* **1979**, *279*, 450–451. [[CrossRef](#)]

63. Dzwigaj, S.; Pezerat, H. Singlet oxygen-trapping reaction as a method of (1)O<sub>2</sub> detection: Role of some reducing agents. *Free Radic. Res.* **1995**, *23*, 103–115. [[CrossRef](#)] [[PubMed](#)]
64. Victória, H.F.V.; Ferreira, D.C.; Filho, J.B.G.; Martins, D.C.S.; Pinheiro, M.V.B.; Sáfar, G.A.M.; Krambrock, K. Detection of singlet oxygen by EPR: The instability of the nitroxyl radicals. *Free Radic. Biol. Med.* **2022**, *180*, 143–152. [[CrossRef](#)] [[PubMed](#)]
65. Jung, M.Y.; Choi, D.S. Electron spin resonance and luminescence spectroscopic observation and kinetic study of chemical and physical singlet oxygen quenching by resveratrol in methanol. *J. Agric. Food Chem.* **2010**, *58*, 11888–11895. [[CrossRef](#)] [[PubMed](#)]
66. Kobayashi, K.; Maehata, Y.; Kawamura, Y.; Kusubata, M.; Hattori, S.; Tanaka, K.; Miyamoto, C.; Yoshino, F.; Yoshida, A.; Wada-Takahashi, S.; et al. Direct assessments of the antioxidant effects of the novel collagen peptide on reactive oxygen species using electron spin resonance spectroscopy. *J. Pharmacol. Sci.* **2011**, *116*, 97–106. [[CrossRef](#)] [[PubMed](#)]
67. Soh, N.; Katayama, Y.; Maeda, M. A fluorescent probe for monitoring nitric oxide production using a novel detection concept. *Analyst* **2001**, *126*, 564–566. [[CrossRef](#)] [[PubMed](#)]
68. Tanaka, K.; Miura, T.; Umezawa, N.; Urano, Y.; Kikuchi, K.; Higuchi, T.; Nagano, T. Rational design of fluorescein-based fluorescence probes. Mechanism-based design of a maximum fluorescence probe for singlet oxygen. *J. Am. Chem. Soc.* **2001**, *123*, 2530–2536. [[CrossRef](#)] [[PubMed](#)]
69. Gomes, A.; Fernandes, E.; Lima, J.L. Fluorescence probes used for detection of reactive oxygen species. *J. Biochem. Biophys. Methods* **2005**, *65*, 45–80. [[CrossRef](#)]
70. Corey, E.J.; Taylor, W.C. Study of the peroxidation of organic compounds by externally generated singlet oxygen molecules. *J. Am. Chem. Soc.* **1964**, *86*, 3881–3882. [[CrossRef](#)]
71. Francis Wilkinson, W.P.H.; Ross, A.B. Rate Constants for the Decay and Reactions of the Lowest Electronically Excited Singlet State of Molecular Oxygen in Solution. *J. Phys. Chem. Ref.* **1995**, *24*, 663–1021.
72. Umezawa, N.; Tanaka, K.; Urano, Y.; Kikuchi, K.; Higuchi, T.; Nagano, T. Novel Fluorescent Probes for Singlet Oxygen. *Angew. Chem. Int. Ed. Engl.* **1999**, *38*, 2899–2901. [[CrossRef](#)]
73. Flors, C.; Fryer, M.J.; Waring, J.; Reeder, B.; Bechtold, U.; Mullineaux, P.M.; Nonell, S.; Wilson, M.T.; Baker, N.R. Imaging the production of singlet oxygen in vivo using a new fluorescent sensor, Singlet Oxygen Sensor Green. *J. Exp. Bot.* **2006**, *57*, 1725–1734. [[CrossRef](#)]
74. Price, M.; Reiners, J.J.; Santiago, A.M.; Kessel, D. Monitoring singlet oxygen and hydroxyl radical formation with fluorescent probes during photodynamic therapy. *Photochem. Photobiol.* **2009**, *85*, 1177–1181. [[CrossRef](#)]
75. Ragas, X.; Jimenez-Banzo, A.; Sanchez-Garcia, D.; Batllori, X.; Nonell, S. Singlet oxygen photosensitisation by the fluorescent probe Singlet Oxygen Sensor Green. *Chem. Commun.* **2009**, *28*, 2920–2922. [[CrossRef](#)]
76. Kim, S.; Tachikawa, T.; Fujitsuka, M.; Majima, T. Far-red fluorescence probe for monitoring singlet oxygen during photodynamic therapy. *J. Am. Chem. Soc.* **2014**, *136*, 11707–11715. [[CrossRef](#)]
77. Murotomi, K.; Umeno, A.; Sugino, S.; Yoshida, Y. Quantitative kinetics of intracellular singlet oxygen generation using a fluorescence probe. *Sci. Rep.* **2020**, *10*, 10616. [[CrossRef](#)]
78. Chen, B.; Yang, Y.; Wang, Y.; Yan, Y.; Wang, Z.; Yin, Q.; Zhang, Q.; Wang, Y. Precise Monitoring of Singlet Oxygen in Specific Endocytic Organelles by Super-pH-Resolved Nanosensors. *ACS Appl. Mater. Interfaces* **2021**, *13*, 18533–18544. [[CrossRef](#)]
79. Nath, P.; Hamadna, S.S.; Karamchand, L.; Foster, J.; Kopelman, R.; Amar, J.G.; Ray, A. Intracellular detection of singlet oxygen using fluorescent nanosensors. *Analyst* **2021**, *146*, 3933–3941. [[CrossRef](#)]
80. Niki, E. Lipid peroxidation products as oxidative stress biomarkers. *Biofactors* **2008**, *34*, 171–180. [[CrossRef](#)]
81. Niki, E. Assessment of antioxidant capacity in vitro and in vivo. *Free Radic. Biol. Med.* **2010**, *49*, 503–515. [[CrossRef](#)]
82. Akazawa-Ogawa, Y.; Shichiri, M.; Nishio, K.; Yoshida, Y.; Niki, E.; Hagihara, Y. Singlet-oxygen-derived products from linoleate activate Nrf2 signaling in skin cells. *Free Radic. Biol. Med.* **2015**, *79*, 164–175. [[CrossRef](#)]
83. Murotomi, K.; Umeno, A.; Yasunaga, M.; Shichiri, M.; Ishida, N.; Abe, H.; Yoshida, Y.; Nakajima, Y. Switching from singlet-oxygen-mediated oxidation to free-radical-mediated oxidation in the pathogenesis of type 2 diabetes in model mouse. *Free Radic. Res.* **2015**, *49*, 133–138. [[CrossRef](#)] [[PubMed](#)]
84. Luchetti, F.; Canonico, B.; Cesarini, E.; Betti, M.; Galluzzi, L.; Galli, L.; Tippins, J.; Zerbinati, C.; Papa, S.; Iuliano, L. 7-Ketocholesterol and 5,6-secosterol induce human endothelial cell dysfunction by differential mechanisms. *Steroids* **2015**, *99*, 204–211. [[CrossRef](#)]
85. Dantas, L.S.; Chaves-Filho, A.B.; Coelho, F.R.; Genaro-Mattos, T.C.; Tallman, K.A.; Porter, N.A.; Augusto, O.; Miyamoto, S. Cholesterol secosterol aldehyde adduction and aggregation of Cu,Zn-superoxide dismutase: Potential implications in ALS. *Redox Biol.* **2018**, *19*, 105–115. [[CrossRef](#)]
86. Niki, E.; Yoshida, Y. Biomarkers for oxidative stress: Measurement, validation, and application. *J. Med. Invest.* **2005**, *52*, 228–230. [[CrossRef](#)]
87. Yoshida, Y.; Niki, E. Bio-markers of lipid peroxidation in vivo: Hydroxyoctadecadienoic acid and hydroxycholesterol. *Biofactors* **2006**, *27*, 195–202. [[CrossRef](#)]
88. Yoshida, Y.; Hayakawa, M.; Habuchi, Y.; Itoh, N.; Niki, E. Evaluation of lipophilic antioxidant efficacy in vivo by the biomarkers hydroxyoctadecadienoic acid and isoprostane. *Lipids* **2007**, *42*, 463–472. [[CrossRef](#)]
89. Yoshida, Y.; Kodai, S.; Takemura, S.; Minamiyama, Y.; Niki, E. Simultaneous measurement of F<sub>2</sub>-isoprostane, hydroxyoctadecadienoic acid, hydroxyeicosatetraenoic acid, and hydroxycholesterols from physiological samples. *Anal. Biochem.* **2008**, *379*, 105–115. [[CrossRef](#)]

90. Yoshida, Y.; Umeno, A.; Shichiri, M. Lipid peroxidation biomarkers for evaluating oxidative stress and assessing antioxidant capacity in vivo. *J. Clin. Biochem. Nutr.* **2013**, *52*, 9–16. [[CrossRef](#)]
91. Yoshida, Y.; Umeno, A.; Akazawa, Y.; Shichiri, M.; Murotomi, K.; Horie, M. Chemistry of lipid peroxidation products and their use as biomarkers in early detection of diseases. *J. Oleo Sci.* **2015**, *64*, 347–356. [[CrossRef](#)]
92. Umeno, A.; Shichiri, M.; Ishida, N.; Hashimoto, Y.; Abe, K.; Kataoka, M.; Yoshino, K.; Hagihara, Y.; Aki, N.; Funaki, M.; et al. Singlet oxygen induced products of linoleates, 10- and 12-(Z,E)-hydroxyoctadecadienoic acids (HODE), can be potential biomarkers for early detection of type 2 diabetes. *PLoS ONE* **2013**, *8*, e63542. [[CrossRef](#)] [[PubMed](#)]
93. Umeno, A.; Yoshino, K.; Hashimoto, Y.; Shichiri, M.; Kataoka, M.; Yoshida, Y. Multi-Biomarkers for Early Detection of Type 2 Diabetes, Including 10- and 12-(Z,E)-Hydroxyoctadecadienoic Acids, Insulin, Leptin, and Adiponectin. *PLoS ONE* **2015**, *10*, e0130971. [[CrossRef](#)] [[PubMed](#)]
94. Umeno, A.; Tanito, M.; Kaidzu, S.; Takai, Y.; Horie, M.; Yoshida, Y. Comprehensive measurements of hydroxylinoleate and hydroxyarachidonate isomers in blood samples from primary open-angle glaucoma patients and controls. *Sci. Rep.* **2019**, *9*, 2171. [[CrossRef](#)] [[PubMed](#)]
95. Kiessling, U.; Spitteller, G. The course of enzymatically induced lipid peroxidation in homogenized porcine kidney tissue. *Z. Naturforsch C J. Biosci.* **1998**, *53*, 431–437. [[CrossRef](#)]
96. Horie, M.; Miura, T.; Hirakata, S.; Hosoyama, A.; Sugino, S.; Umeno, A.; Murotomi, K.; Yoshida, Y.; Koike, T. Comparative analysis of the intestinal flora in type 2 diabetes and nondiabetic mice. *Exp. Anim.* **2017**, *66*, 405–416. [[CrossRef](#)]
97. Ogawa, H.; Azuma, M.; Umeno, A.; Shimizu, M.; Murotomi, K.; Yoshida, Y.; Nishioka, Y.; Tsuneyama, K. Singlet oxygen -derived nerve growth factor exacerbates airway hyperresponsiveness in a mouse model of asthma with mixed inflammation. *Allergol. Int.* **2022**, *71*, 395–404. [[CrossRef](#)]
98. Adachi, J.; Asano, M.; Naito, T.; Ueno, Y.; Imamichi, H.; Tatsuno, Y. Cholesterol hydroperoxides in erythrocyte membranes of alcoholic patients. *Alcohol. Clin. Exp. Res.* **1999**, *23*, 96s–100s. [[CrossRef](#)]
99. Yamazaki, S.; Ozawa, N.; Hiratsuka, A.; Watanabe, T. Quantitative determination of cholesterol 5alpha-, 7alpha-, and 7beta-hydroperoxides in rat skin. *Free Radic. Biol. Med.* **1999**, *27*, 110–118. [[CrossRef](#)]
100. Minami, Y.; Yokoi, S.; Setoyama, M.; Bando, N.; Takeda, S.; Kawai, Y.; Terao, J. Combination of TLC blotting and gas chromatography-mass spectrometry for analysis of peroxidized cholesterol. *Lipids* **2007**, *42*, 1055–1063. [[CrossRef](#)]
101. Minami, Y.; Kawabata, K.; Kubo, Y.; Arase, S.; Hirasaka, K.; Nikawa, T.; Bando, N.; Kawai, Y.; Terao, J. Peroxidized cholesterol-induced matrix metalloproteinase-9 activation and its suppression by dietary beta-carotene in photoaging of hairless mouse skin. *J. Nutr. Biochem.* **2009**, *20*, 389–398. [[CrossRef](#)]
102. Terao, J.; Minami, Y.; Bando, N. Singlet molecular oxygen-quenching activity of carotenoids: Relevance to protection of the skin from photoaging. *J. Clin. Biochem. Nutr.* **2011**, *48*, 57–62. [[CrossRef](#)] [[PubMed](#)]
103. Wentworth, P., Jr.; Nieva, J.; Takeuchi, C.; Galve, R.; Wentworth, A.D.; Dille, R.B.; DeLaria, G.A.; Saven, A.; Babior, B.M.; Janda, K.D.; et al. Evidence for ozone formation in human atherosclerotic arteries. *Science* **2003**, *302*, 1053–1056. [[CrossRef](#)] [[PubMed](#)]
104. Zhang, Q.; Powers, E.T.; Nieva, J.; Huff, M.E.; Dendle, M.A.; Bieschke, J.; Glabe, C.G.; Eschenmoser, A.; Wentworth, P., Jr.; Lerner, R.A.; et al. Metabolite-initiated protein misfolding may trigger Alzheimer's disease. *Proc. Natl. Acad. Sci. USA* **2004**, *101*, 4752–4757. [[CrossRef](#)] [[PubMed](#)]
105. Elshafei, M.E.; Minamiyama, Y.; Ichikawa, H. Singlet oxygen from endoperoxide initiates an intracellular reactive oxygen species release in HaCaT keratinocytes. *J. Clin. Biochem. Nutr.* **2022**, *71*, 198–205. [[CrossRef](#)]
106. Umar, S.A.; Shahid, N.H.; Nazir, L.A.; Tanveer, M.A.; Divya, G.; Archoo, S.; Raghu, S.R.; Tasduq, S.A. Pharmacological Activation of Autophagy Restores Cellular Homeostasis in Ultraviolet-(B)-Induced Skin Photodamage. *Front. Oncol.* **2021**, *11*, 726066. [[CrossRef](#)]
107. Mokrzyński, K.; Krzysztowska-Kuleta, O.; Zawrotniak, M.; Sarna, M.; Sarna, T. Fine Particulate Matter-Induced Oxidative Stress Mediated by UVA-Visible Light Leads to Keratinocyte Damage. *Int. J. Mol. Sci.* **2021**, *22*, 10645. [[CrossRef](#)] [[PubMed](#)]
108. Requena, M.B.; Russignoli, P.E.; Vollet-Filho, J.D.; Salvio, A.G.; Fortunato, T.C.; Pratavieira, S.; Bagnato, V.S. Use of dermograph for improvement of PpIX precursor's delivery in photodynamic therapy: Experimental and clinical pilot studies. *Photodiagnosis Photodyn. Ther.* **2020**, *29*, 101599. [[CrossRef](#)]
109. Pinto, M.A.F.; Ferreira, C.B.R.; de Lima, B.E.S.; Molon, Â.C.; Ibarra, A.M.C.; Cecatto, R.B.; Dos Santos Franco, A.L.; Rodrigues, M. Effects of 5-ALA mediated photodynamic therapy in oral cancer stem cells. *J. Photochem. Photobiol. B* **2022**, *235*, 112552. [[CrossRef](#)]
110. Arakane, K.; Ryu, A.; Hayashi, C.; Masunaga, T.; Shinmoto, K.; Mashiko, S.; Nagano, T.; Hirobe, M. Singlet oxygen ( $^1\Delta_g$ ) generation from coproporphyrin in *Propionibacterium acnes* on irradiation. *Biochem. Biophys. Res. Commun.* **1996**, *223*, 578–582. [[CrossRef](#)]
111. Patwardhan, S.V.; Richter, C.; Vogt, A.; Blume-Peytavi, U.; Canfield, D.; Kottner, J. Measuring acne using Coproporphyrin III, Protoporphyrin IX, and lesion-specific inflammation: An exploratory study. *Arch. Dermatol. Res.* **2017**, *309*, 159–167. [[CrossRef](#)]
112. Zhang, S.; Sun, X.; Wang, Z.; Sun, J.; He, Z.; Sun, B.; Luo, C. Molecularly Self-Engineered Nanoamplifier for Boosting Photodynamic Therapy via Cascade Oxygen Elevation and Lipid ROS Accumulation. *ACS Appl. Mater. Interfaces* **2022**, *14*, 38497–38505. [[CrossRef](#)] [[PubMed](#)]
113. Uliana, M.P.; da Cruz Rodrigues, A.; Ono, B.A.; Pratavieira, S.; de Oliveira, K.T.; Kurachi, C. Photodynamic Inactivation of Microorganisms Using Semisynthetic Chlorophyll a Derivatives as Photosensitizers. *Molecules* **2022**, *27*, 5769. [[CrossRef](#)] [[PubMed](#)]

114. Sugiura, M.; Azami, C.; Koyama, K.; Rutherford, A.W.; Rappaport, F.; Boussac, A. Modification of the pheophytin redox potential in *Thermosynechococcus elongatus* Photosystem II with PsbA3 as D1. *Biochim. Biophys. Acta* **2014**, *1837*, 139–148. [[CrossRef](#)] [[PubMed](#)]
115. Wang, E.; Braun, M.S.; Wink, M. Chlorophyll and Chlorophyll Derivatives Interfere with Multi-Drug Resistant Cancer Cells and Bacteria. *Molecules* **2019**, *24*, 2968. [[CrossRef](#)] [[PubMed](#)]
116. Zhao, Z.; Poojary, M.M.; Skibsted, L.H.; Lund, M.N. Cleavage of Disulfide Bonds in Cystine by UV-B Illumination Mediated by Tryptophan or Tyrosine as Photosensitizers. *J. Agric. Food Chem.* **2020**, *68*, 6900–6909. [[CrossRef](#)]
117. Ionita, G.; Matei, I. Application of Riboflavin Photochemical Properties in Hydrogel Synthesis. In *Biophysical Chemistry Advance Applications*; InTech Open: London, UK, 2020.
118. Wangsuwan, S.; Meephansan, J. Comparative Study Of Photodynamic Therapy With Riboflavin-Tryptophan Gel And 13% 5-Aminolevulinic Acid In The Treatment Of Mild To Moderate Acne Vulgaris. *Clin. Cosmet. Investig. Dermatol.* **2019**, *12*, 805–814. [[CrossRef](#)]
119. Chignell, C.F.; Kukielczak, B.M.; Sik, R.H.; Bilski, P.J.; He, Y.Y. Ultraviolet A sensitivity in Smith-Lemli-Opitz syndrome: Possible involvement of cholesta-5,7,9(11)-trien-3 beta-ol. *Free Radic. Biol. Med.* **2006**, *41*, 339–346. [[CrossRef](#)]
120. Bode, C.W.; Hänsel, W. 5-(3-Phenylpropoxy)psoralen and 5-(4-phenylbutoxy)psoralen: Mechanistic studies on phototoxicity. *Pharmazie* **2005**, *60*, 225–228.
121. Lee, K.P.; Girijala, R.L.; Chon, S.Y. Phytophotodermatitis due to a Citrus-Based Hand Sanitizer: A Case Report. *Korean J. Fam. Med.* **2022**, *43*, 271–273. [[CrossRef](#)]
122. Pappas, A. Epidermal surface lipids. *Dermatoendocrinology* **2009**, *1*, 72–76. [[CrossRef](#)]
123. Chapkin, R.S.; Ziboh, V.A.; Marcelo, C.L.; Voorhees, J.J. Metabolism of essential fatty acids by human epidermal enzyme preparations: Evidence of chain elongation. *J. Lipid Res.* **1986**, *27*, 945–954. [[CrossRef](#)]
124. Ni Raghallaigh, S.; Bender, K.; Lacey, N.; Brennan, L.; Powell, F.C. The fatty acid profile of the skin surface lipid layer in papulopustular rosacea. *Br. J. Dermatol.* **2012**, *166*, 279–287.
125. Shimizu, N.; Ito, J.; Kato, S.; Otoki, Y.; Goto, M.; Eitsuka, T.; Miyazawa, T.; Nakagawa, K. Oxidation of squalene by singlet oxygen and free radicals results in different compositions of squalene monohydroperoxide isomers. *Sci. Rep.* **2018**, *8*, 9116. [[CrossRef](#)] [[PubMed](#)]
126. Chiba, K.; Kawakami, K.; Sone, T.; Onoue, M. Characteristics of skin wrinkling and dermal changes induced by repeated application of squalene monohydroperoxide to hairless mouse skin. *Skin Pharmacol. Appl. Skin Physiol.* **2003**, *16*, 242–251. [[CrossRef](#)]
127. Chiba, K.; Yoshizawa, K.; Makino, I.; Kawakami, K.; Onoue, M. Comedogenicity of squalene monohydroperoxide in the skin after topical application. *J. Toxicol. Sci.* **2000**, *25*, 77–83. [[CrossRef](#)]
128. Khalifa, S.; Enomoto, M.; Kato, S.; Nakagawa, K. Novel Photoinduced Squalene Cyclic Peroxide Identified, Detected, and Quantified in Human Skin Surface Lipids. *Antioxidants* **2021**, *10*, 1760. [[CrossRef](#)]
129. Dalrymple, A.; McEwan, M.; Brandt, M.; Bielfeldt, S.; Bean, E.J.; Moga, A.; Coburn, S.; Hardie, G. A novel clinical method to measure skin staining reveals activation of skin damage pathways by cigarette smoke. *Skin Res. Technol.* **2022**, *28*, 162–170. [[CrossRef](#)] [[PubMed](#)]
130. Minami, Y.; Yokoyama, K.; Bando, N.; Kawai, Y.; Terao, J. Occurrence of singlet oxygen oxygenation of oleic acid and linoleic acid in the skin of live mice. *Free Radic. Res.* **2008**, *42*, 197–204. [[CrossRef](#)]
131. Egawa, M.; Kohno, Y.; Kumano, Y. Oxidative effects of cigarette smoke on the human skin. *Int. J. Cosmet. Sci.* **1999**, *21*, 83–98. [[CrossRef](#)] [[PubMed](#)]
132. Nakagawa, K.; Ibusuki, D.; Suzuki, Y.; Yamashita, S.; Higuchi, O.; Oikawa, S.; Miyazawa, T. Ion-trap tandem mass spectrometric analysis of squalene monohydroperoxide isomers in sunlight-exposed human skin. *J. Lipid Res.* **2007**, *48*, 2779–2787. [[CrossRef](#)] [[PubMed](#)]
133. Ekanayake-Mudiyanselage, S.; Tavakkol, A.; Polefka, T.G.; Nabi, Z.; Elsner, P.; Thiele, J.J. Vitamin E delivery to human skin by a rinse-off product: Penetration of alpha-tocopherol versus wash-out effects of skin surface lipids. *Skin Pharmacol. Physiol.* **2005**, *18*, 20–26. [[CrossRef](#)] [[PubMed](#)]
134. Ekanayake Mudiyanselage, S.; Hamburger, M.; Elsner, P.; Thiele, J.J. Ultraviolet a induces generation of squalene monohydroperoxide isomers in human sebum and skin surface lipids in vitro and in vivo. *J. Invest. Dermatol.* **2003**, *120*, 915–922. [[CrossRef](#)] [[PubMed](#)]
135. Auffray, B. Protection against singlet oxygen, the main actor of sebum squalene peroxidation during sun exposure, using *Commiphora myrrha* essential oil. *Int. J. Cosmet. Sci.* **2007**, *29*, 23–29. [[CrossRef](#)]
136. Lens, M.; Podesta Marty, M.H. Assessment of the kinetics of the antioxidative capacity of topical antioxidants. *J. Drugs Dermatol.* **2011**, *10*, 262–267. [[PubMed](#)]
137. Shimizu, N.; Ito, J.; Kato, S.; Eitsuka, T.; Saito, T.; Nishida, H.; Miyazawa, T.; Nakagawa, K. Evaluation of squalene oxidation mechanisms in human skin surface lipids and shark liver oil supplements. *Ann. N. Y. Acad. Sci.* **2019**, *1457*, 158–165. [[CrossRef](#)]
138. Jourdain, R.; Moga, A.; Vingler, P.; El Rawadi, C.; Pouradier, F.; Souverain, L.; Bastien, P.; Amalric, N.; Breton, L. Exploration of scalp surface lipids reveals squalene peroxide as a potential actor in dandruff condition. *Arch. Dermatol. Res.* **2016**, *308*, 153–163. [[CrossRef](#)] [[PubMed](#)]

139. Mountfort, K.A.; Bronstein, H.; Archer, N.; Jickells, S.M. Identification of oxidation products of squalene in solution and in latent fingerprints by ESI-MS and LC/APCI-MS. *Anal. Chem.* **2007**, *79*, 2650–2657. [[CrossRef](#)]
140. Curpen, S.; Francois-Newton, V.; Moga, A.; Hosenally, M.; Petkar, G.; Soobramaney, V.; Ruchaia, B.; Lutchmanen Kolanthan, V.; Roheemun, N.; Sokeechand, B.N.; et al. A novel method for evaluating the effect of pollution on the human skin under controlled conditions. *Skin Res. Technol.* **2020**, *26*, 50–60. [[CrossRef](#)]
141. Bielfeldt, S.; Jung, K.; Laing, S.; Moga, A.; Wilhelm, K.P. Anti-pollution effects of two antioxidants and a chelator-Ex vivo electron spin resonance and in vivo cigarette smoke model assessments in human skin. *Skin Res. Technol.* **2021**, *27*, 1092–1099. [[CrossRef](#)]
142. Someya, K.; Totsuka, Y.; Murakoshi, M.; Kitano, H.; Miyazawa, T. The antioxidant effect of palm fruit carotene on skin lipid peroxidation in guinea pigs as estimated by chemiluminescence-HPLC method. *J. Nutr. Sci. Vitaminol.* **1994**, *40*, 315–324. [[CrossRef](#)] [[PubMed](#)]
143. Pena, A.M.; Baldewick, T.; Decencièrre, E.; Koudoro, S.; Victorin, S.; Raynaud, E.; Ngo, B.; Bastien, P.; Brizion, S.; Tancredi-Bohin, E. In vivo multiphoton multiparametric 3D quantification of human skin aging on forearm and face. *Sci. Rep.* **2022**, *12*, 14863. [[CrossRef](#)] [[PubMed](#)]
144. Scharffetter, K.; Wlaschek, M.; Hogg, A.; Bolsen, K.; Schothorst, A.; Goerz, G.; Krieg, T.; Plewig, G. UVA irradiation induces collagenase in human dermal fibroblasts in vitro and in vivo. *Arch. Dermatol. Res.* **1991**, *283*, 506–511. [[CrossRef](#)]
145. Nakamura, T.; Noma, A.; Shimada, S.; Ishii, N.; Bando, N.; Kawai, Y.; Terao, J. Non-selective distribution of isomeric cholesterol hydroperoxides to microdomains in cell membranes and activation of matrix metalloproteinase activity in a model of dermal cells. *Chem. Phys. Lipids* **2013**, *174*, 17–23. [[CrossRef](#)] [[PubMed](#)]
146. Cadet, J.; Douki, T.; Ravanat, J.L. Oxidatively generated damage to the guanine moiety of DNA: Mechanistic aspects and formation in cells. *Acc. Chem. Res.* **2008**, *41*, 1075–1083. [[CrossRef](#)] [[PubMed](#)]
147. Cadet, J.; Douki, T.; Ravanat, J.L. Oxidatively generated damage to cellular DNA by UVB and UVA radiation. *Photochem. Photobiol.* **2015**, *91*, 140–155. [[CrossRef](#)] [[PubMed](#)]
148. Ravanat, J.L.; Di Mascio, P.; Martinez, G.R.; Medeiros, M.H.; Cadet, J. Singlet oxygen induces oxidation of cellular DNA. *J. Biol. Chem.* **2000**, *275*, 40601–40604. [[CrossRef](#)] [[PubMed](#)]
149. Yagura, T.; Schuch, A.P.; Garcia, C.C.M.; Rocha, C.R.R.; Moreno, N.C.; Angeli, J.P.F.; Mendes, D.; Severino, D.; Bianchini Sanchez, A.; Di Mascio, P.; et al. Direct participation of DNA in the formation of singlet oxygen and base damage under UVA irradiation. *Free Radic. Biol. Med.* **2017**, *108*, 86–93. [[CrossRef](#)]
150. Cadet, J.; Sage, E.; Douki, T. Ultraviolet radiation-mediated damage to cellular DNA. *Mutat. Res.* **2005**, *571*, 3–17. [[CrossRef](#)]
151. Mouret, S.; Baudouin, C.; Charveron, M.; Favier, A.; Cadet, J.; Douki, T. Cyclobutane pyrimidine dimers are predominant DNA lesions in whole human skin exposed to UVA radiation. *Proc. Natl. Acad. Sci. USA* **2006**, *103*, 13765–13770. [[CrossRef](#)]
152. Prat, F.; Hou, C.-C.; Foote, C.S. Determination of the Quenching Rate Constants of Singlet Oxygen by Derivatized Nucleosides in Nonaqueous Solution. *J. Am. Chem. Soc.* **1997**, *119*, 5051–5052. [[CrossRef](#)]
153. David, S.S.; O’Shea, V.L.; Kundu, S. Base-excision repair of oxidative DNA damage. *Nature* **2007**, *447*, 941–950. [[CrossRef](#)] [[PubMed](#)]
154. Hsu, G.W.; Ober, M.; Carell, T.; Beese, L.S. Error-prone replication of oxidatively damaged DNA by a high-fidelity DNA polymerase. *Nature* **2004**, *431*, 217–221. [[CrossRef](#)] [[PubMed](#)]
155. Greenman, C.; Stephens, P.; Smith, R.; Dalgliesh, G.L.; Hunter, C.; Bignell, G.; Davies, H.; Teague, J.; Butler, A.; Stevens, C.; et al. Patterns of somatic mutation in human cancer genomes. *Nature* **2007**, *446*, 153–158. [[CrossRef](#)] [[PubMed](#)]
156. Lindahl, T.; Barnes, D.E. Repair of endogenous DNA damage. *Cold Spring Harb. Symp. Quant. Biol.* **2000**, *65*, 127–133. [[CrossRef](#)]
157. Greinert, R.; Volkmer, B.; Henning, S.; Breitbart, E.W.; Greulich, K.O.; Cardoso, M.C.; Rapp, A. UVA-induced DNA double-strand breaks result from the repair of clustered oxidative DNA damages. *Nucleic Acids Res.* **2012**, *40*, 10263–10273. [[CrossRef](#)] [[PubMed](#)]
158. Agar, N.S.; Halliday, G.M.; Barnetson, R.S.; Ananthaswamy, H.N.; Wheeler, M.; Jones, A.M. The basal layer in human squamous tumors harbors more UVA than UVB fingerprint mutations: A role for UVA in human skin carcinogenesis. *Proc. Natl. Acad. Sci. USA* **2004**, *101*, 4954–4959. [[CrossRef](#)]
159. Kunisada, M.; Sakumi, K.; Tominaga, Y.; Budiyo, A.; Ueda, M.; Ichihashi, M.; Nakabeppu, Y.; Nishigori, C. 8-Oxoguanine formation induced by chronic UVB exposure makes Ogg1 knockout mice susceptible to skin carcinogenesis. *Cancer Res.* **2005**, *65*, 6006–6010. [[CrossRef](#)]
160. Kunisada, M.; Kumimoto, H.; Ishizaki, K.; Sakumi, K.; Nakabeppu, Y.; Nishigori, C. Narrow-band UVB induces more carcinogenic skin tumors than broad-band UVB through the formation of cyclobutane pyrimidine dimer. *J. Invest. Dermatol.* **2007**, *127*, 2865–2871. [[CrossRef](#)]
161. Zhang, R.B.; Eriksson, L.A. A triplet mechanism for the formation of cyclobutane pyrimidine dimers in UV-irradiated DNA. *J. Phys. Chem. B* **2006**, *110*, 7556–7562. [[CrossRef](#)]
162. You, Y.; Zhu, F.; Li, Z.; Zhang, L.; Xie, Y.; Chinnathambi, A.; Alahmadi, T.A.; Lu, B. Phyllanthin prevents diethylnitrosamine (DEN) induced liver carcinogenesis in rats and induces apoptotic cell death in HepG2 cells. *Biomed. Pharmacother.* **2021**, *137*, 111335. [[CrossRef](#)]
163. Yuan, H.; Guo, L.; Su, Q.; Su, X.; Wen, Y.; Wang, T.; Yang, P.; Xu, M.; Li, F. Afterglow Amplification for Fast and Sensitive Detection of Porphyrin in Whole Blood. *ACS Appl. Mater. Interfaces* **2021**, *13*, 27991–27998. [[CrossRef](#)]

164. Ventura, P.; Brancaleoni, V.; Di Pierro, E.; Graziadei, G.; Macrì, A.; Carmine Guida, C.; Nicolli, A.; Rossi, M.T.; Granata, F.; Fiorentino, V.; et al. Clinical and molecular epidemiology of erythropoietic protoporphyria in Italy. *Eur. J. Dermatol.* **2020**, *30*, 532–540. [[CrossRef](#)] [[PubMed](#)]
165. Balwani, M. Erythropoietic Protoporphyria and X-Linked Protoporphyria: Pathophysiology, genetics, clinical manifestations, and management. *Mol. Genet. Metab.* **2019**, *128*, 298–303. [[CrossRef](#)] [[PubMed](#)]
166. Mathews-Roth, M.M.; Pathak, M.A.; Fitzpatrick, T.B.; Harber, L.C.; Kass, E.H. Beta-carotene as a photoprotective agent in erythropoietic protoporphyria. *N. Engl. J. Med.* **1970**, *282*, 1231–1234. [[CrossRef](#)] [[PubMed](#)]
167. Black, H.S.; Boehm, F.; Edge, R.; Truscott, T.G. The Benefits and Risks of Certain Dietary Carotenoids that Exhibit both Anti- and Pro-Oxidative Mechanisms—A Comprehensive Review. *Antioxidants* **2020**, *9*, 264. [[CrossRef](#)]
168. Mathews-Roth, M.M.; Pathak, M.A.; Fitzpatrick, T.B.; Harber, L.H.; Kass, E.H. Beta carotene therapy for erythropoietic protoporphyria and other photosensitivity diseases. *Arch. Dermatol.* **1977**, *113*, 1229–1232. [[CrossRef](#)]
169. Maitra, D.; Bragazzi Cunha, J.; Elenbaas, J.S.; Bonkovsky, H.L.; Shavit, J.A.; Omary, M.B. Porphyrin-Induced Protein Oxidation and Aggregation as a Mechanism of Porphyria-Associated Cell Injury. *Cell Mol Gastroenterol. Hepatol.* **2019**, *8*, 535–548. [[CrossRef](#)]
170. Maitra, D.; Carter, E.L.; Richardson, R.; Rittié, L.; Basrur, V.; Zhang, H.; Nesvizhskii, A.I.; Osawa, Y.; Wolf, M.W.; Ragsdale, S.W.; et al. Oxygen and Conformation Dependent Protein Oxidation and Aggregation by Porphyrins in Hepatocytes and Light-Exposed Cells. *Cell Mol. Gastroenterol. Hepatol.* **2019**, *8*, 659–682.e651. [[CrossRef](#)]
171. Maitra, D.; Elenbaas, J.S.; Whitesall, S.E.; Basrur, V.; D’Alec, L.G.; Omary, M.B. Ambient Light Promotes Selective Subcellular Proteotoxicity after Endogenous and Exogenous Porphyrinogenic Stress. *J. Biol. Chem.* **2015**, *290*, 23711–23724. [[CrossRef](#)]
172. Tomita, H.; Hines, K.M.; Herron, J.M.; Li, A.; Baggett, D.W.; Xu, L. 7-Dehydrocholesterol-derived oxysterols cause neurogenic defects in Smith-Lemli-Opitz syndrome. *Elife* **2022**, *11*, e67141. [[CrossRef](#)]
173. Luo, Y.; Zhang, C.; Ma, L.; Zhang, Y.; Liu, Z.; Chen, L.; Wang, R.; Luan, Y.; Rao, Y. Measurement of 7-dehydrocholesterol and cholesterol in hair can be used in the diagnosis of Smith-Lemli-Opitz syndrome. *J. Lipid Res.* **2022**, *63*, 100228. [[CrossRef](#)]
174. Koczok, K.; Horváth, L.; Korade, Z.; Mezei, Z.A.; Szabó, G.P.; Porter, N.A.; Kovács, E.; Mirnics, K.; Balogh, I. Biochemical and Clinical Effects of Vitamin E Supplementation in Hungarian Smith-Lemli-Opitz Syndrome Patients. *Biomolecules* **2021**, *11*, 1228. [[CrossRef](#)] [[PubMed](#)]
175. Quiec, D.; Mazière, C.; Auclair, M.; Santus, R.; Gardette, J.; Redziniak, G.; Franchi, J.; Dubertret, L.; Mazière, J.C. Lovastatin enhances the photocytotoxicity of UVA radiation towards cultured N.C.T.C. 2544 human keratinocytes: Prevention by cholesterol supplementation and by a cathepsin inhibitor. *Biochem. J.* **1995**, *310 Pt 1*, 305–309. [[CrossRef](#)] [[PubMed](#)]
176. Alrashidi, A.; Rhodes, L.E.; Sharif, J.C.H.; Kreeshan, F.C.; Farrar, M.D.; Ahad, T. Systemic drug photosensitivity—Culprits, impact and investigation in 122 patients. *Photodermatol. Photoimmunol. Photomed.* **2020**, *36*, 441–451. [[CrossRef](#)]
177. Chen, H.L.; Chang, H.M.; Wu, H.J.; Lin, Y.C.; Chang, Y.H.; Chang, Y.C.; Lee, W.H.; Chang, C.T. Effect of hydrophilic and lipophilic statins on early onset cataract: A nationwide case-control study. *Regul. Toxicol. Pharmacol.* **2021**, *124*, 104970. [[CrossRef](#)] [[PubMed](#)]
178. Yang, J.; Zhang, B.W.; Lin, L.N.; Zan, X.L.; Zhang, G.C.; Chen, G.S.; Ji, J.Y.; Ma, W.H. Key factors affecting photoactivated fungicidal activity of sodium pheophorbide a against *Pestalotiopsis neglecta*. *Pestic. Biochem. Physiol.* **2020**, *167*, 104584. [[CrossRef](#)]
179. Kobayashi, T.; Sugaya, K.; Onose, J.I.; Abe, N. Peppermint (*Mentha piperita* L.) extract effectively inhibits cytochrome P450 3A4 (CYP3A4) mRNA induction in rifampicin-treated HepG2 cells. *Biosci. Biotechnol. Biochem.* **2019**, *83*, 1181–1192. [[CrossRef](#)]
180. Puschner, B.; Chen, X.; Read, D.; Affolter, V.K. Alfalfa hay induced primary photosensitization in horses. *Vet. J.* **2016**, *211*, 32–38. [[CrossRef](#)]
181. Bayoumy, A.B.; Crouwel, F.; Chanda, N.; Florin, T.H.J.; Buijter, H.J.C.; Mulder, C.J.J.; de Boer, N.K.H. Advances in Thiopurine Drug Delivery: The Current State-of-the-Art. *Eur. J. Drug Metab. Pharmacokinet.* **2021**, *46*, 743–758. [[CrossRef](#)]
182. Euvrard, S.; Kanitakis, J.; Claudy, A. Skin cancers after organ transplantation. *N. Engl. J. Med.* **2003**, *348*, 1681–1691. [[CrossRef](#)]
183. Bignon, E.; Marazzi, M.; Besancenot, V.; Gattuso, H.; Drouot, G.; Morell, C.; Eriksson, L.A.; Grandemange, S.; Dumont, E.; Monari, A. Ibuprofen and ketoprofen potentiate UVA-induced cell death by a photosensitization process. *Sci. Rep.* **2017**, *7*, 8885. [[CrossRef](#)] [[PubMed](#)]
184. Zawadzka, M.; Rącz, B.; Ambrosini, D.; Görbitz, C.H.; Morth, J.P.; Wilkins, A.L.; Østeby, A.; Elgstøen, K.B.P.; Lundanes, E.; Rise, F.; et al. Searching for a UV-filter in the eyes of high-flying birds. *Sci. Rep.* **2021**, *11*, 273. [[CrossRef](#)] [[PubMed](#)]
185. Guan, L.L.; Lim, H.W.; Mohammad, T.F. Sunscreens and Photoaging: A Review of Current Literature. *Am. J. Clin. Dermatol.* **2021**, *22*, 819–828. [[CrossRef](#)]
186. Behar-Cohen, F.; Martinsons, C.; Viénot, F.; Zissis, G.; Barlier-Salsi, A.; Cesarini, J.P.; Enouf, O.; Garcia, M.; Picaud, S.; Attia, D. Light-emitting diodes (LED) for domestic lighting: Any risks for the eye? *Prog. Retin. Eye Res.* **2011**, *30*, 239–257. [[CrossRef](#)] [[PubMed](#)]
187. Tao, J.X.; Zhou, W.C.; Zhu, X.G. Mitochondria as Potential Targets and Initiators of the Blue Light Hazard to the Retina. *Oxid. Med. Cell. Longev.* **2019**, *2019*, 6435364. [[CrossRef](#)] [[PubMed](#)]
188. Kaarniranta, K.; Blasiak, J.; Liton, P.; Boulton, M.; Klionsky, D.J.; Sinha, D. Autophagy in age-related macular degeneration. *Autophagy* **2023**, *19*, 388–400. [[CrossRef](#)] [[PubMed](#)]
189. Rózanowska, M.B.; Pawlak, A.; Rózanowski, B. Products of Docosahexaenoate Oxidation as Contributors to Photosensitising Properties of Retinal Lipofuscin. *Int. J. Mol. Sci.* **2021**, *22*, 3525. [[CrossRef](#)]
190. Höhn, A.; Grune, T. Lipofuscin: Formation, effects and role of macroautophagy. *Redox Biol.* **2013**, *1*, 140–144. [[CrossRef](#)]

191. Singh Kushwaha, S.; Patro, N.; Kumar Patro, I. A Sequential Study of Age-Related Lipofuscin Accumulation in Hippocampus and Striate Cortex of Rats. *Ann. Neurosci.* **2018**, *25*, 223–233. [[CrossRef](#)]
192. Gao, Z.; Liao, Y.; Chen, C.; Liao, C.; He, D.; Chen, J.; Ma, J.; Liu, Z.; Wu, Y. Conversion of all-trans-retinal into all-trans-retinal dimer reflects an alternative metabolic/antidotal pathway of all-trans-retinal in the retina. *J. Biol. Chem.* **2018**, *293*, 14507–14519. [[CrossRef](#)]
193. Parish, C.A.; Hashimoto, M.; Nakanishi, K.; Dillon, J.; Sparrow, J. Isolation and one-step preparation of A2E and iso-A2E, fluorophores from human retinal pigment epithelium. *Proc. Natl. Acad. Sci. USA* **1998**, *95*, 14609–14613. [[CrossRef](#)] [[PubMed](#)]
194. Marie, M.; Bigot, K.; Angebault, C.; Barrau, C.; Gondouin, P.; Pagan, D.; Fouquet, S.; Villette, T.; Sahel, J.A.; Lenaers, G.; et al. Light action spectrum on oxidative stress and mitochondrial damage in A2E-loaded retinal pigment epithelium cells. *Cell Death Dis.* **2018**, *9*, 287. [[CrossRef](#)] [[PubMed](#)]
195. Bernstein, P.S.; Li, B.; Vachali, P.P.; Gorusupudi, A.; Shyam, R.; Henriksen, B.S.; Nolan, J.M. Lutein, zeaxanthin, and meso-zeaxanthin: The basic and clinical science underlying carotenoid-based nutritional interventions against ocular disease. *Prog. Retin. Eye Res.* **2016**, *50*, 34–66. [[CrossRef](#)] [[PubMed](#)]
196. Lem, D.W.; Davey, P.G.; Gierhart, D.L.; Rosen, R.B. A Systematic Review of Carotenoids in the Management of Age-Related Macular Degeneration. *Antioxidants* **2021**, *10*, 1255. [[CrossRef](#)] [[PubMed](#)]
197. Shyam, R.; Gorusupudi, A.; Nelson, K.; Horvath, M.P.; Bernstein, P.S. RPE65 has an additional function as the lutein to meso-zeaxanthin isomerase in the vertebrate eye. *Proc. Natl. Acad. Sci. USA* **2017**, *114*, 10882–10887. [[CrossRef](#)] [[PubMed](#)]
198. Johra, F.T.; Bepari, A.K.; Bristy, A.T.; Reza, H.M. A Mechanistic Review of  $\beta$ -Carotene, Lutein, and Zeaxanthin in Eye Health and Disease. *Antioxidants* **2020**, *9*, 1046. [[CrossRef](#)] [[PubMed](#)]
199. Mizdrak, J.; Hains, P.G.; Truscott, R.J.; Jamie, J.F.; Davies, M.J. Tryptophan-derived ultraviolet filter compounds covalently bound to lens proteins are photosensitizers of oxidative damage. *Free Radic. Biol. Med.* **2008**, *44*, 1108–1119. [[CrossRef](#)]
200. Ouyang, X.; Yang, J.; Hong, Z.; Wu, Y.; Xie, Y.; Wang, G. Mechanisms of blue light-induced eye hazard and protective measures: A review. *Biomed. Pharmacother.* **2020**, *130*, 110577. [[CrossRef](#)]
201. Boulton, M.; Rozanowska, M.; Rozanowski, B.; Wess, T. The photoreactivity of ocular lipofuscin. *Photochem. Photobiol. Sci. Off. J. Eur. Photochem. Assoc. Eur. Soc. Photobiol.* **2004**, *3*, 759–764. [[CrossRef](#)]
202. Weinreb, R.N.; Khaw, P.T. Primary open-angle glaucoma. *Lancet* **2004**, *363*, 1711–1720. [[CrossRef](#)]
203. Foster, A.; Resnikoff, S. The impact of Vision 2020 on global blindness. *Eye* **2005**, *19*, 1133–1135. [[CrossRef](#)] [[PubMed](#)]
204. Tanito, M.; Kaidzu, S.; Takai, Y.; Ohira, A. Status of systemic oxidative stresses in patients with primary open-angle glaucoma and pseudoexfoliation syndrome. *PLoS ONE* **2012**, *7*, e49680. [[CrossRef](#)] [[PubMed](#)]
205. Alvarado, J.A.; Murphy, C.G. Outflow obstruction in pigmentary and primary open angle glaucoma. *Arch. Ophthalmol.* **1992**, *110*, 1769–1778. [[CrossRef](#)] [[PubMed](#)]
206. Himori, N.; Yamamoto, K.; Maruyama, K.; Ryu, M.; Taguchi, K.; Yamamoto, M.; Nakazawa, T. Critical role of Nrf2 in oxidative stress-induced retinal ganglion cell death. *J. Neurochem.* **2013**, *127*, 669–680. [[CrossRef](#)] [[PubMed](#)]
207. Yokoyama, Y.; Maruyama, K.; Yamamoto, K.; Omodaka, K.; Yasuda, M.; Himori, N.; Ryu, M.; Nishiguchi, K.M.; Nakazawa, T. The role of calpain in an in vivo model of oxidative stress-induced retinal ganglion cell damage. *Biochem. Biophys. Res. Commun.* **2014**, *451*, 510–515. [[CrossRef](#)]
208. Inomata, Y.; Nakamura, H.; Tanito, M.; Teratani, A.; Kawaji, T.; Kondo, N.; Yodoi, J.; Tanihara, H. Thioredoxin inhibits NMDA-induced neurotoxicity in the rat retina. *J. Neurochem.* **2006**, *98*, 372–385. [[CrossRef](#)]
209. Munemasa, Y.; Ahn, J.H.; Kwong, J.M.; Caprioli, J.; Piri, N. Redox proteins thioredoxin 1 and thioredoxin 2 support retinal ganglion cell survival in experimental glaucoma. *Gene Ther.* **2009**, *16*, 17–25. [[CrossRef](#)]
210. Umeno, A.; Tanito, M.; Kaidzu, S.; Takai, Y.; Yoshida, Y. Involvement of free radical-mediated oxidation in the pathogenesis of pseudoexfoliation syndrome detected based on specific hydroxylinoleate isomers. *Free Radic. Biol. Med.* **2020**, *147*, 61–68. [[CrossRef](#)] [[PubMed](#)]
211. Umeno, A.; Yoshida, Y.; Kaidzu, S.; Tanito, M. Positive Association between Aqueous Humor Hydroxylinoleate Levels and Intraocular Pressure. *Molecules* **2022**, *27*, 2215. [[CrossRef](#)]
212. Schafheimer, N.; King, J. Tryptophan cluster protects human  $\gamma$ D-crystallin from ultraviolet radiation-induced photoaggregation in vitro. *Photochem. Photobiol.* **2013**, *89*, 1106–1115. [[CrossRef](#)] [[PubMed](#)]
213. Yoshida, Y.; Hayakawa, M.; Habuchi, Y.; Niki, E. Evaluation of the dietary effects of coenzyme Q in vivo by the oxidative stress marker, hydroxyoctadecadienoic acid and its stereoisomer ratio. *Biochim. Biophys. Acta* **2006**, *1760*, 1558–1568. [[CrossRef](#)] [[PubMed](#)]
214. Hirashima, Y.; Doshi, M.; Hayashi, N.; Endo, S.; Akazawa, Y.; Shichiri, M.; Yoshida, Y. Plasma platelet-activating factor-acetyl hydrolase activity and the levels of free forms of biomarker of lipid peroxidation in cerebrospinal fluid of patients with aneurysmal subarachnoid hemorrhage. *Neurosurgery* **2012**, *70*, 602–609. [[CrossRef](#)]
215. Fan Gaskin, J.C.; Shah, M.H.; Chan, E.C. Oxidative Stress and the Role of NADPH Oxidase in Glaucoma. *Antioxidants* **2021**, *10*, 238. [[CrossRef](#)] [[PubMed](#)]
216. Garcia-Medina, J.J.; Rubio-Velazquez, E.; Lopez-Bernal, M.D.; Cobo-Martinez, A.; Zanon-Moreno, V.; Pinazo-Duran, M.D.; Del-Rio-Vellosillo, M. Glaucoma and Antioxidants: Review and Update. *Antioxidants* **2020**, *9*, 1031. [[CrossRef](#)] [[PubMed](#)]
217. Tang, B.; Li, S.; Cao, W.; Sun, X. The Association of Oxidative Stress Status with Open-Angle Glaucoma and Exfoliation Glaucoma: A Systematic Review and Meta-Analysis. *J. Ophthalmol.* **2019**, *2019*, 1803619. [[CrossRef](#)]

218. Neale, R.E.; Purdie, J.L.; Hirst, L.W.; Green, A.C. Sun exposure as a risk factor for nuclear cataract. *Epidemiology* **2003**, *14*, 707–712. [[CrossRef](#)]
219. Garzón-Chavez, D.R.; Quentin, E.; Harrison, S.L.; Parisi, A.V.; Butler, H.J.; Downs, N.J. The geospatial relationship of pterygium and senile cataract with ambient solar ultraviolet in tropical Ecuador. *Photochem. Photobiol. Sci. Off. J. Eur. Photochem. Assoc. Eur. Soc. Photobiol.* **2018**, *17*, 1075–1083. [[CrossRef](#)]
220. Dillon, J.; Atherton, S.J. Time resolved spectroscopic studies on the intact human lens. *Photochem. Photobiol.* **1990**, *51*, 465–468. [[CrossRef](#)]
221. Kessel, L.; Eskildsen, L.; Lundeman, J.H.; Jensen, O.B.; Larsen, M. Optical effects of exposing intact human lenses to ultraviolet radiation and visible light. *BMC Ophthalmol.* **2011**, *11*, 41. [[CrossRef](#)]
222. Davies, M.J.; Truscott, R.J. Photo-oxidation of proteins and its role in cataractogenesis. *J. Photochem. Photobiol. B* **2001**, *63*, 114–125. [[CrossRef](#)]
223. Ehrenshaft, M.; Zhao, B.; Andley, U.P.; Mason, R.P.; Roberts, J.E. Immunological detection of N-formylkynurenine in porphyrin-mediated photooxidized lens  $\alpha$ -crystallin. *Photochem. Photobiol.* **2011**, *87*, 1321–1329. [[CrossRef](#)] [[PubMed](#)]
224. Benedek, G.B. Theory of transparency of the eye. *Appl. Opt.* **1971**, *10*, 459–473. [[CrossRef](#)] [[PubMed](#)]
225. Ávila, F.; Ravello, N.; Zanicco, A.L.; Gamon, L.F.; Davies, M.J.; Silva, E. 3-Hydroxykynurenine bound to eye lens proteins induces oxidative modifications in crystalline proteins through a type I photosensitizing mechanism. *Free Radic. Biol. Med.* **2019**, *141*, 103–114. [[CrossRef](#)]
226. Parker, N.R.; Jamie, J.F.; Davies, M.J.; Truscott, R.J. Protein-bound kynurenine is a photosensitizer of oxidative damage. *Free Radic. Biol. Med.* **2004**, *37*, 1479–1489. [[CrossRef](#)]
227. Ratter-Rieck, J.M.; Maalmi, H.; Trenkamp, S.; Zaharia, O.P.; Rathmann, W.; Schloot, N.C.; Straßburger, K.; Szendroedi, J.; Herder, C.; Roden, M. Leukocyte Counts and T-Cell Frequencies Differ Between Novel Subgroups of Diabetes and Are Associated With Metabolic Parameters and Biomarkers of Inflammation. *Diabetes* **2021**, *70*, 2652–2662. [[CrossRef](#)] [[PubMed](#)]
228. Penno, G.; Solini, A.; Orsi, E.; Bonora, E.; Fondelli, C.; Trevisan, R.; Vedovato, M.; Cavalot, F.; Zerbini, G.; Lamacchia, O.; et al. Insulin resistance, diabetic kidney disease, and all-cause mortality in individuals with type 2 diabetes: A prospective cohort study. *BMC Med.* **2021**, *19*, 66. [[CrossRef](#)] [[PubMed](#)]
229. Li, Z.; Xu, Y.; Liu, X.; Nie, Y.; Zhao, Z. Urinary heme oxygenase-1 as a potential biomarker for early diabetic nephropathy. *Nephrology* **2017**, *22*, 58–64. [[CrossRef](#)]
230. Xu, G.W.; Yao, Q.H.; Weng, Q.F.; Su, B.L.; Zhang, X.; Xiong, J.H. Study of urinary 8-hydroxydeoxyguanosine as a biomarker of oxidative DNA damage in diabetic nephropathy patients. *J. Pharm. Biomed. Anal.* **2004**, *36*, 101–104. [[CrossRef](#)]
231. Maschirow, L.; Khalaf, K.; Al-Aubaidy, H.A.; Jelinek, H.F. Inflammation, coagulation, endothelial dysfunction and oxidative stress in prediabetes—Biomarkers as a possible tool for early disease detection for rural screening. *Clin. Biochem.* **2015**, *48*, 581–585. [[CrossRef](#)] [[PubMed](#)]
232. Lv, C.; Zhou, Y.H.; Wu, C.; Shao, Y.; Lu, C.L.; Wang, Q.Y. The changes in miR-130b levels in human serum and the correlation with the severity of diabetic nephropathy. *Diabetes Metab. Res. Rev.* **2015**, *31*, 717–724. [[CrossRef](#)]
233. Sánchez-Gómez, F.J.; Espinosa-Díez, C.; Dubey, M.; Dikshit, M.; Lamas, S. S-glutathionylation: Relevance in diabetes and potential role as a biomarker. *Biol. Chem.* **2013**, *394*, 1263–1280. [[CrossRef](#)] [[PubMed](#)]
234. Liang, M.; Wang, J.; Xie, C.; Yang, Y.; Tian, J.W.; Xue, Y.M.; Hou, F.F. Increased plasma advanced oxidation protein products is an early marker of endothelial dysfunction in type 2 diabetes patients without albuminuria 2. *J. Diabetes* **2014**, *6*, 417–426. [[CrossRef](#)]
235. Ceriello, A.; Testa, R.; Genovese, S. Clinical implications of oxidative stress and potential role of natural antioxidants in diabetic vascular complications. *Nutr. Metab. Cardiovasc. Dis.* **2016**, *26*, 285–292. [[CrossRef](#)] [[PubMed](#)]
236. Paneni, F.; Costantino, S.; Cosentino, F. Molecular mechanisms of vascular dysfunction and cardiovascular biomarkers in type 2 diabetes. *Cardiovasc. Diagn. Ther.* **2014**, *4*, 324–332. [[PubMed](#)]
237. Molnar, J.; Garamvolgyi, Z.; Herold, M.; Adanyi, N.; Somogyi, A.; Rigo, J., Jr. Serum selenium concentrations correlate significantly with inflammatory biomarker high-sensitive CRP levels in Hungarian gestational diabetic and healthy pregnant women at mid-pregnancy. *Biol. Trace Elem. Res.* **2008**, *121*, 16–22. [[CrossRef](#)] [[PubMed](#)]
238. Basu, A.; Yu, J.Y.; Jenkins, A.J.; Nankervis, A.J.; Hanssen, K.F.; Henriksen, T.; Lorentzen, B.; Garg, S.K.; Menard, M.K.; Hammad, S.M.; et al. Trace elements as predictors of preeclampsia in type 1 diabetic pregnancy. *Nutr. Res.* **2015**, *35*, 421–430. [[CrossRef](#)]
239. Morabito, R.; Remigante, A.; Spinelli, S.; Vitale, G.; Trichilo, V.; Loddo, S.; Marino, A. High Glucose Concentrations Affect Band 3 Protein in Human Erythrocytes. *Antioxidants* **2020**, *9*, 365. [[CrossRef](#)]
240. Chai, J.F.; Kao, S.L.; Wang, C.; Lim, V.J.; Khor, I.W.; Dou, J.; Podgornaia, A.I.; Chothani, S.; Cheng, C.Y.; Sabanayagam, C.; et al. Genome-Wide Association for HbA1c in Malay Identified Deletion on SLC4A1 that Influences HbA1c Independent of Glycemia. *J. Clin. Endocrinol. Metab.* **2020**, *105*, dgaa658. [[CrossRef](#)]
241. Zhekova, H.R.; Jiang, J.; Wang, W.; Tsirulnikov, K.; Kayik, G.; Khan, H.M.; Azimov, R.; Abuladze, N.; Kao, L.; Newman, D.; et al. CryoEM structures of anion exchanger 1 capture multiple states of inward- and outward-facing conformations. *Commun. Biol.* **2022**, *5*, 1372. [[CrossRef](#)]
242. Kostopoulou, E.; Kalaitzopoulou, E.; Papadea, P.; Skipitari, M.; Rojas Gil, A.P.; Spiliotis, B.E.; Georgiou, C.D. Oxidized lipid-associated protein damage in children and adolescents with type 1 diabetes mellitus: New diagnostic/prognostic clinical markers. *Pediatr. Diabetes* **2021**, *22*, 1135–1142. [[CrossRef](#)]

243. Veitch, S.; Njock, M.S.; Chandy, M.; Siraj, M.A.; Chi, L.; Mak, H.; Yu, K.; Rathnakumar, K.; Perez-Romero, C.A.; Chen, Z.; et al. MiR-30 promotes fatty acid beta-oxidation and endothelial cell dysfunction and is a circulating biomarker of coronary microvascular dysfunction in pre-clinical models of diabetes. *Cardiovasc. Diabetol.* **2022**, *21*, 31. [[CrossRef](#)] [[PubMed](#)]
244. Griesser, E.; Vemula, V.; Raulien, N.; Wagner, U.; Reeg, S.; Grune, T.; Fedorova, M. Cross-talk between lipid and protein carbonylation in a dynamic cardiomyocyte model of mild nitroxidative stress. *Redox Biol* **2017**, *11*, 438–455. [[CrossRef](#)]
245. Schöttker, B.; Xuan, Y.; Gào, X.; Anusruti, A.; Brenner, H. Oxidatively Damaged DNA/RNA and 8-Isoprostane Levels Are Associated with the Development of Type 2 Diabetes at Older Age: Results From a Large Cohort Study. *Diabetes Care* **2020**, *43*, 130–136. [[CrossRef](#)]
246. Leinisch, F.; Mariotti, M.; Hägglund, P.; Davies, M.J. Structural and functional changes in RNase A originating from tyrosine and histidine cross-linking and oxidation induced by singlet oxygen and peroxy radicals. *Free Radic. Biol. Med.* **2018**, *126*, 73–86. [[CrossRef](#)] [[PubMed](#)]
247. Miyamoto, S.; Martinez, G.R.; Medeiros, M.H.; Di Mascio, P. Singlet molecular oxygen generated by biological hydroperoxides. *J. Photochem. Photobiol. B* **2014**, *139*, 24–33. [[CrossRef](#)]
248. Umeno, A.; Fukui, T.; Hashimoto, Y.; Kataoka, M.; Hagihara, Y.; Nagai, H.; Horie, M.; Shichiri, M.; Yoshino, K.; Yoshida, Y. Early diagnosis of type 2 diabetes based on multiple biomarkers and non-invasive indices. *J. Clin. Biochem. Nutr.* **2018**, *62*, 187–194. [[CrossRef](#)]
249. Hampton, M.B.; Kettle, A.J.; Winterbourn, C.C. Inside the neutrophil phagosome: Oxidants, myeloperoxidase, and bacterial killing. *Blood* **1998**, *92*, 3007–3017. [[CrossRef](#)]
250. Badwey, J.A.; Karnovsky, M.L. Active oxygen species and the functions of phagocytic leukocytes. *Annu. Rev. Biochem.* **1980**, *49*, 695–726. [[CrossRef](#)] [[PubMed](#)]
251. Kanofsky, J.R. Singlet oxygen production from the peroxidase-catalyzed oxidation of indole-3-acetic acid. *J. Biol. Chem.* **1988**, *263*, 14171–14175. [[CrossRef](#)] [[PubMed](#)]
252. Miyamoto, S.; Martinez, G.R.; Rettori, D.; Augusto, O.; Medeiros, M.H.; Di Mascio, P. Linoleic acid hydroperoxide reacts with hypochlorous acid, generating peroxy radical intermediates and singlet molecular oxygen. *Proc. Natl. Acad. Sci. USA* **2006**, *103*, 293–298. [[CrossRef](#)]
253. Tian, R.; Ding, Y.; Peng, Y.Y.; Lu, N. Myeloperoxidase amplified high glucose-induced endothelial dysfunction in vasculature: Role of NADPH oxidase and hypochlorous acid. *Biochem. Biophys. Res. Commun.* **2017**, *484*, 572–578. [[CrossRef](#)] [[PubMed](#)]
254. Zhang, C.; Yang, J.; Jennings, L.K. Leukocyte-derived myeloperoxidase amplifies high-glucose-induced endothelial dysfunction through interaction with high-glucose—Stimulated, vascular non—Leukocyte-derived reactive oxygen species. *Diabetes* **2004**, *53*, 2950–2959. [[CrossRef](#)] [[PubMed](#)]
255. Zhang, C.; Yang, J.; Jacobs, J.D.; Jennings, L.K. Interaction of myeloperoxidase with vascular NAD(P)H oxidase-derived reactive oxygen species in vasculature: Implications for vascular diseases. *Am. J. Physiol. Heart Circ. Physiol.* **2003**, *285*, H2563–H2572. [[CrossRef](#)] [[PubMed](#)]
256. Eiserich, J.P.; Baldus, S.; Brennan, M.L.; Ma, W.; Zhang, C.; Tousson, A.; Castro, L.; Lusa, A.J.; Nauseef, W.M.; White, C.R.; et al. Myeloperoxidase, a leukocyte-derived vascular NO oxidase. *Science* **2002**, *296*, 2391–2394. [[CrossRef](#)] [[PubMed](#)]
257. Nussbaum, C.; Klinke, A.; Adam, M.; Baldus, S.; Sperandio, M. Myeloperoxidase: A leukocyte-derived protagonist of inflammation and cardiovascular disease. *Antioxid. Redox Signal* **2013**, *18*, 692–713. [[CrossRef](#)]
258. Tian, R.; Jin, Z.; Zhou, L.; Zeng, X.P.; Lu, N. Quercetin Attenuated Myeloperoxidase-Dependent HOCl Generation and Endothelial Dysfunction in Diabetic Vasculature. *J. Agric. Food Chem.* **2021**, *69*, 404–413. [[CrossRef](#)]
259. Onyango, A.N. The Contribution of Singlet Oxygen to Insulin Resistance. *Oxid. Med. Cell. Longev.* **2017**, *2017*, 8765972. [[CrossRef](#)]
260. Nakamura, Y.; Tamaoki, J.; Nagase, H.; Yamaguchi, M.; Horiguchi, T.; Hozawa, S.; Ichinose, M.; Iwanaga, T.; Kondo, R.; Nagata, M.; et al. Japanese guidelines for adult asthma 2020. *Allergol. Int.* **2020**, *69*, 519–548. [[CrossRef](#)]
261. Kaur, R.; Chupp, G. Phenotypes and endotypes of adult asthma: Moving toward precision medicine. *J. Allergy Clin. Immunol.* **2019**, *144*, 1–12. [[CrossRef](#)]
262. Hekking, P.W.; Wener, R.R.; Amelink, M.; Zwinderman, A.H.; Bouvy, M.L.; Bel, E.H. The prevalence of severe refractory asthma. *J. Allergy Clin. Immunol.* **2015**, *135*, 896–902. [[CrossRef](#)]
263. Hammad, H.; Lambrecht, B.N. The basic immunology of asthma. *Cell* **2021**, *184*, 1469–1485. [[CrossRef](#)]
264. Lambrecht, B.N.; Hammad, H. The immunology of asthma. *Nat. Immunol.* **2015**, *16*, 45–56. [[CrossRef](#)] [[PubMed](#)]
265. Trevor, J.L.; Deshane, J.S. Refractory asthma: Mechanisms, targets, and therapy. *Allergy* **2014**, *69*, 817–827. [[CrossRef](#)] [[PubMed](#)]
266. Woodruff, P.G.; Khashayar, R.; Lazarus, S.C.; Janson, S.; Avila, P.; Boushey, H.A.; Segal, M.; Fahy, J.V. Relationship between airway inflammation, hyperresponsiveness, and obstruction in asthma. *J. Allergy Clin. Immunol.* **2001**, *108*, 753–758. [[CrossRef](#)] [[PubMed](#)]
267. Shaw, D.E.; Berry, M.A.; Hargadon, B.; McKenna, S.; Shelley, M.J.; Green, R.H.; Brightling, C.E.; Wardlaw, A.J.; Pavord, I.D. Association between neutrophilic airway inflammation and airflow limitation in adults with asthma. *Chest* **2007**, *132*, 1871–1875. [[CrossRef](#)]
268. Moore, W.C.; Hastie, A.T.; Li, X.; Li, H.; Busse, W.W.; Jarjour, N.N.; Wenzel, S.E.; Peters, S.P.; Meyers, D.A.; Bleecker, E.R.; et al. Sputum neutrophil counts are associated with more severe asthma phenotypes using cluster analysis. *J. Allergy Clin. Immunol.* **2014**, *133*, 1557–1563. [[CrossRef](#)]
269. Jatakanon, A.; Uasuf, C.; Maziak, W.; Lim, S.; Chung, K.F.; Barnes, P.J. Neutrophilic inflammation in severe persistent asthma. *Am. J. Respir. Crit. Care Med.* **1999**, *160*, 1532–1539. [[CrossRef](#)]

270. Rosales, C. Neutrophil: A Cell with Many Roles in Inflammation or Several Cell Types? *Front. Physiol.* **2018**, *9*, 113. [CrossRef]
271. Li, Y.; Wang, W.; Yang, F.; Xu, Y.; Feng, C.; Zhao, Y. The regulatory roles of neutrophils in adaptive immunity. *Cell Commun. Signal* **2019**, *17*, 147. [CrossRef]
272. Giacalone, V.D.; Margaroli, C.; Mall, M.A.; Tirouvanziam, R. Neutrophil Adaptations upon Recruitment to the Lung: New Concepts and Implications for Homeostasis and Disease. *Int. J. Mol. Sci.* **2020**, *21*, 851. [CrossRef]
273. Wills-Karp, M. Neutrophil ghosts worsen asthma. *Sci. Immunol.* **2018**, *3*, eaau0112. [CrossRef] [PubMed]
274. Ray, A.; Kolls, J.K. Neutrophilic Inflammation in Asthma and Association with Disease Severity. *Trends Immunol.* **2017**, *38*, 942–954. [CrossRef] [PubMed]
275. Chen, F.; Yu, M.; Zhong, Y.; Wang, L.; Huang, H. Characteristics and Role of Neutrophil Extracellular Traps in Asthma. *Inflammation.* **2022**, *45*, 6–13. [CrossRef]
276. Chen, X.; Li, Y.; Qin, L.; He, R.; Hu, C. Neutrophil Extracellular Trapping Network Promotes the Pathogenesis of Neutrophil-associated Asthma through Macrophages. *Immunol. Invest.* **2021**, *50*, 544–561. [CrossRef]
277. Varricchi, G.; Modestino, L.; Poto, R.; Cristinziano, L.; Gentile, L.; Postiglione, L.; Spadaro, G.; Galdiero, M.R. Neutrophil extracellular traps and neutrophil-derived mediators as possible biomarkers in bronchial asthma. *Clin. Exp. Med.* **2022**, *22*, 285–300. [CrossRef] [PubMed]
278. Lu, Y.; Huang, Y.; Li, J.; Huang, J.; Zhang, L.; Feng, J.; Li, J.; Xia, Q.; Zhao, Q.; Huang, L.; et al. Eosinophil extracellular traps drive asthma progression through neuro-immune signals. *Nat. Cell Biol.* **2021**, *23*, 1060–1072. [CrossRef]
279. Michaeloudes, C.; Abubakar-Waziri, H.; Lakhdar, R.; Raby, K.; Dixey, P.; Adcock, I.M.; Mumby, S.; Bhavsar, P.K.; Chung, K.F. Molecular mechanisms of oxidative stress in asthma. *Mol. Aspects Med.* **2022**, *85*, 101026. [CrossRef]
280. Crisford, H.; Sapey, E.; Rogers, G.B.; Taylor, S.; Nagakumar, P.; Lokwani, R.; Simpson, J.L. Neutrophils in asthma: The good, the bad and the bacteria. *Thorax* **2021**, *76*, 835–844. [CrossRef]
281. Andreadis, A.A.; Hazen, S.L.; Comhair, S.A.; Erzurum, S.C. Oxidative and nitrosative events in asthma. *Free Radic Biol. Med.* **2003**, *35*, 213–225. [CrossRef]
282. Obaid Abdullah, S.; Ramadan, G.M.; Makki Al-Hindy, H.A.; Mousa, M.J.; Al-Mumin, A.; Jihad, S.; Hafidh, S.; Kadhum, Y. Serum Myeloperoxidase as a Biomarker of Asthma Severity Among Adults: A Case Control Study. *Rep. Biochem. Mol. Biol.* **2022**, *11*, 182–189. [CrossRef]
283. Olgart Hoglund, C.; de Blay, F.; Oster, J.P.; Duvernelle, C.; Kassel, O.; Pauli, G.; Frossard, N. Nerve growth factor levels and localisation in human asthmatic bronchi. *Eur. Respir. J.* **2002**, *20*, 1110–1116. [CrossRef] [PubMed]
284. Ogawa, H.; Azuma, M.; Tsunematsu, T.; Morimoto, Y.; Kondo, M.; Tezuka, T.; Nishioka, Y.; Tsuneyama, K. Neutrophils induce smooth muscle hyperplasia via neutrophil elastase-induced FGF-2 in a mouse model of asthma with mixed inflammation. *Clin. Exp. Allergy* **2018**, *48*, 1715–1725. [CrossRef] [PubMed]
285. Chen, J.; Kou, L.; Kong, L. Anti-nerve growth factor antibody improves airway hyperresponsiveness by down-regulating RhoA. *J. Asthma* **2018**, *55*, 1079–1085. [CrossRef] [PubMed]
286. Liu, P.; Li, S.; Tang, L. Nerve Growth Factor: A Potential Therapeutic Target for Lung Diseases. *Int. J. Mol. Sci.* **2021**, *22*, 9112. [CrossRef] [PubMed]
287. Saffar, A.S.; Ashdown, H.; Gounni, A.S. The molecular mechanisms of glucocorticoids-mediated neutrophil survival. *Curr. Drug Targets* **2011**, *12*, 556–562. [CrossRef]
288. Tamura, H.; Ishikita, H. Quenching of Singlet Oxygen by Carotenoids via Ultrafast Superexchange Dynamics. *J. Phys. Chem. A* **2020**, *124*, 5081–5088. [CrossRef]
289. Stratton, S.P.; Schaefer, W.H.; Liebler, D.C. Isolation and identification of singlet oxygen oxidation products of beta-carotene. *Chem. Res. Toxicol.* **1993**, *6*, 542–547. [CrossRef]
290. Zbyradowski, M.; Duda, M.; Wisniewska-Becker, A.; Heriyanto; Rajwa, W.; Fiedor, J.; Cvetkovic, D.; Pilch, M.; Fiedor, L. Triplet-driven chemical reactivity of  $\beta$ -carotene and its biological implications. *Nat. Commun.* **2022**, *13*, 2474. [CrossRef]
291. Montenegro, M.A.; Nazareno, M.A.; Durantini, E.N.; Borsarelli, C.D. Singlet molecular oxygen quenching ability of carotenoids in a reverse-micelle membrane mimetic system. *Photochem. Photobiol.* **2002**, *75*, 353–361. [CrossRef]
292. Ramel, F.; Birtic, S.; Cuiné, S.; Triantaphylidès, C.; Ravanat, J.L.; Havaux, M. Chemical quenching of singlet oxygen by carotenoids in plants. *Plant Physiol.* **2012**, *158*, 1267–1278. [CrossRef]
293. Kruk, J.; Szymańska, R. Singlet oxygen oxidation products of carotenoids, fatty acids and phenolic prennylipids. *J. Photochem. Photobiol. B* **2021**, *216*, 112148. [CrossRef]
294. Di Mascio, P.; Devasagayam, T.P.; Kaiser, S.; Sies, H. Carotenoids, tocopherols and thiols as biological singlet molecular oxygen quenchers. *Biochem. Soc. Trans.* **1990**, *18*, 1054–1056. [CrossRef] [PubMed]
295. Cantrell, A.; McGarvey, D.J.; Truscott, T.G.; Rancan, F.; Böhm, F. Singlet oxygen quenching by dietary carotenoids in a model membrane environment. *Arch. Biochem. Biophys.* **2003**, *412*, 47–54. [CrossRef]
296. Ukai, N.; Lu, Y.; Etoh, H.; Yagi, A.; Ina, K.; Oshima, S.; Ojima, F.; Sakamoto, H.; Ishiguro, Y. Photosensitized Oxygenation of Lycopene. *Biosci. Biotechnol. Biochem.* **1994**, *58*, 1718–1719. [CrossRef]
297. Naik, P.; Kumar, M. Receptor interactions of constituents of *Zingiber officinalis* and *Solanum lycopersicum* on COX. *J. Pharmacogn. Phytochem.* **2019**, *8*, 4637–4641.
298. Hayashi, R.; Hayashi, S.; Machida, S. Changes in Aqueous Humor Lutein Levels of Patients with Cataracts after a 6-Week Course of Lutein-Containing Antioxidant Supplementation. *Curr. Eye Res.* **2022**, *47*, 1016–1023. [CrossRef]

299. Sideri, O.; Tsaousis, K.T.; Li, H.J.; Viskadouraki, M.; Tsinopoulos, I.T. The potential role of nutrition on lens pathology: A systematic review and meta-analysis. *Surv. Ophthalmol.* **2019**, *64*, 668–678. [[CrossRef](#)]
300. Groten, K.; Marini, A.; Grether-Beck, S.; Jaenicke, T.; Ibbotson, S.H.; Moseley, H.; Ferguson, J.; Krutmann, J. Tomato Phytonutrients Balance UV Response: Results from a Double-Blind, Randomized, Placebo-Controlled Study. *Skin Pharmacol. Physiol.* **2019**, *32*, 101–108. [[CrossRef](#)]
301. Fam, V.W.; Holt, R.R.; Keen, C.L.; Sivamani, R.K.; Hackman, R.M. Prospective Evaluation of Mango Fruit Intake on Facial Wrinkles and Erythema in Postmenopausal Women: A Randomized Clinical Pilot Study. *Nutrients* **2020**, *12*, 3381. [[CrossRef](#)]
302. Ouchi, A.; Aizawa, K.; Iwasaki, Y.; Inakuma, T.; Terao, J.; Nagaoka, S.; Mukai, K. Kinetic study of the quenching reaction of singlet oxygen by carotenoids and food extracts in solution. Development of a singlet oxygen absorption capacity (SOAC) assay method. *J. Agric. Food Chem.* **2010**, *58*, 9967–9978. [[CrossRef](#)]
303. Fukuzawa, K.; Inokami, Y.; Tokumura, A.; Terao, J.; Suzuki, A. Rate constants for quenching singlet oxygen and activities for inhibiting lipid peroxidation of carotenoids and alpha-tocopherol in liposomes. *Lipids* **1998**, *33*, 751–756. [[CrossRef](#)] [[PubMed](#)]
304. Foote, C.S.; Ching, T.Y.; Geller, G.G. Chemistry of singlet oxygen. XVIII. Rates of reaction and quenching of alpha-tocopherol and singlet oxygen. *Photochem. Photobiol.* **1974**, *20*, 511–513. [[PubMed](#)]
305. Gruszka, J.; Pawlak, A.; Kruk, J. Tocochromanols, plastoquinol, and other biological prenyllipids as singlet oxygen quenchers—determination of singlet oxygen quenching rate constants and oxidation products. *Free Radic. Biol. Med.* **2008**, *45*, 920–928. [[CrossRef](#)] [[PubMed](#)]
306. Shichiri, M.; Yoshida, Y.; Ishida, N.; Hagihara, Y.; Iwahashi, H.; Tamai, H.; Niki, E.  $\alpha$ -Tocopherol suppresses lipid peroxidation and behavioral and cognitive impairments in the Ts65Dn mouse model of Down syndrome. *Free Radic. Biol. Med.* **2011**, *50*, 1801–1811. [[CrossRef](#)] [[PubMed](#)]
307. Shichiri, M.; Harada, N.; Ishida, N.; Komaba, L.K.; Iwaki, S.; Hagihara, Y.; Niki, E.; Yoshida, Y. Oxidative stress is involved in fatigue induced by overnight deskwork as assessed by increase in plasma tocopherylhydroquinone and hydroxycholesterol. *Biol. Psychol.* **2013**, *94*, 527–533. [[CrossRef](#)]
308. Shichiri, M.; Ishida, N.; Hagihara, Y.; Yoshida, Y.; Kume, A.; Suzuki, H. Probucol induces the generation of lipid peroxidation products in erythrocytes and plasma of male cynomolgus macaques. *J. Clin. Biochem. Nutr.* **2019**, *64*, 129–142. [[CrossRef](#)]
309. Krasnovsky, A.A.; Kagan, V.E.; Minin, A.A. Quenching of singlet oxygen luminescence by fatty acids and lipids: Contribution of physical and chemical mechanisms. *FEBS Lett.* **1983**, *155*, 233–236. [[CrossRef](#)]
310. Chaudhuri, R.K.; Bojanowski, K. Bakuchiol: A retinol-like functional compound revealed by gene expression profiling and clinically proven to have anti-aging effects. *Int. J. Cosmet. Sci.* **2014**, *36*, 221–230. [[CrossRef](#)]
311. Chaudhuri, R.K.; Marchio, F. Bakuchiol in the Management of Acne-affected Skin. *Cosmet. Toilet.* **2011**, *126*, 502–510.
312. Dhaliwal, S.; Rybak, I.; Ellis, S.R.; Notay, M.; Trivedi, M.; Burney, W.; Vaughn, A.R.; Nguyen, M.; Reiter, P.; Bosanac, S.; et al. Prospective, randomized, double-blind assessment of topical bakuchiol and retinol for facial photoaging. *Br. J. Dermatol.* **2019**, *180*, 289–296. [[CrossRef](#)]
313. Krishnakantha, T.P.; Lokesh, B.R. Scavenging of superoxide anions by spice principles. *Indian J. Biochem. Biophys.* **1993**, *30*, 133–134.
314. Swindell, W.R.; Bojanowski, K.; Chaudhuri, R.K. A Zingerone Analog, Acetyl Zingerone, Bolsters Matrisome Synthesis, Inhibits Matrix Metallopeptidases, and Represses IL-17A Target Gene Expression. *J. Invest. Dermatol.* **2020**, *140*, 602–614.e615. [[CrossRef](#)] [[PubMed](#)]
315. Das, K.C.; Das, C.K. Curcumin (diferuloylmethane), a singlet oxygen ( $(^1O_2)$ ) quencher. *Biochem. Biophys. Res. Commun.* **2002**, *295*, 62–66. [[CrossRef](#)] [[PubMed](#)]
316. Chaudhuri, R.K.; Meyer, T.; Premi, S.; Brash, D. Acetyl zingerone: An efficacious multifunctional ingredient for continued protection against ongoing DNA damage in melanocytes after sun exposure ends. *Int. J. Cosmet. Sci.* **2020**, *42*, 36–45. [[CrossRef](#)]
317. Dhaliwal, S.; Rybak, I.; Pourang, A.; Burney, W.; Haas, K.; Sandhu, S.; Crawford, R.; Sivamani, R.K. Randomized double-blind vehicle controlled study of the effects of topical acetyl zingerone on photoaging. *J. Cosmet. Dermatol.* **2021**, *20*, 166–173. [[CrossRef](#)] [[PubMed](#)]
318. Aratani, Y. Myeloperoxidase: Its role for host defense, inflammation, and neutrophil function. *Arch. Biochem. Biophys.* **2018**, *640*, 47–52. [[CrossRef](#)] [[PubMed](#)]

**Disclaimer/Publisher’s Note:** The statements, opinions and data contained in all publications are solely those of the individual author(s) and contributor(s) and not of MDPI and/or the editor(s). MDPI and/or the editor(s) disclaim responsibility for any injury to people or property resulting from any ideas, methods, instructions or products referred to in the content.